

BULLETIN 44

OFFICE COPY

STATE OF ILLINOIS

WILLIAM G. STRATTON, Governor

DEPARTMENT OF REGISTRATION AND EDUCATION

VERA M. BINKS, Director



**RAINFALL RELATIONS
ON
SMALL AREAS IN ILLINOIS**

BY

F. A. HUFF AND J. C. NEILL

**ILLINOIS STATE WATER SURVEY
WILLIAM C. ACKERMANN, Chief**

**URBANA
1957**

STATE OF ILLINOIS

WILLIAM G. STRATTON, Governor

DEPARTMENT OF REGISTRATION AND EDUCATION

VERA M. BINKS, Director

RAINFALL RELATIONS
ON
SMALL AREAS IN ILLINOIS

BY

F. A. HUFF AND J. C. NEHL



STATE WATER SURVEY DIVISION

WILLIAM C. ACKERMANN, Chief

URBANA

1957

TABLE OF CONTENTS

	Page
INTRODUCTION	9
ACKNOWLEDGMENTS	9
RAIN-GAGING FACILITIES.....	11
El Paso Network	11
Panther Creek Network	11
Goose Creek Network	12
East Central Illinois Network	12
Boneyard Creek Network	12
Monticello Network	13
Airport Network	13
RAINFALL VARIABILITY.	15
Introduction	15
Rainfall Relative Variability.	15
Results of Analysis.	15
Effect of Gage Density on Maximum Recorded Point Rainfall.	20
FREQUENCY OF POINT AND AREAL MEAN RAINFALL RATES.	21
Introduction	21
Data Used in Analysis	21
Frequency of Point Rainfall Rates.	22
Frequency of Areal Mean Rainfall Rates.	23
Discussion of Results.	23
AREA-DEPTH RELATIONS.	25
Introduction	25
Analysis and Results.	25
VARIATION OF POINT RAINFALL WITH DISTANCE	31
Introduction	31
Analysis of Average Differences.	31
Confidence Limits.	31
Equation Comparisons.	31
Consideration of Additional Variables.	32
AREAL REPRESENTATIVENESS OF POINT RAINFALL	35
Introduction	35
Available Data	35
Accuracy of Areal Rainfall Estimates From a Centered Gage.	35
Average Error	35
Confidence Limits.	38
Areal Rainfall Estimates From an Off-Center Gage.	39

TABLE OF CONTENTS (continued)

	Page
RELIABILITY OF STORM MEAN RAINFALL ESTIMATES.	43
Introduction	43
Data Used	43
Sampling Procedures.	43
Random Start	43
Combined Sampling Plan.	43
Best-Centered.	45
Analytical Procedure.	46
Results of Analysis on 100-Square Mile Network	46
Random Start	46
Combined Sampling Plan	46
Best-Centered	47
Comparison of Results from Three Sampling Plans.	47
Results of Analysis for Areas of Different Size.	47
Average Error.	47
Confidence Limits.	50
EXCESSIVE RAINFALL RELATIONS ON 100-SQUARE MILE AREA.	51
Gage Density to Observational Frequency Relations.	51
Effect of Gage Density on Observed Maximum.	51
Point-Areal Mean Relations.	52
RELATION BETWEEN POINT AND AREAL RAINFALL FREQUENCIES.	55
A MICROMETEOROLOGICAL STUDY OF RAINFALL VARIABILITY.	57
Introduction	57
Description of Network.	57
Analysis of Data	57

TABLE OF CONTENTS (continued)

LIST OF ILLUSTRATIONS

Figure	Title	Page
1	Reference map10
2	El Paso network, 280 square miles.....	.11
3	Panther Creek network, 100 square miles11
4	Goose Creek network, 100 square miles.12
5	East central Illinois network, 400 square miles12
6	Boneyard Creek network, 8.5 square miles12
7	Monticello network, 400 acres13
8	Airport network, 19 acres13
9	Storm rainfall variability.15
10	Examples of rainfall variability.17
11	One-minute mean rates.18
12	Time variations in rainfall pattern19
13	Effect of gage density on maximum recorded point rainfall.20
14	Distribution of point rainfall rates in individual storms.21
15	Distribution of point rainfall rates during average season.22
16	Time distribution of point rainfall22
17	Point rainfall time-rate relation.23
18	Distribution of areal mean rainfall rates.23
19	Effect of gage density on isohyetal pattern.26
20	Area-depth relations for heaviest storms, 5.5-square mile area27
21	Area-depth relations for heaviest storms, 100-square mile area27
22	Area-depth relations for heaviest storms, 280-square mile area27
23	Average area-depth relations, 5.5-square mile area, mean rainfall = 1.00 inch.28
24	Average area-depth relations, 100-square mile area, mean rainfall = 1.00 inch28
25	Average area-depth relations, 5.5-square mile area, 6-hour storm duration.28
26	Average area-depth relations, 100-square mile area, 6-hour storm duration.28
27	Extreme area-depth relations, 5.5-square mile area, mean rainfall = 1.00 inch29
28	Extreme area-depth relations, 100-square mile area, mean rainfall = 1.00 inch.29
29	Extreme area-depth curve slopes, 5.5-square mile area, selected areal mean rainfalls.29

TABLE OF CONTENTS (continued)

LIST OF ILLUSTRATIONS (continued)

Figure	Title	Page
30	Extreme area-depth curve slopes, 100-square mile area, selected areal mean rainfalls	29
31	Variation of point rainfall with distance	32
32	95 per cent confidence range for variation of point rainfall with distance	32
33	25, 50 and 100-square mile areas, Goose Creek 1954.	35
34	Storm relation between point and areal mean rainfall based on average deviations.	36
35	Weekly relation between point and areal mean rainfall based on average deviations.	36
36	Monthly relation between point and areal mean rainfall based on individual deviations.	37
37	Storm relation between point and areal mean rainfall based on standard errors.	38
38	Weekly relation between point and areal mean rainfall based on standard errors.	39
39	95 per cent confidence range for storm rainfall	40
40	95 per cent confidence range for weekly rainfall	41
41	Effect of gage location on single gage estimates of mean rainfall on 100-square mile area	42
42	Groups of gages from which 3 random start systematic samples of size 16 were selected	43
43	Combined sampling plan for samples of Size 1, 2, 3, 4, 6 and 8	44
44	Best-centered sampling plan for Panther Creek network	45
45	Comparison of storm sampling plans on a 100-square mile area	47
46	Relation between sampling error, storm size, and gage density on 100-square mile area	48
47	95 per cent confidence range of storm mean rainfall for various gage densities.	49
48	Effect of gage density on maximum observed excessive rates.	51
49	Relation between point and areal mean rates under excessive rate conditions.	52
50	30-minute excessive rates, July 8, 1951.	53
51	Excessive rate area-depth relations, July 8, 1951.	53
52	Comparison between point and areal mean rainfall at equal frequencies on 25-square mile area	55
53	Effect of several meteorological factors on relative variability of storm rainfall.	60

TABLE OF CONTENTS (continued)

TABLES

Table	Title	Page
1	Storm rainfall variability, 100-square mile area16
2	Storm rainfall variability, 280-square mile area16
3	Monthly rainfall variability, 100-square mile area16
4	Frequency of point rainfall rates calculated from different base periods	22
5	Frequency of areal mean rainfall rates	24
6	Time distribution of areal mean rainfall rates	24
7	Correlation coefficients30
8	Comparisons between Equations (3) and (4)31
9	Multiple correlation coefficients33
10	Regression constants for storm, weekly and monthly equations on various areas.35
11	Multiple correlation coefficients37
12	Comparisons between Equations (4) and (8).38
13	Comparison between storm, weekly and monthly relations.38
14	Storm groups used in standard error computations.39
15	Regression constants.47
16	Equations for average and standard deviations.48
17	Relation between excessive rainfall frequency and gage density.51
18	Effect of gage density on observed maximum amounts.51
19	Differences between gage pairs.57
20	Relative variability trends for 6-foot gage pairs.58
21	Variation of point rainfall with distance.58
22	Monthly and seasonal differences between gage pairs.59
23	Relation between areal mean rainfall and central gage point rainfall59

INTRODUCTION

During the period 1948-55, the State Water Survey Meteorology Subdivision operated several concentrated rain gage networks on small areas to collect detailed precipitation data which can further our knowledge of the water resources of Illinois. The collected data have been used in a number of studies to obtain information on precipitation pertinent to hydrologic analysis, design, and planning. This bulletin presents current results of several of these studies. Some of the studies are of a continuing nature and as additional data become available, refinements will be published. However, it is felt that adequate analysis has now been completed to present results that may be beneficial to hydrologists and engineers actively engaged in the field of water resources.

Although these studies are based on Illinois data, the results should be approximately representative of conditions in the Midwest and of other areas having similar climate and topography. The studies to date have been concentrated on the analysis of rainfall during the spring to fall thunderstorm season on relatively small areas ranging from less than one square mile to 400 square miles. The extreme variability in precipitation experienced during the thunderstorm season creates difficult problems for the hydrologist concerned with small watersheds, which are subject to flash floods and rapidly affected by drought conditions. The major portion of the surface-water supplies for municipalities in the state are obtained from lakes having watershed areas under 400 square miles.

Included in this bulletin are results of studies on: the relative variability of storm and monthly rainfall over small areas; the distribution of point and areal mean rainfall rates in shower-type precipitation; area-depth relations on small watersheds; the variation of point rainfall with distance; the areal representativeness of point rainfall in measuring areal mean rainfall on a storm, weekly, and monthly basis; the combined effect of storm size, area, and number of rain gages on the accuracy of storm mean rainfall estimates; relations during periods of excessive rainfall over a 100-

square mile basin; the relation between point and areal mean rainfall frequencies; and micro-meteorological variations in storm rainfall.

ACKNOWLEDGMENTS

This bulletin was prepared under the direction of William C. Ackermann, Chief of the Illinois State Water Survey. Research was accomplished under the general guidance of Glenn E. Stout, Head, Meteorology Subdivision.

The authors are indebted to A. M. Buswell, former Chief, and H. E. Hudson, Jr., former Head of the Engineering Subdivision, for suggestions and guidance in the early phases of the research incorporated in the bulletin.

Within the Meteorology Subdivision, special credit is due Douglas M. A. Jones, who supervised a major portion of the data collection and Carol Verseman, who performed or supervised a major portion of the routine analysis. Drafting of the illustrations and cover was done by John Wesselhoff. Numerous research assistants helped with the installation and servicing of rain gages, collection and tabulation of data, and computation.

Credit is due Lester Pfister, President of the Pfister Hybrid Corn Company, the U. S. Soil Conservation Service, and the Civil Engineering Department of the University of Illinois, who provided some of the rain gages for the studies. Operation of the Goose Creek network and data collection were sponsored in part by the Signal Corps Engineering Laboratories, Belmar, New Jersey under Contract DA-36-039 SC-42446. The Agricultural Engineering Department of the University of Illinois furnished data from its 400-acre rain-gage network.

Certain phases of the analyses were greatly expedited through use of facilities at the Statistical Service Unit and the Digital Computer Laboratory at the University of Illinois.

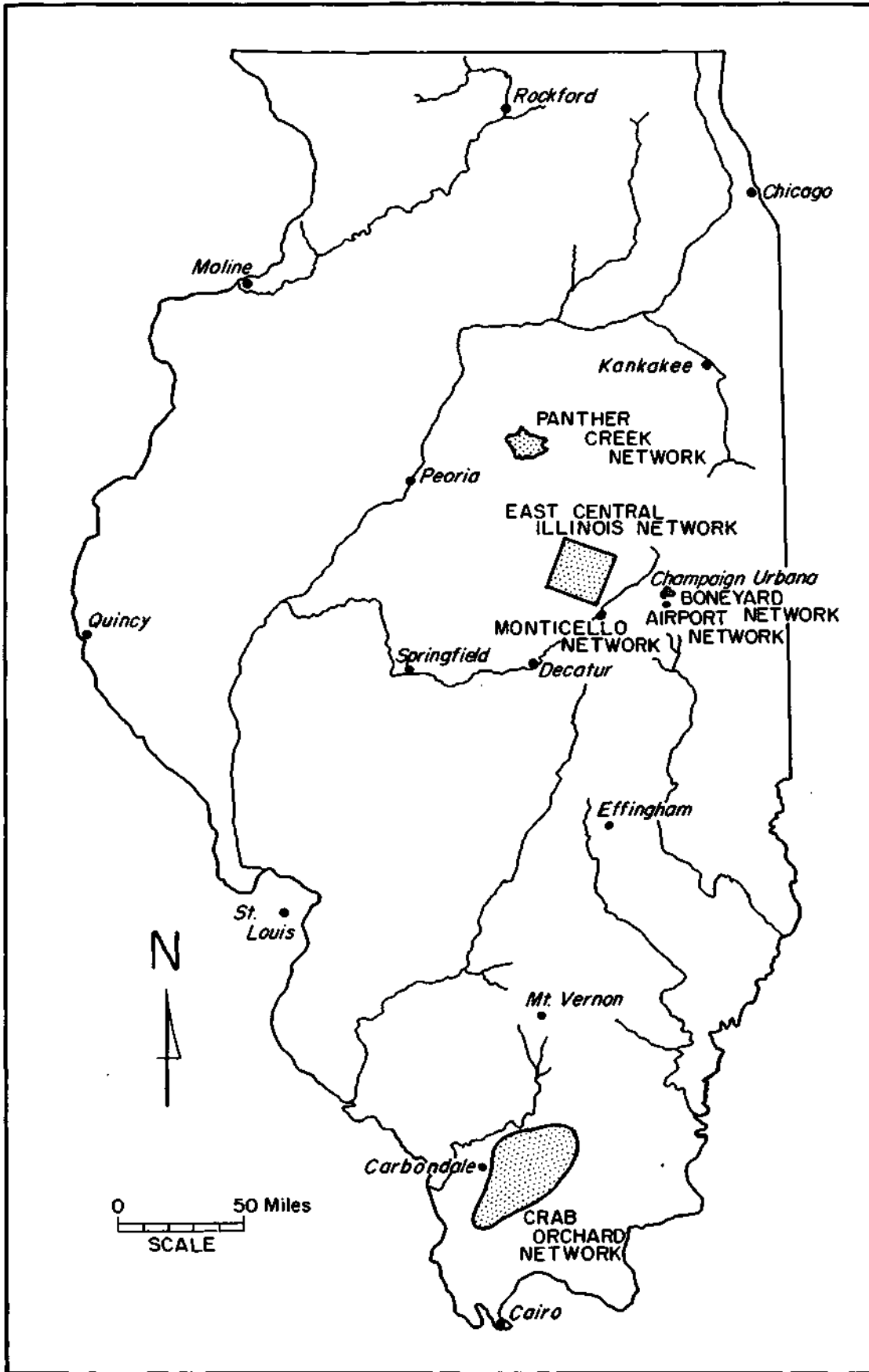


FIGURE 1 REFERENCE MAP

RAIN-GAGING FACILITIES

Rainfall data from seven rain-gage networks located in central Illinois were available for studies described in this bulletin. Generally, the networks were in full operation during the warm season from April through October, after which they were closed or reduced to relatively few gages for the winter season. The network locations within the state are shown on the reference map in Figure 1. The 1948 El Paso network which is not illustrated was a southward and westward extension of the Panther Creek network. The Goose Creek network was located in the southeastern portion of the present east central Illinois network. The Crab Orchard network in southern Illinois was not installed until the fall of 1954. Data from it have not been analyzed adequately to be presented in this bulletin.

The terrain within the central Illinois experimental areas is relatively flat with no distinct topographic features to influence storm behavior. All gages were located with open exposures. The recording gages, from which the majority of the analytical data were obtained, were serviced by trained technicians. The non-recording gages were installed by Water Survey technicians, and the measurements were taken by nearby residents who had been carefully instructed in the proper operation of the gages. In most cases, these cooperative observers were farmers having a lively interest in the measurement of rainfall.

Statistical tests were performed to determine the homogeneity of data obtained from the various networks. These tests indicated that no significant

differences existed, thus permitting utilization of combined network data for the derivation of various empirical rainfall relations.

El Paso Network

The first of these rain-gage networks located on an area of 280 square miles in the vicinity of El Paso, Illinois (Fig. 2) was established in the spring of 1948. During 1948 and 1949 a total of 17 recording and 31 non-recording gages, or an average of one gage per 5.8 square miles, was operated on this area.

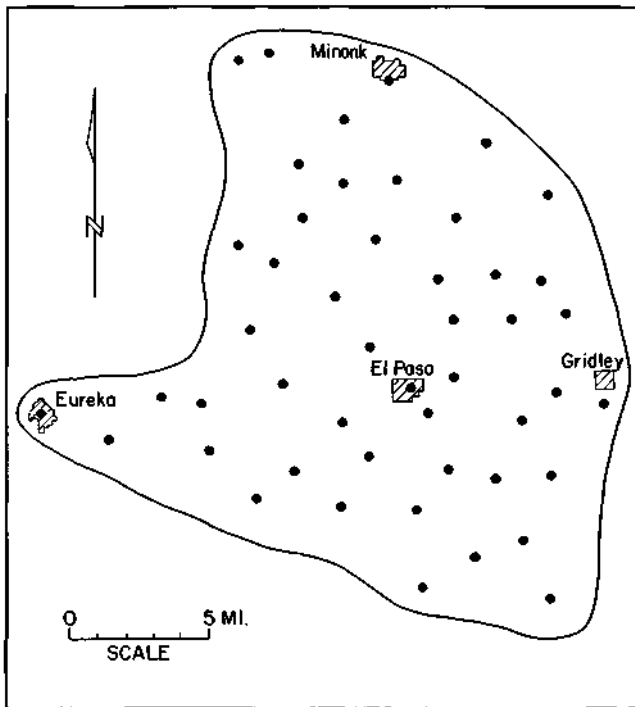


FIGURE 2 EL PASO NETWORK, 230 SQUARE MILES

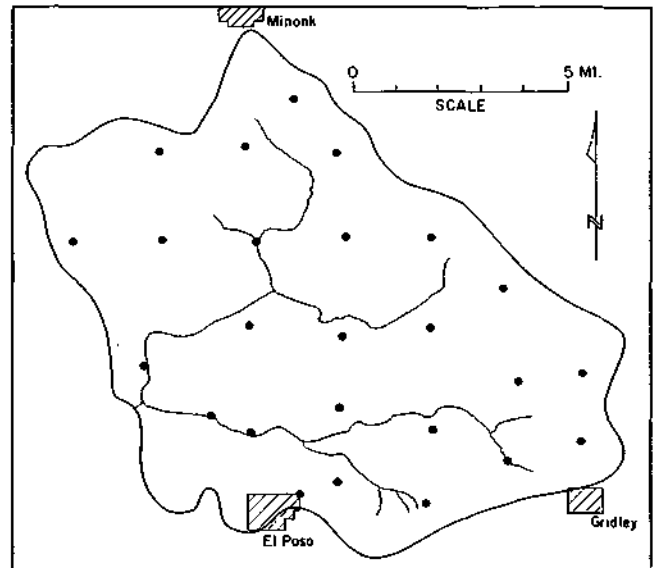


FIGURE 3 PANTHER CREEK NETWORK, 100 SQUARE MILES

Panther Creek Network

The network in the El Paso area was reduced in size at the close of the 1949 thunderstorm season. Beginning in the spring of 1950, a network of 100 square miles within the El Paso network was continued on the Panther Creek watershed. This area had been gaged with 6 recording and 14 non-recording gages during the 1948 and 1949 seasons, corresponding to an average of one gage per 4.75 square miles. Employing both recording and non-recording gages, the Panther Creek network was expanded to 40 gages in 1950. During 1951-53, the network of 25 recording gages illustrated in Figure 3 was maintained. In 1954, the Panther Creek network was reduced to 10 recording gages, since the gages were needed elsewhere and 10 was considered a sufficient number for the Panther Creek study.

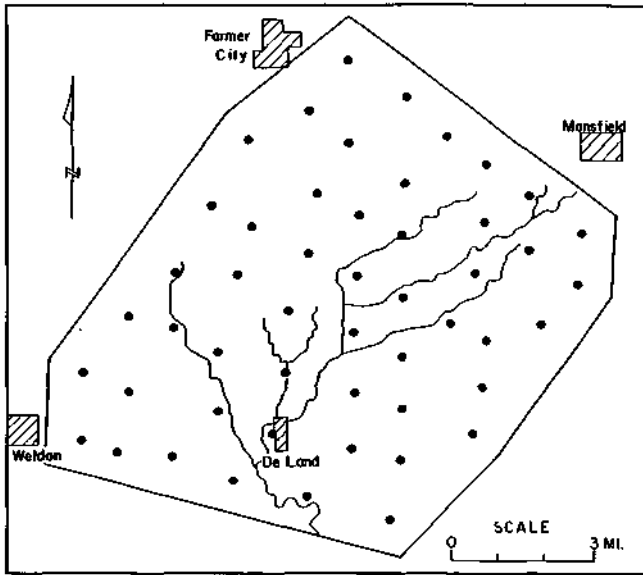


FIGURE 4 GOOSE CREEK NETWORK, 100 SQUARE MILES

one revolution every six hours. The Goose Creek network was enlarged during July 1952 to include 100 square miles (Fig. 4). A total of 50 recording rain gages, equipped with the 12.65-inch diameter collector and the 6-hour chart drive, was operated on this area during the remainder of the 1952 thunderstorm season and during the 1953 thunderstorm season. This network was reorganized somewhat in 1954; however, the area of the network was maintained at 100 square miles. A total of 48 recording gages was used during the 1954 season.

East Central Illinois Network

In order to obtain data over an area larger than 100 square miles, the Goose creek network was reorganized and expanded north and west during the spring of 1955. The new network (Fig. 5) includes an area of 400 square miles. A total of 49 recording gages was used on this area during the 1955 thunderstorm season.

Goose Creek Network

During the spring of 1951, a network was installed over an area of 50 square miles on the Goose Creek watershed in the vicinity of Deland, Illinois. This network consisted of 33 recording rain gages which were equipped with 12.65-inch diameter collectors and with chart drums making

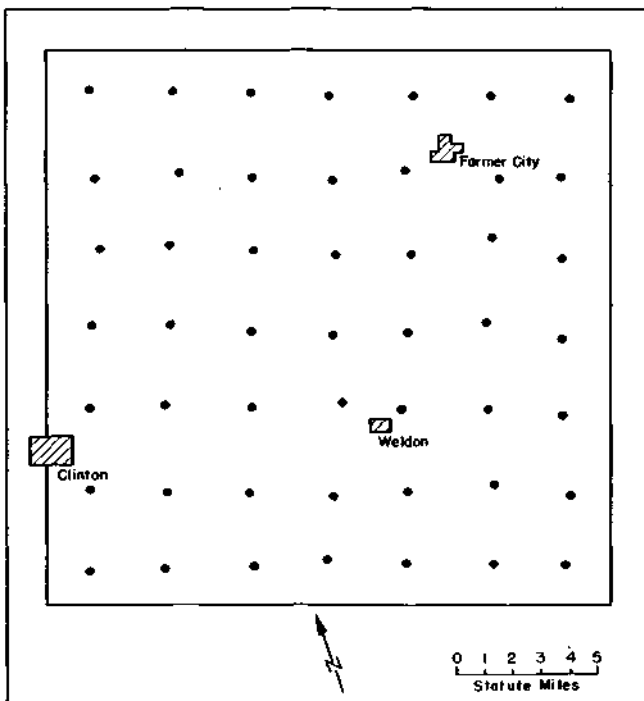


FIGURE 5 EAST CENTRAL ILLINOIS NETWORK, 400 SQUARE MILES

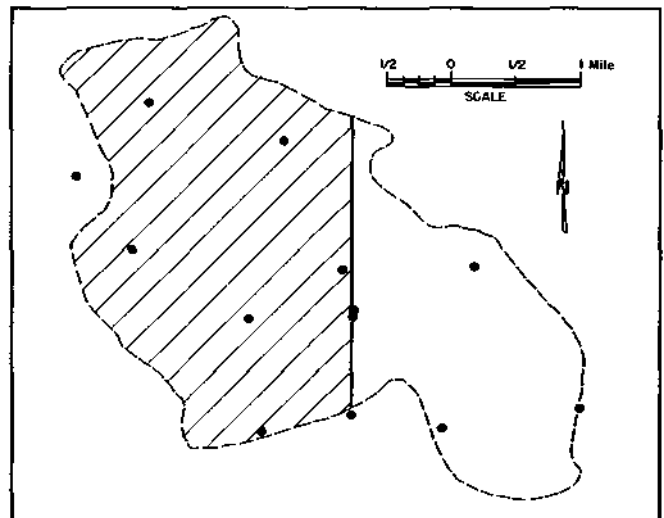


FIGURE 6 BONEYARD CREEK NETWORK, 8.5 SQUARE MILES

Boneyard Creek Network

A 12-station network for sampling an area of approximately 8.5 square miles on the Boneyard Creek watershed at Champaign-Urbana, Illinois is shown in Figure 6. This network has been operated since the fall of 1948 in cooperation with the Civil Engineering Department, University of Illinois. The majority of the rainfall analysis has been confined to data from an area of 5.5 square miles within the watershed (cross-hatched in Fig. 6). Streamflow measurements are made on this area, and the rain gage density is greater than over the remaining portion of the watershed.

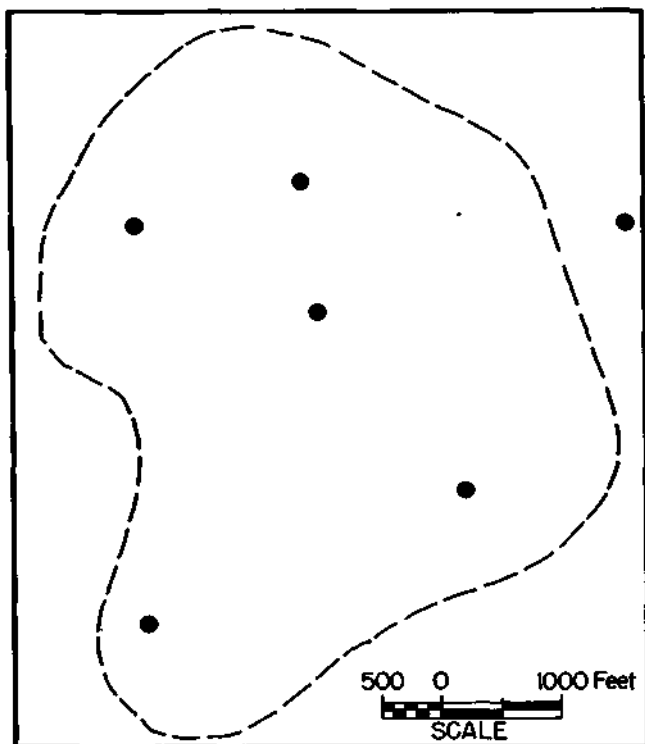


FIGURE 7 MONTICELLO NETWORK, 400 ACRES

Monticello Network

The Monticello network (Fig. 7) consisting of 400 acres (0.6 sq. mi.) is operated by the Agricultural Engineering Department, University of Illinois. For the Survey studies six recording gages were used from this network, which has been operated

since 1949. Data from the network were made available to the authors for analysis and inclusion in this bulletin.

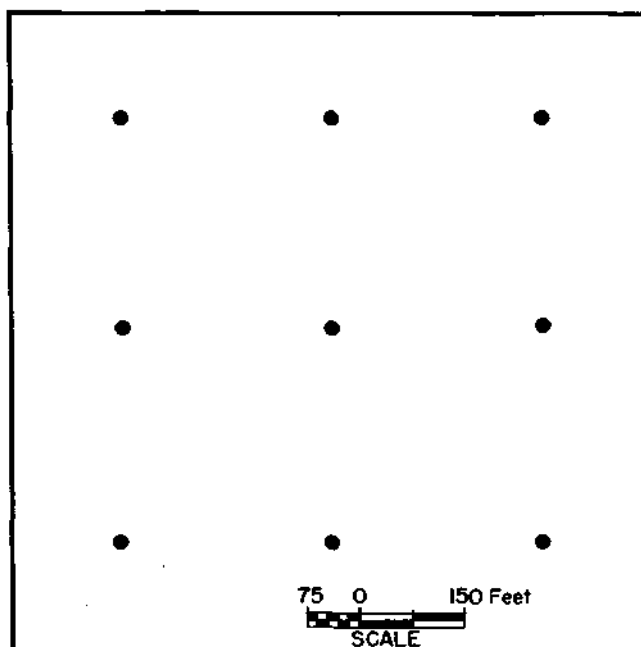


FIGURE 8 AIRPORT NETWORK, 19 ACRES

Airport Network

During 1953-55, a micro-network of 18 non-recording gages was operated at the University of Illinois Airport, six miles south of Champaign-Urbana. This network consisted of pairs of gages spaced six feet apart at each of nine stations. These stations were located at intervals of 300 feet to form a square grid pattern on 19 acres (0.03 sq. mi.) as shown in Figure 8.

RAINFALL VARIABILITY

Introduction

The great variability of thunderstorm and rain-shower precipitation within relatively short distances is generally recognized by meteorologists and hydrologists. However, information concerning the degree of this variability is limited, especially for small watersheds. Obviously, rainfall variability is pertinent to hydrologists and meteorologists concerned with rain gaging of watersheds and the interpretation of rainfall data for application to hydrologic analysis. For example, the area-depth relation and, consequently, the rainfall-runoff relation are closely related to the variability within a given watershed.

Data from two concentrated networks, the 280-square mile El Paso network (Fig.2) and the 100-square mile Panther Creek network (Fig. 3) have been used for a limited study on thundershower and rainshower variability. Data for 1948-49 on the El Paso network and for 1948-53 on the Panther Creek network were used in the study.

Rainfall Relative Variability

The relative variability for these areas was obtained by calculating the coefficient of variation in each storm on each network. There were 48 gages in the El Paso network and 20 gages on the Panther Creek network used for calculations. For convenience, the variability factor (coefficient of variation) was expressed in per cent and was obtained from the following equation:

$$CV = \frac{SD}{P} \times 100 \quad (1)$$

where CV is the coefficient of variation in per cent, SD is the standard deviation of all the network observations, and P is the areal mean rainfall.

The variability factor is a measure of the dispersion of point rainfall values about the areal mean rainfall. In addition to the actual variations in the storm rainfall the variability factor includes the effects of instrumental or observational errors and gage non-representativeness. However, no distinct topographic features existed in the experimental area, and all gages were located with open exposures. Therefore, the effect of gage non-representativeness is eliminated for all practical purposes. A close check was maintained on the operation of the rain gages, so the variability data should be reasonably accurate and representative.

Results of Analysis

The data were first analyzed to determine the general effects of storm mean rainfall and area on relative variability. The results of this analysis are summarized in Tables 1 and 2. Both tables clearly indicate that for a given basin the relative variability tends to decrease with increasing storm mean rainfall. This tendency is accounted for by the nature of shower-type rainfall and the location of the heavier storm cores with respect to the

basin. Considering the multi-cellular nature of thunderstorms, it appears logical that an area comes under the influence of more cells with heavy rainfall and, consequently, a tendency exists for greater relative uniformity in the rainfall pattern. It was found on the Thunderstorm Project⁽¹⁾ that single-celled thunderstorms were generally weak compared to the multi-cellular storms. The expected tendency for the variability to increase with area is apparent from a comparison of average values in Tables 1 and 2. The maximum and minimum values in these tables are the extremes observed for individual storms in each mean rainfall class.

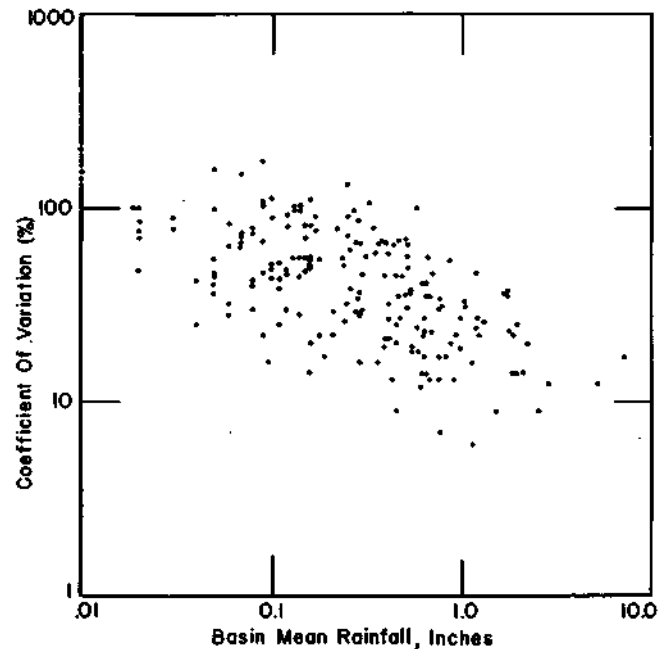


FIGURE 9 STORM RAINFALL VARIABILITY

Table 3 shows the relative variability calculated on a monthly basis for the 100-square mile drainage basin. Comparing Tables 1 and 3, it is seen that the relative variability tends to decrease as the rainfall increases and the totalizing period is increased. Figure 9 is a scatter diagram for the 100-square mile basin, illustrating the relationship between storm mean rainfall and relative variability based on 185 cases. The trend for the relative variability to decrease with increasing mean rainfall is apparent. However, a close correlation does not exist as shown by the amount of scatter on the diagram. Other factors, such as storm duration, movement of storm with respect to basin, and the internal structure of thunderstorms and rain showers undoubtedly contributed to the observed scatter.

TABLE 1
STORM RAINFALL VARIABILITY
100 SQ. MI. AREA

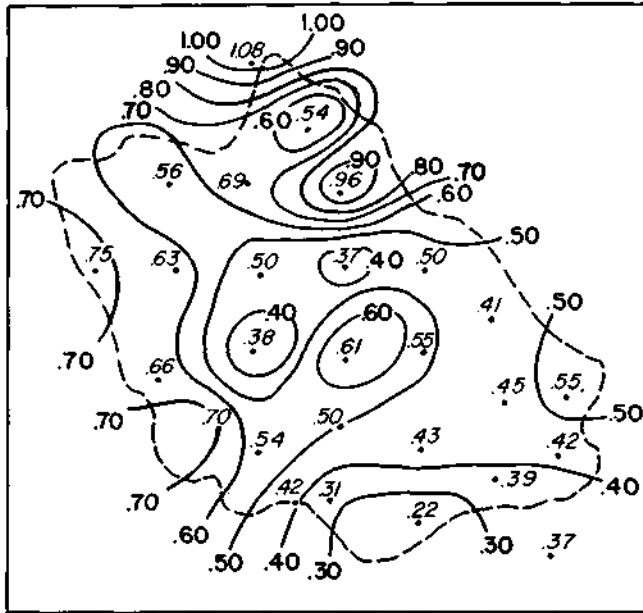
Mean Rainfall (in.)	Coefficient of Variation (%)		Min.	Number of Cases
	Av.	Max.		
0.01 - 0.20	72	200	14	75
0.21 - 0.50	48	133	9	44
0.51 - 1.00	30	100	7	42
1.01 - 2.00	25	37	6	18
Over 2.00	14	20	9	6

TABLE 2
STORM RAINFALL VARIABILITY
280 SQ. MI. AREA

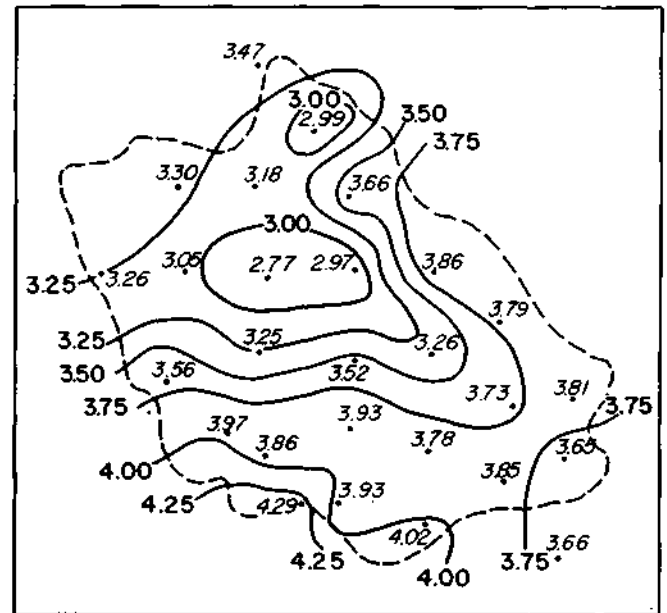
Mean Rainfall (in.)	Coefficient of Variation (%)		Min.	Number of Cases
	Av.	Max.		
0.01 - 0.20	81	127	23	17
0.21 - 0.50	56	78	16	14
0.51 - 1.00	42	64	22	15
1.01 - 3.00	31	47	14	5

TABLE 3
MONTHLY RAINFALL VARIABILITY
100 SQ. MI. AREA

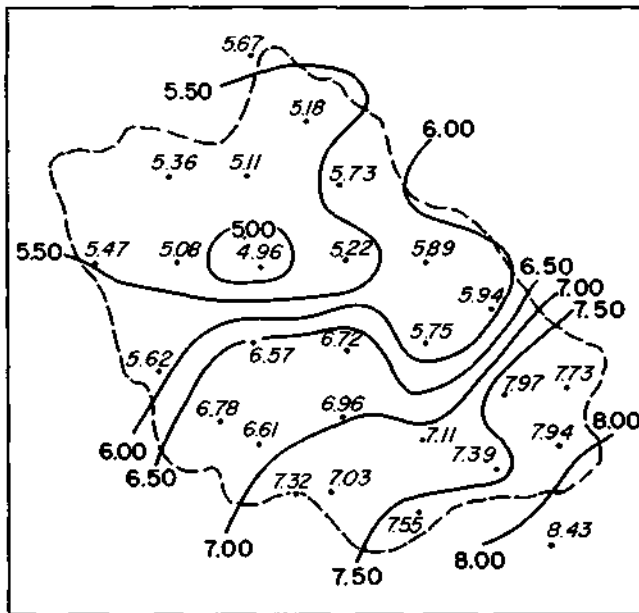
Mean Rainfall (in.)	Coefficient of Variation (%)		Min.	Number of Cases
	Av.	Max.		
0.01 - 2.00	31	37	16	6
2.01 - 4.00	15	19	9	9
4.01 - 6.00	18	26	12	4
6.01 - 8.00	12	25	8	7



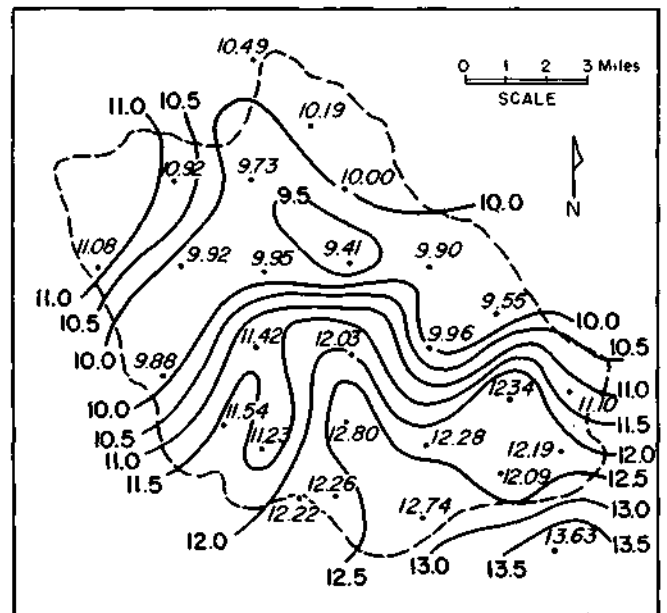
A. STORM RAINFALL, JULY 1, 1953
($\bar{P} = .52$, $CV = .30$)



B. WEEKLY RAINFALL, JULY 1-7, 1953
($\bar{P} = 3.57$, $CV = .11$)



C. JULY 1953 RAINFALL
($\bar{P} = 6.36$, $CV = .15$)



D. JUNE-AUG. 1953 RAINFALL
($\bar{P} = 11.03$, $CV = .10$)

FIGURE 10 EXAMPLES OF RAINFALL VARIABILITY

The tendency for the relative variability to decrease with increasing mean rainfall and with the length of observation period is illustrated in Figure 10. This figure shows the isohyetal maps for storm, weekly, monthly, and seasonal (June-

August) rainfall during the summer of 1951 on the Panther Creek network. In the illustration, \bar{P} is the mean rainfall and CV is the coefficient of variation.

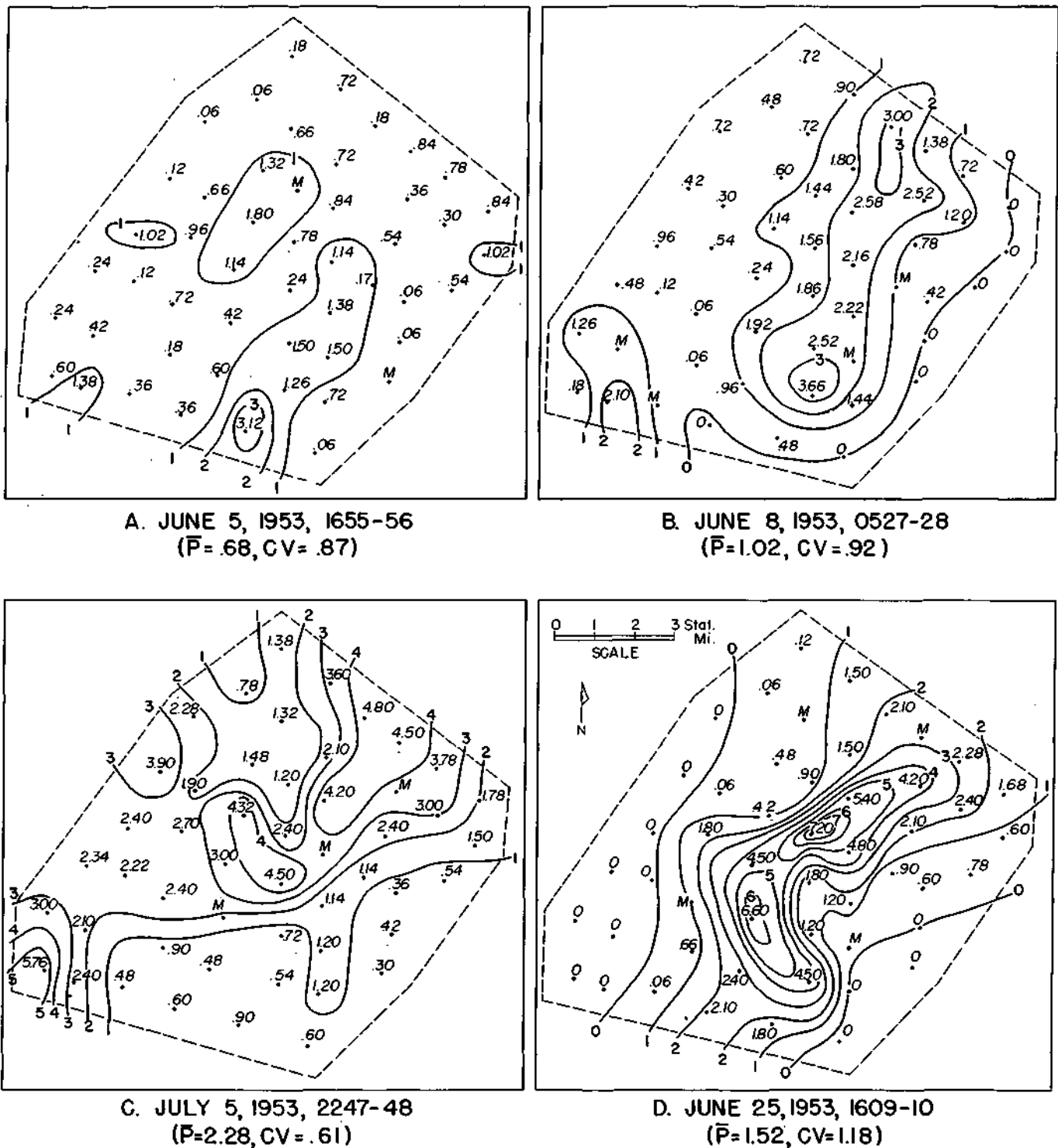
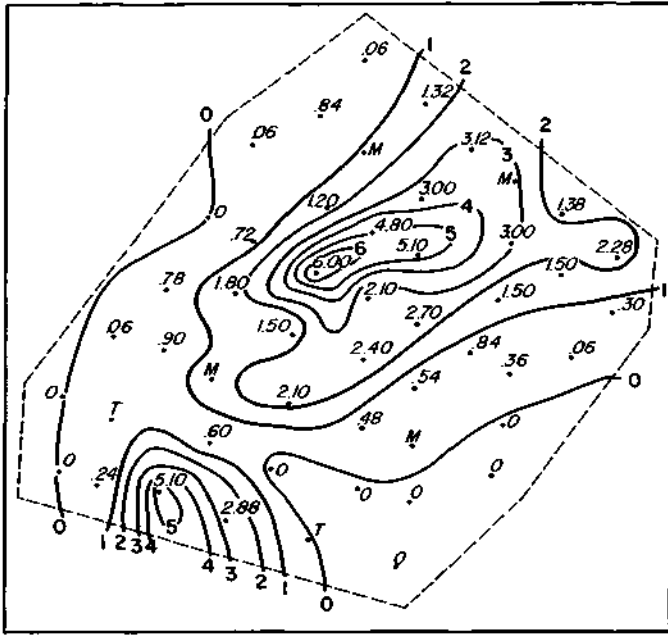


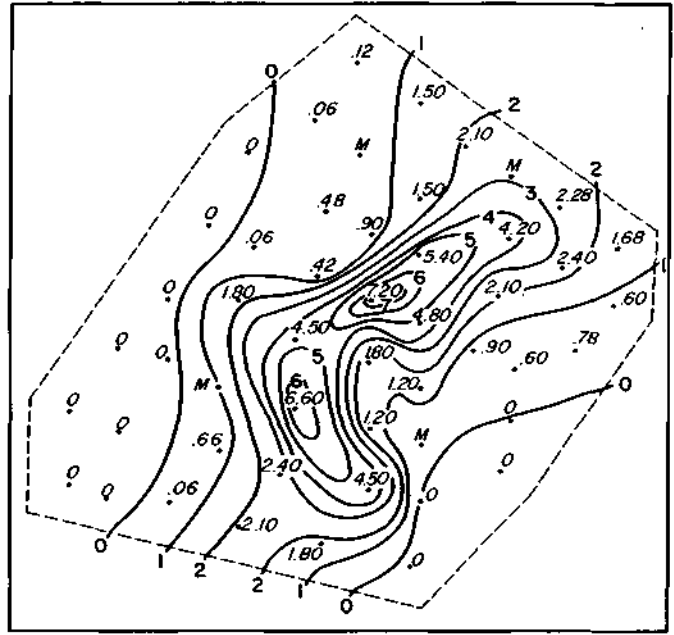
FIGURE 11 ONE-MINUTE MEAN RATES

Figure 11 shows some examples of relative variability in thunderstorms when mean rainfall is calculated on a very short time basis. The four isohyetal maps are for one-minute periods measured on the Goose Creek network during 1953, using special recording rain gages (see previous section and Figure 4). Isohyetal values in Figure 11 represent one-minute amounts expressed in rainfall rate in inches per hour. \bar{P} represents the mean rainfall rate and CV the coefficient of variation. Since the

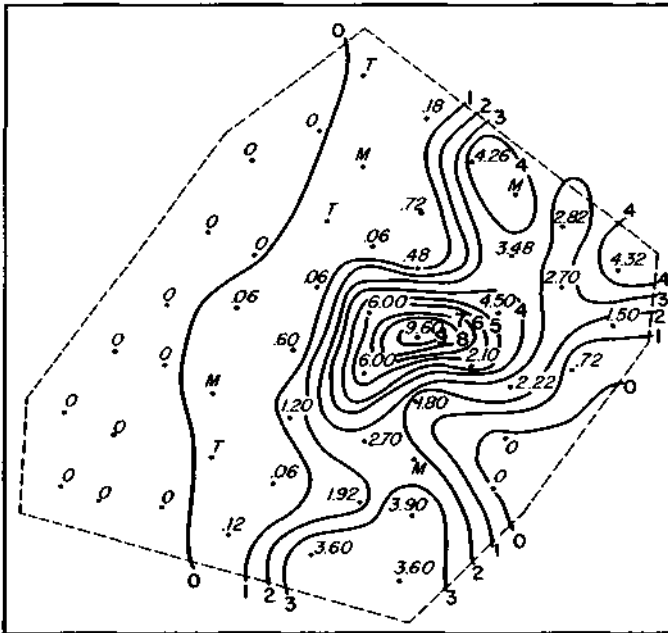
rainfall values on the maps represent nearly instantaneous values, the isohyetal patterns are approximately representative of the instantaneous pattern of rainfall within thunderstorms. The great variability existing in the internal structure of thunderstorms is apparent and helps explain the great variability observed in total storm rainfall in thunderstorms and the scatter in the coefficient of variation shown in Figure 9.



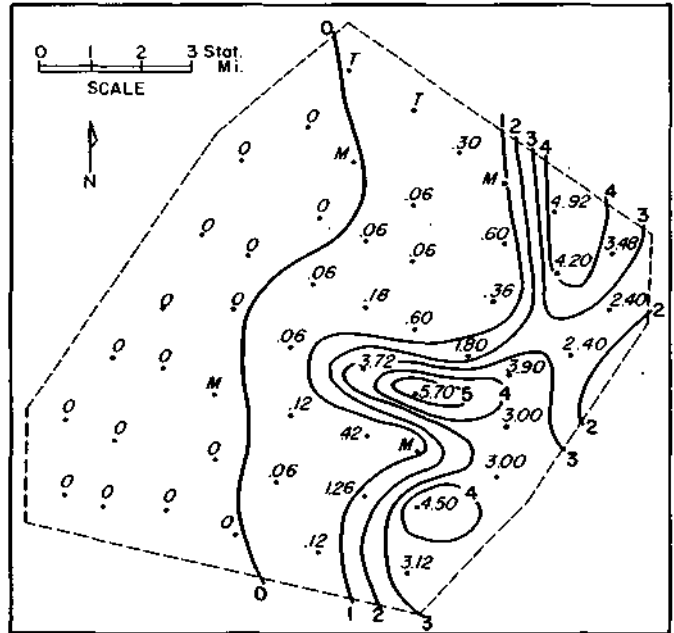
A. 1605-06 CST



B. 1609-10 CST



C. 1613-14 CST



D. 1617-18 CST

FIGURE 12 TIME VARIATIONS IN RAINFALL PATTERN

Figure 12 is a series of one-minute isohyetal maps spaced four minutes apart in an intense thunderstorm and illustrates the rapid changes which may take place in the internal structure of thunderstorms.

The effects of storm rainfall variability will be discussed in the section on area-depth curves, where its application to hydrologic analysis and design will be shown.

Effect of Gage Density on Maximum Recorded Point Rainfall

The peak rainfall occurring within basin storms is a useful factor in hydrologic analysis. Obviously, the maximum recorded rainfall in shower-type storms is closely related to the gage density on a given basin.

Using rainfall data collected from 70 storms on the Panther Creek Basin during 1948-50, a study was made of the effect of gage density on the observed maximum point rainfall within an area. To study this effect, point rainfall recorded at the most centrally-located station in the 100-square mile basin was compared with the maximum point rainfall obtained by increasing the network progressively to 3, 5, 10, and 20 gages. These networks, corresponding to gage densities of 33, 20, 10, and 5 square miles per gage, were chosen to give the most uniform distribution of gages possible.

For each of the four gage densities in each storm, the ration of network maximum to single gage amount was determined from the rain-gage charts. These data were then grouped, based upon class intervals for single gage rainfall of 0.01 - 0.20, 0.21 - 0.50, 0.51 - 1.00 and 1.01 - 2.00 inches. The grouped data were then used to obtain an empirical relation between network maximum rainfall, single gage rainfall, and gage density. The empirical equation obtained is

$$\frac{R_m}{R_s} = 2.5 G^{-.20} \quad (2)$$

where R_m is the maximum recorded point rainfall (in.), R_s is the central gage amount (in.) and G is the gage density (sq. mi./gage). The developed relation is illustrated in Figure 13.

Reference to Figure 13 shows the expected trend for the maximum recorded point rainfall to increase significantly as the gage density decreases (number of gages increases). The average

ratio of maximum recorded to central gage rainfall was found to increase from 1.15 at a gage density of 50 square miles per gage to 1.38, 1.58 and 1.83 at gage densities of 20, 10 and 5 square miles per gage, respectively.

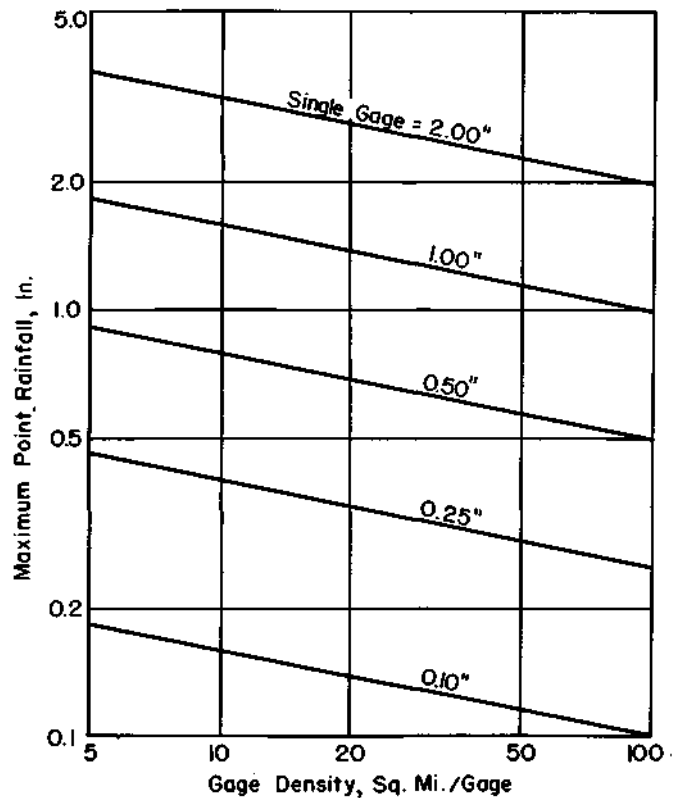


FIGURE 13 EFFECT OF GAGE DENSITY ON MAXIMUM RECORDED POINT RAINFALL

FREQUENCY OF POINT AND AREAL MEAN RAINFALL RATES

Introduction

During 1952-53, one minute rainfall totals for a number of storms were tabulated in conjunction with a project concerned with the investigation of the utility of radar for quantitative rainfall measurements.⁽²⁾ Use of special recording rain gages with 12.6 -inch diameter orifices and six-hour charts enabled recording of one-minute amounts over an area of 100 square miles. Information on the distribution of rainfall rates within storms should be of interest to hydrologists, especially to those concerned with sedimentation. Areal distributions of one-minute rates, which closely approximate the actual pattern of rainfall rates within storms, are pertinent in studying the physical structure of storms. Information on short-period rates is also valuable in evaluating radar for quantitative precipitation measurements and other meteorological uses, since precipitation attenuation is proportional to the rainfall rates within a storm, and attenuation presents an outstanding problem in applying radar to the measurement of rainfall intensity.⁽³⁾ Consequently, an analysis was made of the frequency of occurrence of point and areal mean rainfall rates. The available data were restricted to shower-type rainfall occurring during the thunderstorm season from late spring to early fall.

Data Used in Analysis

One-minute rainfall amounts from 19 storms during 1952-53, tabulated in conjunction with the

radar-rainfall project mentioned previously, were used in the study. The one-minute amounts were obtained from 50 recording gages located on the 100-square mile Goose Creek Network (Fig.4).* The distribution of gages on the network was approximately uniform, the uniformity being limited only by existing road systems and suitable exposures. The network terrain is relatively flat with no distinct topographic features to influence storm behavior.

Careful attention was given to synchronizing the gages so that one-minute rainfall patterns and areal means could be reliably represented. All clocks were checked for accurate timing before installation each spring. Before proceeding to the network to change charts, observers synchronized their watches with a master clock, which was checked daily with time signals from radio station WWV, the National Bureau of Standards Station at Washington, D.C. When installing and removing charts from the drum, the observer made a vertical time check mark with the pen on the chart and entered the exact "on" or "off" time from his watch. Charts were changed after each storm and twice a week during periods of no rain to minimize any clock timing errors. When a rain-gage record indicated the gage clock had gained or lost a small amount of time, the error was prorated over the period of record. As a further check, after isohyetal maps were plotted for each minute of a storm, gage charts were reexamined if doubtful values appeared at any stations on a one-minute map.

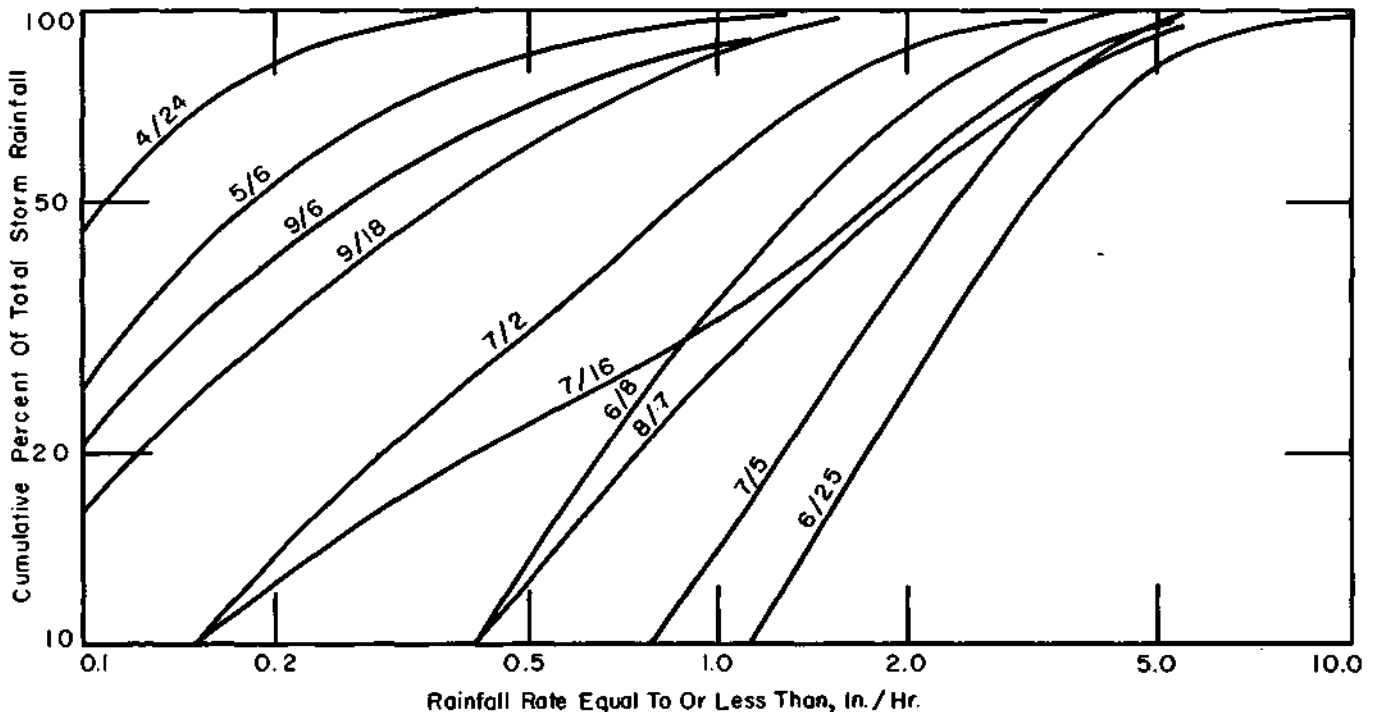


FIGURE 14 DISTRIBUTION OF POINT RAINFALL RATES IN INDIVIDUAL STORMS

*Operation of the network and data reduction were sponsored in part by the Signal Corps Engineering Laboratories, Belmar, New Jersey under contract DA-36-039 SC-42446

Frequency of Point Rainfall Rates

The frequency with which various point rainfall rates occurred in each storm was calculated first, using the data from all 50 gages. Figure 14 shows cumulative frequency curves for the ten 1953 storms. The graph shows cumulative percentages plotted against rainfall rate in inches per hour, based upon one-minute amounts from all 50 gages. For example, in the storm for July 2, 50 per cent of the rainfall occurred at rates exceeding 0.90 inch per hour, while for the storm of June 25, 50 per cent of the total rainfall occurred at rates exceeding 3.10 inches per hour.

Examination of the 19 storms indicated that the group should be approximately representative of conditions experienced during the warm season in the Midwest. Consequently, the data were combined to determine the frequency of point rainfall rates under average conditions during a warm season. Results of this analysis are shown in columns 1 and 2 of Table 4. It will be noted that on the average, based on one-minute rates in the 19-storm sample, 50 per cent of the warm season rainfall occurs at rates exceeding 1.45 inches per hour. However, the median rate in individual storms in the 19-storm sample was highly variable, ranging from 0.10 to 3.10 inches per hour.

For comparison purposes, the per cent of total storm rainfall occurring at various rainfall rates when these rates are based on 5-, 10-, 15-, and 30-minute summation periods was determined. Obviously, the averaging process suppresses details of the high rates occurring during the averaging period. Most studies in the past, such as those of Yarnell⁽⁴⁾ and the U.S. Weather Bureau⁽⁵⁾ on which engineering design has been based, were calculated on the basis of periods from five minutes upward. Hydrologists have found that rainfall rates for periods less than 10 to 15 minutes seldom have practical significance with respect to runoff from a drainage area. However, as mentioned previously, shorter period rates have application in sedimentation studies, in gaining an understanding of the physical structure of storms, and in the evaluation of radar for meteorological purposes. In the present study, an attempt was made to ascertain the effect of the averaging process on the observed frequency of rainfall rates.

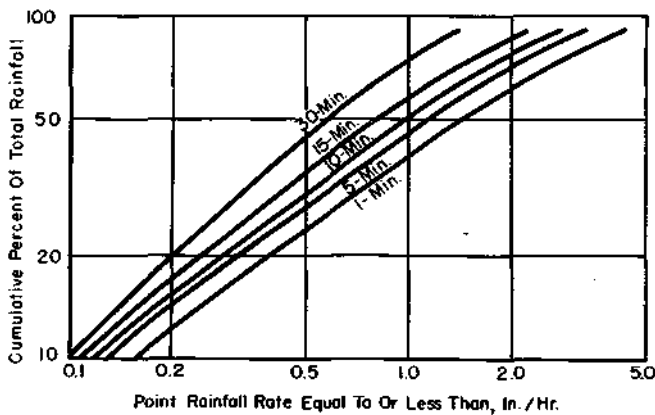


FIGURE 15 DISTRIBUTION OF POINT RAINFALL RATES DURING AVERAGE SEASON

TABLE 4

FREQUENCY OF POINT RAINFALL RATES CALCULATED FROM DIFFERENT BASE PERIODS

Rainfall Rate (in/hr) Equaled or Exceeded For Several Base Periods (Min.)

Cumulative Per Cent	1	5	10	15	30
Max.	13.80	7.50	5.72	4.20	2.45
5	5.35	4.10	3.25	2.64	1.62
10	4.20	3.35	2.80	2.34	1.41
20	3.25	2.58	2.13	1.93	1.15
30	2.45	2.02	1.75	1.42	0.88
40	1.90	1.52	1.34	1.07	0.69
50	1.45	1.16	0.97	0.82	0.56
60	1.05	0.83	0.70	0.62	0.44
70	0.68	0.54	0.46	0.41	0.33
80	0.37	0.28	0.25	0.23	0.21
90	0.15	0.12	0.11	0.11	0.10
95	0.08	0.07	0.07	0.07	0.06

Per Cent of 1-Min. Rate for Several Periods (Min.)

Cumulative Per Cent	5	10	15	30	
Max.		54	41	30	18
5		77	61	49	30
10		80	67	56	34
20		79	66	59	35
30		82	71	58	36
40		80	71	56	36
50		80	67	57	39
60		79	67	59	42
70		79	68	60	48
80		76	68	62	57
90		80	73	73	67
95		87	87	87	75

Results are illustrated in Figure 15 and Table 4. In Table 4 (upper part) it is seen that when one-minute totals are used, 50 per cent of the rain was found to occur at rates exceeding 1.45 inches per hour. When a five-minute base period was used, the 50 per cent value dropped to 1.16 inches per hour and then to 0.97 inch per hour for a 10-minute base period, 0.82 inch per hour for a 15-minute base period, and 0.56 inch per hour for a 30-minute base period. Also, in Table 4 note the rapid decrease in the maximum observed rainfall rate when this rate is based on various averaging periods. The averaging effect is further illustrated in the lower part of Table 4, where the longer period values have been expressed as percentages of the one-minute values.

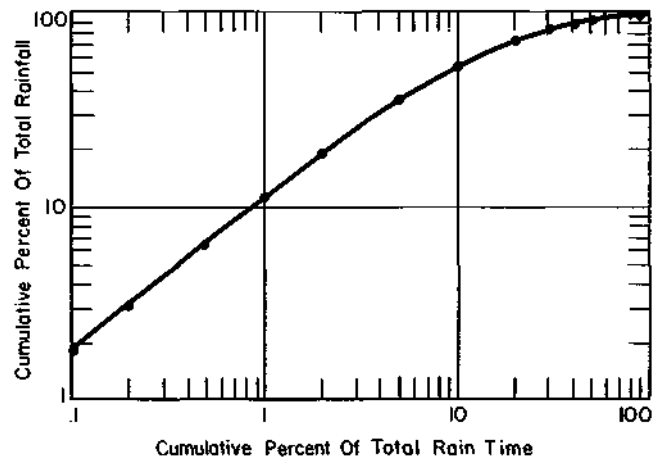


FIGURE 16 TIME DISTRIBUTION OF POINT RAINFALL

The time distribution of point rainfall was studied next, combining data from all 19 storms. Results of this analysis are shown in Figure 16 where per cent of total time of rainfall in the 19 storms has been plotted against per cent of total rainfall in these storms. From this curve it is seen that 10 per cent of the season rainfall, based on the 19-storm sample, occurs in approximately one per cent of the time it is raining, 50 per cent of the rain occurs during about 9 per cent of the time that rain is falling, and 90 per cent of the total rain occurs in 50 per cent of the time that it is raining. Thus, it is apparent that warm season rainfall tends to occur in strong bursts within a storm period; that is, most of the rain tends to occur in a small portion of the storm.

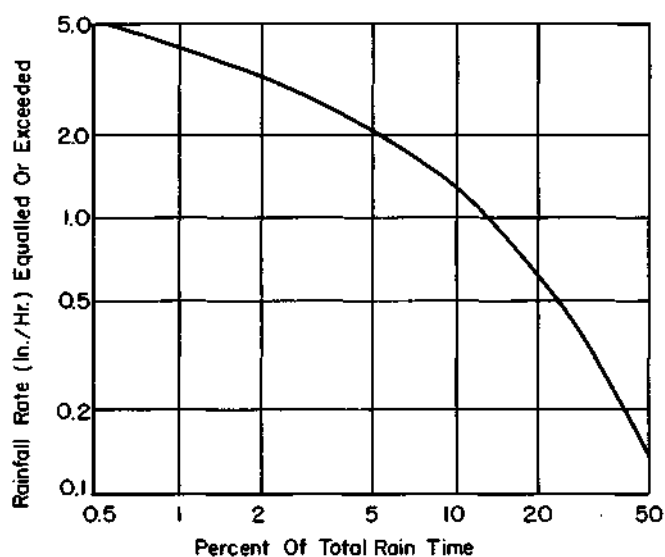


FIGURE 17 POINT RAINFALL TIME-RATE RELATION

Figure 17 shows a time-rate relation for point rainfall derived from the combined data for the 19 storms. This graph further emphasizes the burst nature of shower-type rainfall. Reference to Figure 17 shows that rates equalling or exceeding 1.45 inches per hour, which accounted for 50 per cent of the total rainfall according to Figure 15, occurred only 9 per cent of the time it was raining. Similarly, rates exceeding 4.25 inches per hour occurred only one per cent of the time rain was falling, while rates exceeding 0.14 inch per hour were recorded during 50 per cent of the time it was raining.

Frequency of Areal Mean Rainfall Rates

The foregoing discussion has been concerned with the frequency of point rainfall rates. Often, hydrologists are more concerned with areal than with point relationships. Consequently, data from the 50-gage network on the 100-square mile area were further analyzed to obtain areal frequency relationships. For this purpose, the 100-square

mile network was subdivided to give areas of 10, 25, and 50 square miles for comparisons with areal mean storm rainfall relations on the 100-square mile network. One-minute areal mean rates were calculated for each minute in each storm for each of the areas mentioned above.

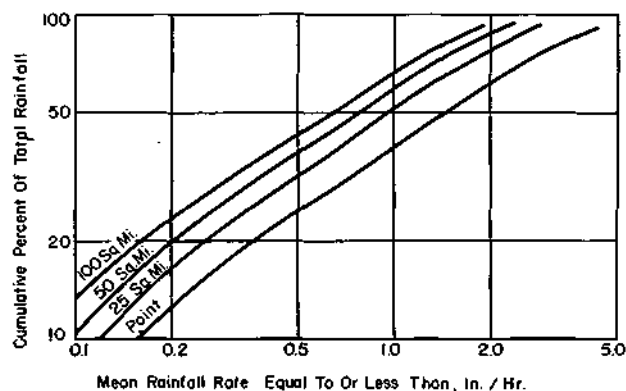


FIGURE 18 DISTRIBUTION OF AREAL MEAN RAINFALL RATES

All 19 storms were combined to obtain average relationships for the various areas. The results are summarized in Tables 5 and 6 and Figure 18. Reference to Table 5 shows the expected trend. For example, 50 per cent of the point rainfall was found to occur at a rate exceeding 1.45 inches per hour, while 50 per cent of the areal mean rainfall occurred at rates of 1.02, 0.96, 0.78 and 0.66 inches per hour, respectively, for the 10-, 25-, 50-, and 100-square mile areas. Table 6 illustrates the variation in the time distribution of rainfall rates as the area is increased. For example, 50 per cent of the point rainfall was found to occur during 9 per cent of the time it was raining. At 25 square miles, 50 per cent of the areal mean rainfall occurred in 11 per cent of the time, while for 100 square miles 50 per cent occurred in 12 per cent of the rain time. This table shows a tendency for the time distribution to change only very slowly with increasing area.

Discussion of Results

Although the results in this study are based upon a relatively small sample, the variety of storms incorporated in the 19-storm sample should make the results approximately representative of average warm season conditions. It would have been desirable to have included more storms; however, the great amount of hand tabulation required did not permit it. It is hoped that the results will prove useful in evaluating the actual distribution of rainfall rates in warm season rainfall in Illinois and the Midwest. At the present time, machine processing of the rain-gage charts is being investigated, and if it is feasible, the present investigation can be greatly expanded since a large amount of unprocessed data are available which were collected from 1951-54.

TABLE 5
FREQUENCY OF AREAL MEAN RAINFALL RATES

Cumulative Per Cent of Rainfall	Point	Rainfall Rate (in/hr) Equaled or Exceeded for Given Area (Mi. ²)				Per Cent of Point Rate				
		<u>10</u>	<u>25</u>	<u>50</u>	<u>100</u>	<u>10</u>	<u>25</u>	<u>50</u>	<u>100</u>	
Max.	13.80	4.08	4.02	3.18	2.88	30	29	23	21	
5	5.50	3.48	2.82	2.52	2.40	63	51	46	44	
10	4.20	3.18	2.55	2.22	1.86	76	61	53	44	
20	3.25	2.28	2.22	1.74	1.35	70	68	54	42	
30	2.45	1.80	1.77	1.32	1.11	73	72	54	45	
40	1.90	1.26	1.26	1.02	0.90	66	66	54	47	
50	1.45	1.02	0.96	0.78	0.66	70	66	54	46	
60	1.05	0.72	0.72	0.54	0.48	69	69	51	46	
70	0.68	0.48	0.48	0.36	0.28	71	71	53	41	
80	0.37	0.25	0.26	0.18	0.16	68	70	49	43	
90	0.15	0.11	0.12	0.10	0.08	73	80	67	53	
95	0.08	0.07	0.07	0.05	0.04	87	87	62	50	

TABLE 6
TIME DISTRIBUTION OF AREAL MEAN
RAINFALL RATES

Area (Mi.)	Per Cent of Total Rain Time Accounting for Given Per Cent of Total Rainfall				
	<u>10</u>	<u>25</u>	<u>50</u>	<u>75</u>	<u>90</u>
Point	1	3	9	25	48
10	1	3	10	26	51
25	1	4	11	27	53
50	1	4	12	28	55
100	1	4	12	30	58

AREA-DEPTH RELATIONS

Introduction

For engineering design purposes, a knowledge of detailed area-depth relations for small areas is often essential. Few detailed data for areal units under 300 square miles have been published. Rain-gage networks of sufficient density to define area-depth relations accurately from isohyetal maps for such small areas are uncommon. While publications of the Miami Conservancy District⁽⁶⁾ and the U.S. Corps of Engineers⁽⁷⁾ include data on small watersheds, the data are based on relatively sparse spacing of rain gages. The concentrated networks employed in this study were designed for collecting more precise data.

To obtain detailed information on the characteristics of the area-depth curve for small watersheds, thunderstorm and rainshower data collected on four densely-gaged networks in central Illinois have been analyzed. These three networks consist of the 280-square mile El Paso network (Fig. 2), the 100-square mile Panther Creek (Fig. 3) and Goose Creek (Fig. 4) networks, and the Boneyard Creek network of 5.5 square miles (Fig. 6). The necessity for concentrated networks, which can be used to obtain detailed isohyetal patterns and thereby minimize interpolation errors in the construction of area-depth curves, is illustrated by the series of isohyetal maps in Figure 19. These maps were drawn for the same storm on the 100-square mile Panther Creek watershed using the various gage densities indicated.

Analysis and Results

Most previous investigations of area-depth relations have been concerned with relatively large watersheds, employing less dense networks than those utilized in this study. It has been observed that area-depth curves derived from isohyetal maps sometimes approach straight lines or flat curves when the logarithm of area is plotted against average rainfall.⁽⁸⁾ This often results from a liberal envelopment of points. Curved lines were obtained with the Illinois area-depth data in most cases by plotting the data on semi-logarithmic paper with depth on the linear scale and area on the logarithmic scale.

Since a straight-line representation is desirable, several hypotheses were investigated in an effort to obtain an easily computed straight-line relation. Within the limits tested for the four small areas, it was found that the data conformed closely to the general equation⁽⁹⁾

$$Y = a + b X^{1/2} \quad (1)$$

where Y is average rainfall depth in inches, X is the area enveloped in square miles, and a and b are constants representing maximum storm point rainfall and mean rainfall gradient, respectively.

The area-depth curve is a two-dimensional representation of rainfall distribution over area, in which values of average rainfall within an isohyet are plotted against the area enveloped. The area-

depth curve is constructed as though the highest value of rainfall occurred at one point, and lower values appeared (in an isohyetal representation) roughly concentrically around the higher values.

Chow⁽¹⁰⁾ has pointed out that Equation (1) indicates that the three-dimensional representation of the rainfall isohyets, which he calls the "storm pile," of thunderstorms or rainshowers is very close to the form of a cone. He indicated that additional terms of higher orders of X' must be considered when the straight-line relationship of the depth plotted against the square root of the area does not apply to storms covering larger areas, that is more than 300 square miles.

Within the "storm pile," point rainfall is also linearly related to the distance from the center of the storm as represented by the following equation

$$y = A + Br \quad (2)$$

where y is the point rainfall at a distance, r, from the center of the storm, and for a given storm, A and B are constants, representing maximum point rainfall and point rainfall gradient. Analysis⁽¹¹⁾ has shown that A = a in Equation (1) and b = 0.376B, so that

$$Y = A + 0.376B X^{1/2} \quad (3)$$

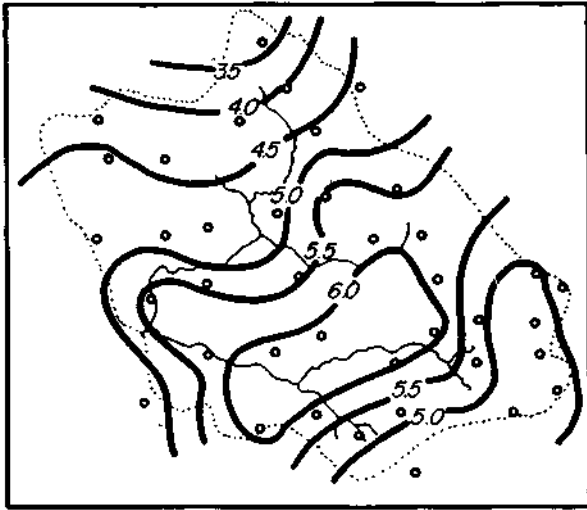
Equations (1) to (3) can be used to construct hypothetical area-depth curves for design purposes on small basins, when the maximum point rainfall of the storm center can be obtained from frequency data, such as those obtained by Yarnell,⁽⁴⁾ provided that the rainfall gradient or mean rainfall on the basin can be estimated from a local rain-gage network. Development of a relationship for rainfall gradient will be discussed later.

Equation (1) was tested on storms ranging from one to 24 hours duration on the four areas. Only storms in which the areal mean rainfall equaled or exceeded 0.50 inch were used. These included 126 storms on the two 100-square mile networks, 72 on the 5.5-square mile area, and 19 on the 280-square mile network. Results for the heaviest storms in each area are illustrated in Figures 20-22.

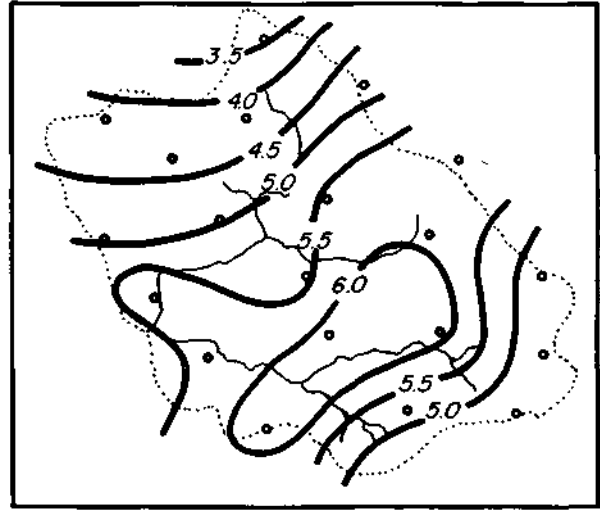
To make the area-depth relation developed in Equation (1) more applicable for engineering design purposes, data from the 5.5- and 100-square mile areas were analyzed further to determine the relationship between the curve slope (rainfall gradient) and other storm parameters. Analysis was not accomplished for the 280-square mile area due to the limited data available. Examination of the data for the two smaller areas indicated that the best fit would be obtained with a relationship of the form

$$b = K P^1 T^m \quad (4)$$

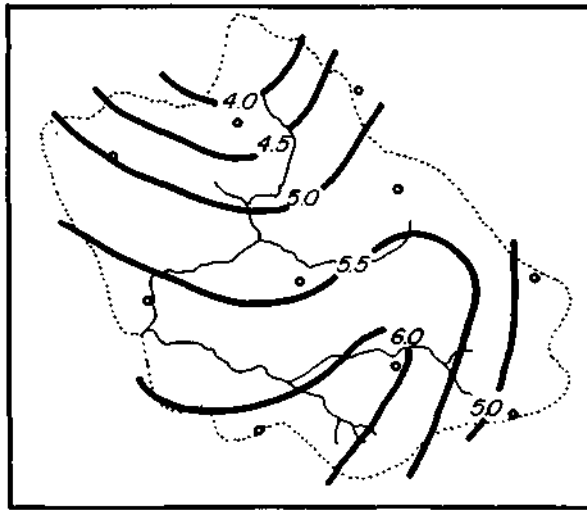
where b is the mean rainfall gradient in Equation (1), P is areal mean rainfall, T is storm duration, and K, 1, and m are constants.



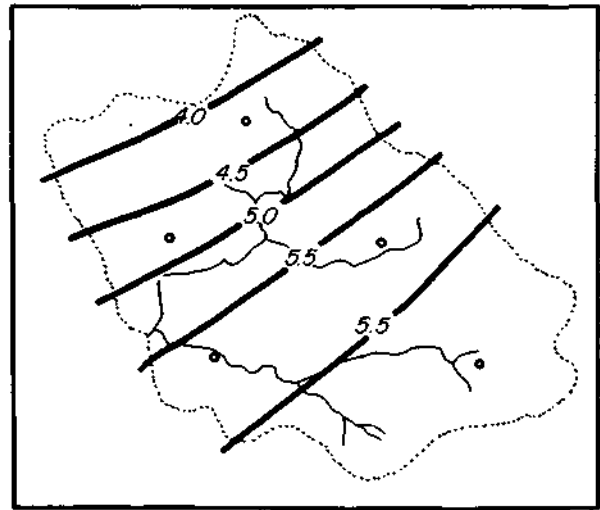
2.4 sq.mi. per gage



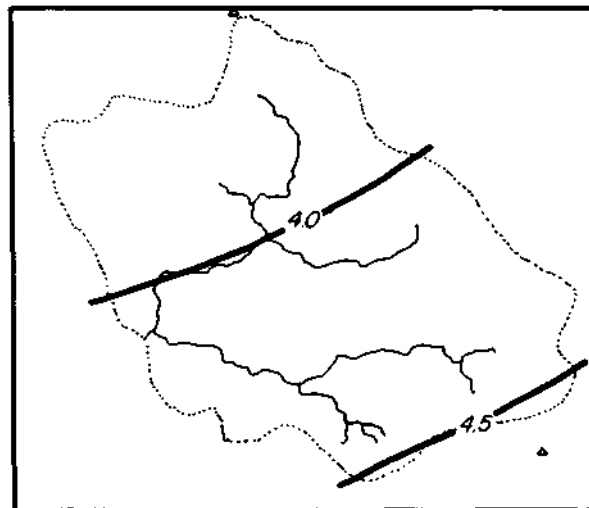
4.75 sq. mi. per gage



9.5 sq.mi. per gage



19.5 sq. mi. per gage



U.S. Weather Bureau Climatological Network, 225 sq. mi. per gage.

FIGURE 19 EFFECT OF GAGE DENSITY ON ISOHYETAL PATTERN

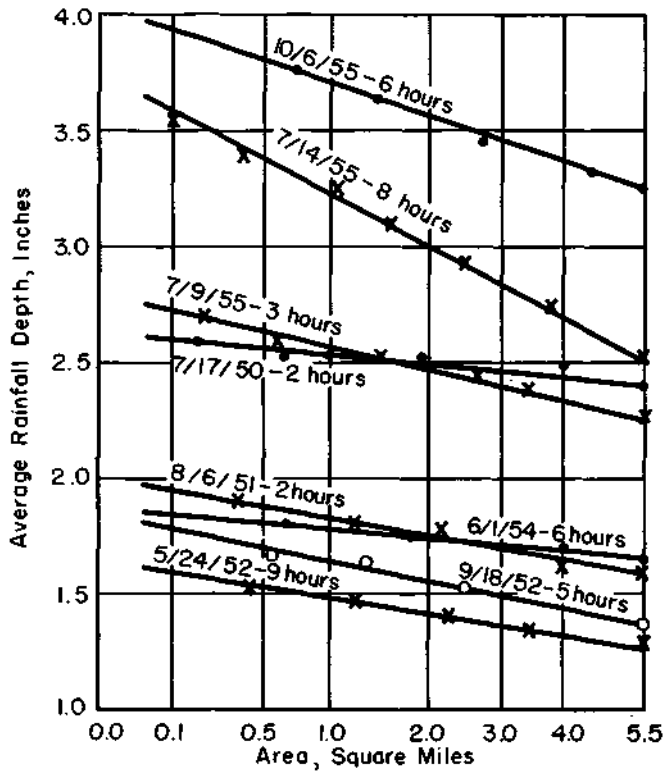


FIGURE 20 AREA-DEPTH RELATIONS FOR HEAVIEST STORMS, 5.5 SQUARE MILE AREA

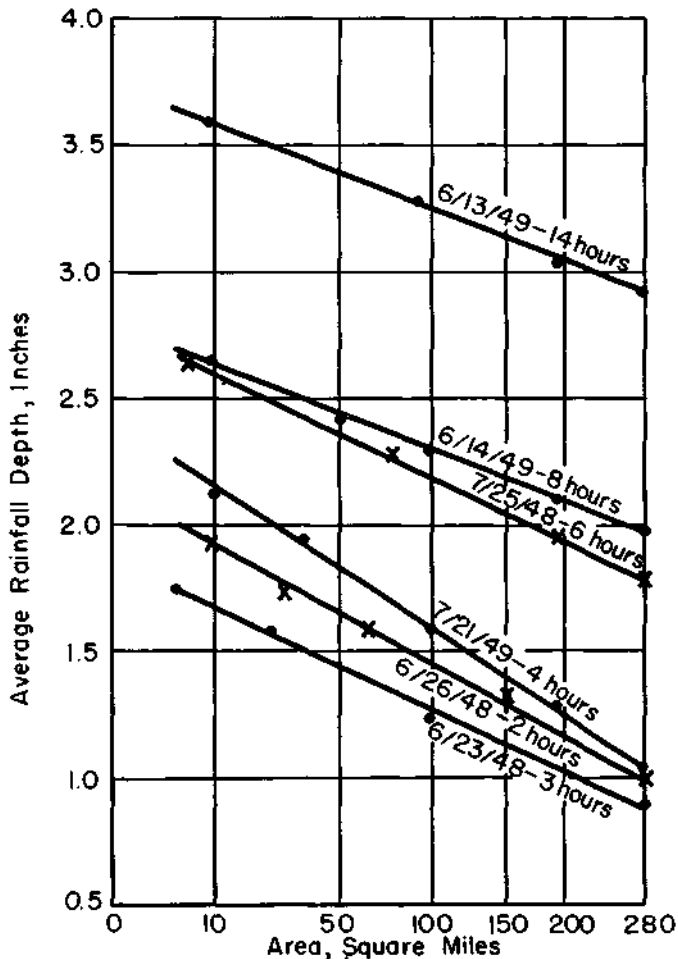


FIGURE 22 AREA-DEPTH RELATIONS FOR HEAVIEST STORMS, 280 SQUARE MILE AREA

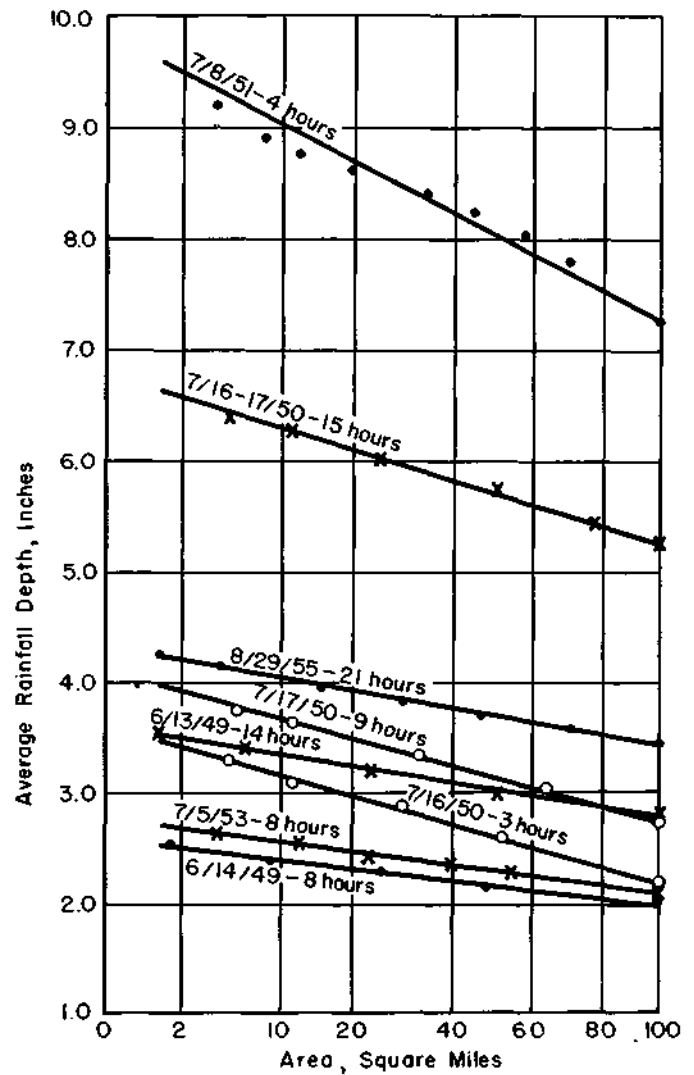


FIGURE 21 AREA-DEPTH RELATIONS FOR HEAVIEST STORMS, 100 SQUARE MILE AREA

Results of this study yielded Equations (5) and (6) for the 100- and 5.5-square mile basins, respectively,

$$b = 0.094 \quad P^{.83} \quad T^{-.28} \quad (5)$$

$$b = 0.169 \quad P^{.89} \quad T^{-.15} \quad (6)$$

As expected, the data indicated considerable variability in the rainfall gradient among storms of similar mean rainfall and duration. Obviously, there are other factors in addition to storm size and storm duration, that are not easily reduced to mathematical expression, which affect the calculated rainfall gradient within storms. For example, the area-depth curve for a given basin will be influenced by the location of the storm core with respect to the basin, movement of the storm with respect to the axis of the basin, and the internal structure of the storm. A multiple correlation coefficient of 0.65 was obtained from Equation (5) and a coefficient of 0.55 for Equation (6). These relatively low coefficients reflect the high variance of the data.

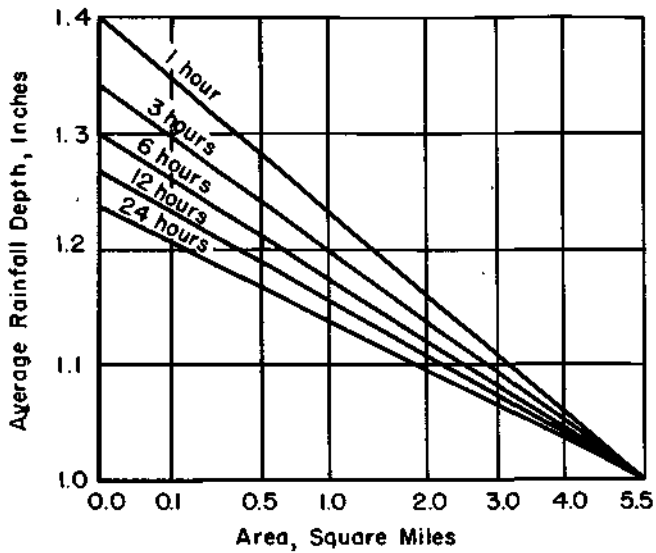


FIGURE 23 AVERAGE AREA-DEPTH RELATIONS, 5.5 SQUARE MILE AREA, MEAN RAINFALL = 1.00 INCH

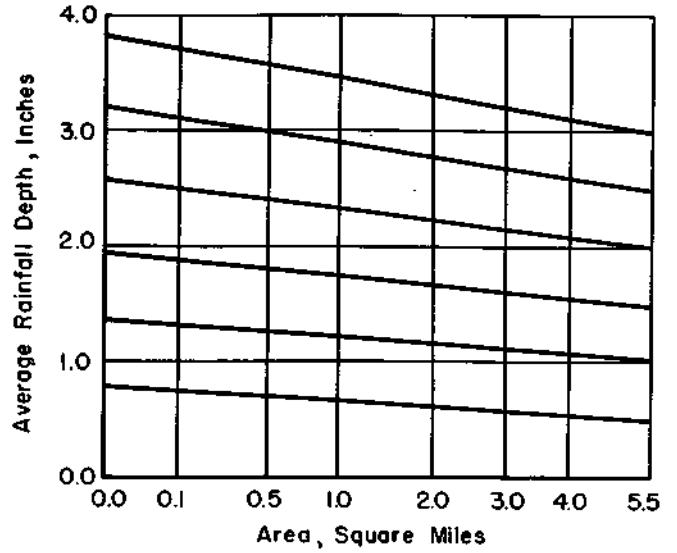


FIGURE 25 AVERAGE AREA-DEPTH RELATIONS, 5.5 SQUARE MILE AREA, 6-HOUR STORM DURATION

Applying the relations for the curve slope or rainfall gradient in Equations (5) and (6) to Equation (1), average area-depth relations were developed for the two areas and are illustrated in Figures 23 to 26. Figures 23 and 24 show average area-depth relations for various storm durations based on an areal mean rainfall of one inch. Figures 25 and 26 show average area-depth relations for storms of various magnitude (mean rainfall) for a storm duration of six hours. Obviously, the developed equations can be used in calculations for other storm sizes and durations.

All data for both areas are for storm durations up to 24 hours; consequently, their curves should not be used for longer period storms. It should also be pointed out that the mean rainfalls tested for the 5.5-square mile area did not exceed 3.5 inches. Except for two storms, all storms observed on the 100-square mile networks had less than 5-inch means. Consequently, upper limits of 3-inch and 4-inch means have been used in Figures 25 and 26.

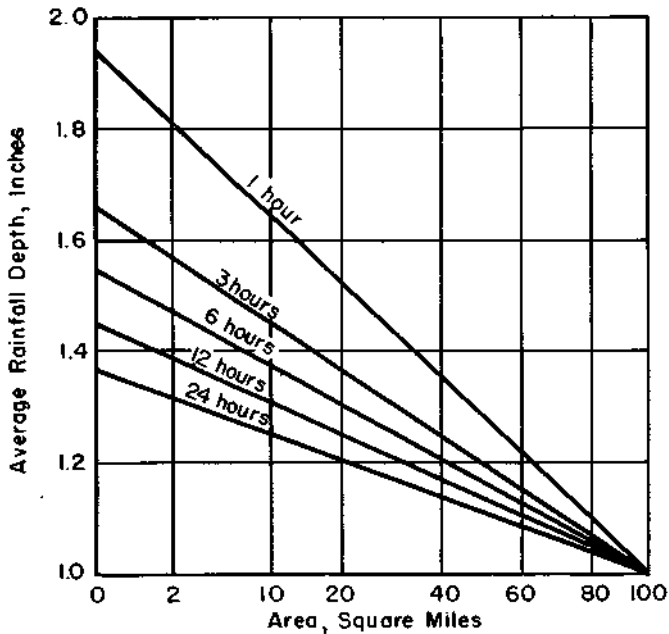


FIGURE 24 AVERAGE AREA-DEPTH RELATIONS, 100 SQUARE MILE AREA, MEAN RAINFALL = 1.00 INCH

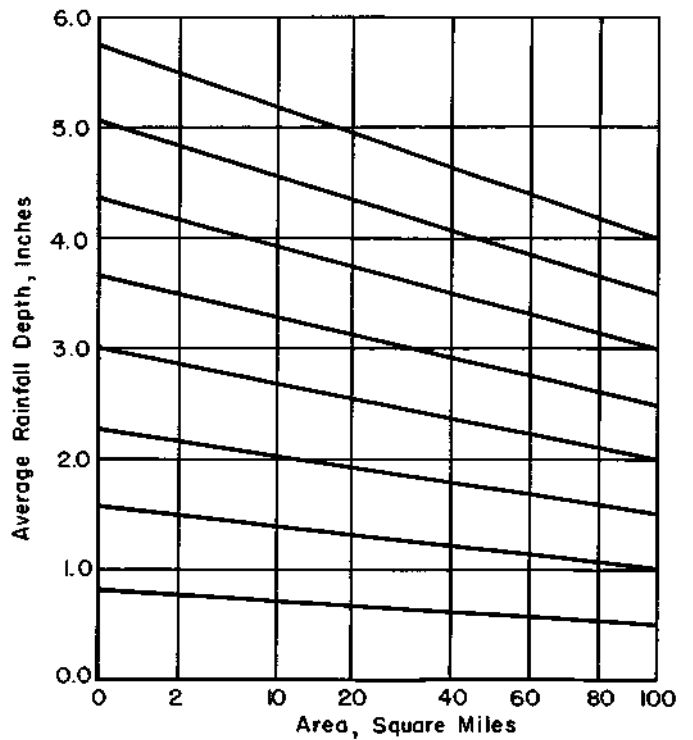


FIGURE 26 AVERAGE AREA-DEPTH RELATIONS, 100 SQUARE MILE AREA, 6-HOUR STORM DURATION

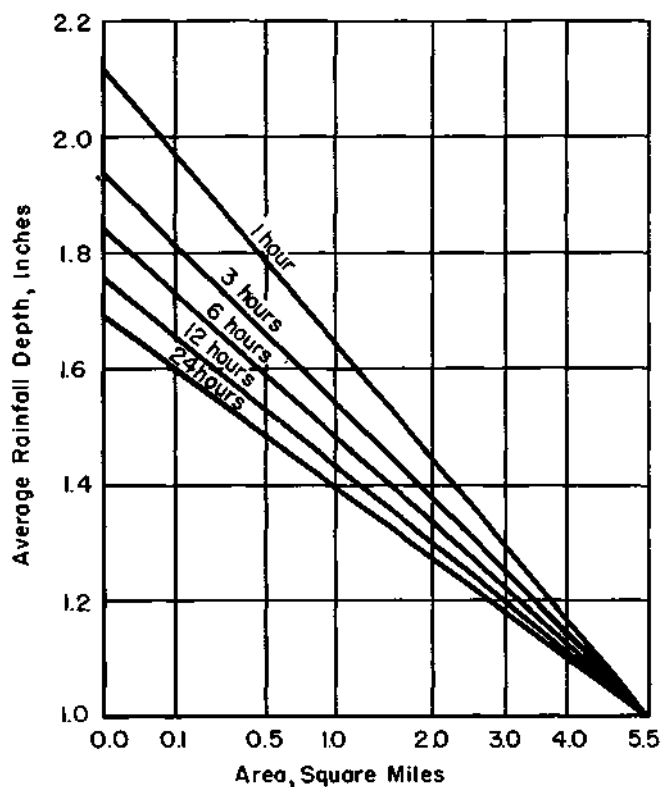


FIGURE 27 EXTREME AREA-DEPTH RELATIONS, 5.5 SQUARE MILE AREA, MEAN RAINFALL = 1.00 INCH

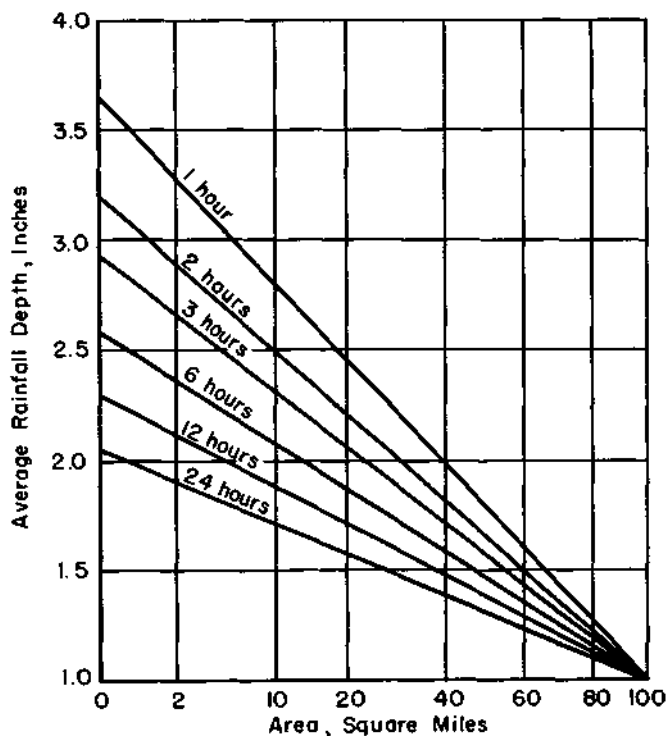


FIGURE 28 EXTREME AREA-DEPTH RELATIONS, 100 SQUARE MILE AREA, MEAN RAINFALL = 1.00 INCH

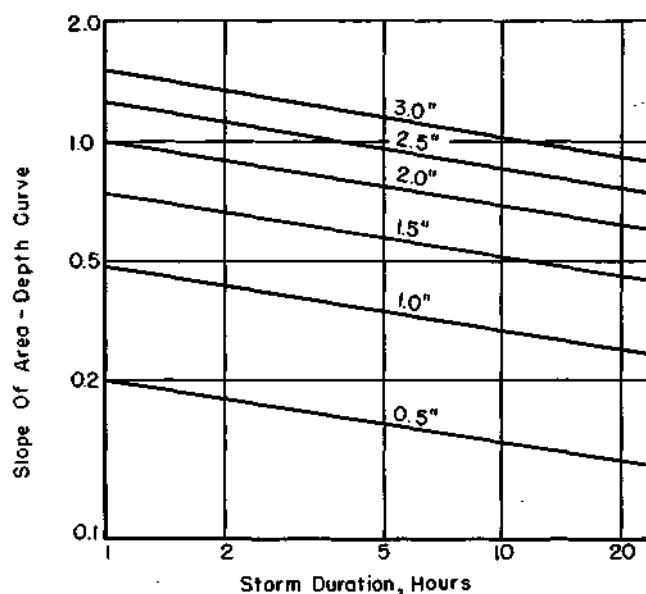


FIGURE 29 EXTREME AREA-DEPTH CURVE SLOPES, 5.5 SQUARE MILE AREA, SELECTED AREAL MEAN RAINFALLS

The curves in Figures 23 to 26, of course, are for average values of rainfall gradient (curve slope). For both Equations (5) and (6), 95 per cent confidence bands were determined. The upper 95 per cent confidence band in both cases has been used in Figures 27 and 28 to show extreme area-depth relations for the two basins with a mean rainfall of one inch. Figures 29 and 30 show extreme curve slopes for durations of 1 to 24 hours and for various mean rainfalls. These figures may be used in conjunction with Equation (1) to obtain

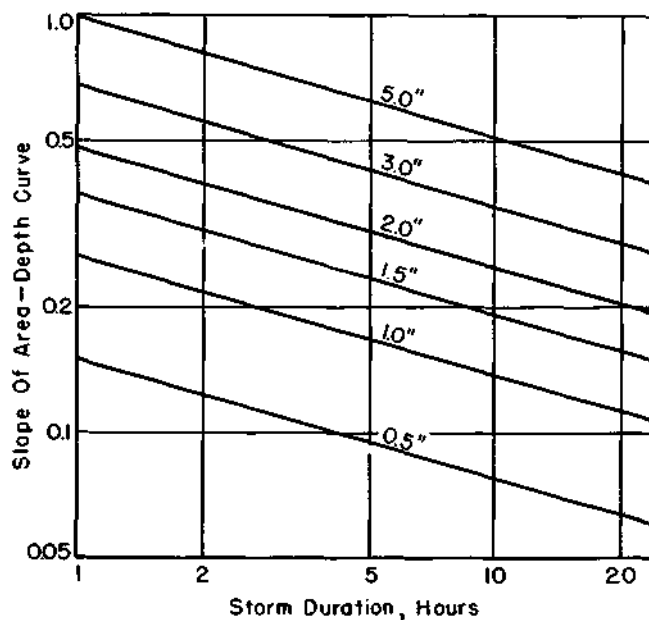


FIGURE 30 EXTREME AREA-DEPTH CURVE SLOPES, 100 SQUARE MILE AREA, SELECTED AREAL MEAN RAINFALLS

extreme area-depth curves under various conditions. Whether average or extreme values should be used depends upon the purpose for which area-depth relations are to be utilized. Again, the large differences between the average curves in Figures 23-24 and the extreme curves in Figures 27-28 result from the large variability in rainfall gradients among storms of similar size and duration.

In Equations (5) and (6) for the slope of area-depth curves, it is interesting to note the relative weight of the two parameters, mean rainfall and storm duration. The relative importance of mean rainfall is greater in the equations for both basins as illustrated by the exponents on P and T. Results indicate that, as the area decreases, storm duration becomes less important in determining rainfall gradients within the basin. Characteristics of the storm passing over the basin are perhaps of greatest importance here.

The relative weights of P and T in determining the characteristic of the area-depth curve are further illustrated in Table 7 where partial correlation coefficients between b and P and between b and T are given for the two areas.

TABLE 7
CORRELATION COEFFICIENTS

Type	Items	Basin Areas	
		5.5 Sq. Mi.	100 Sq. Mi.
Partial	b vs. P	0.45	0.60
Partial	b vs. T	0.21	0.38
Multiple	b vs. P, T	0.55	0.65

While the results of the area-depth study are based on Illinois data, the relations should be generally applicable to shower-type rainfall in the Midwest or other areas having similar climate and topography.

Limited tests made on published area-depth data for the 8000-square mile Muskingum Basin⁽⁸⁾ indicated that Equation (1) is not applicable to large basins. Chow⁽¹⁰⁾ has suggested that an equation of the form

$$Y = a + b X^{1/2} + cX + dX^{3/2} + \dots \quad (7)$$

maybe more applicable to larger basins, the number of higher terms depending on the basin size.

VARIATION OF POINT RAINFALL WITH DISTANCE

Introduction

The variation of rainfall with distance is an important factor in hydrologic and agricultural studies where analysis of precipitation effects is required. Due to the ordinary spacing of rain gages, estimates of point rainfall are frequently needed for locations which may be several miles from the nearest rain gage. The U.S. Weather Bureau (8) has presented some limited results for distances up to four miles, based upon data from five stations on Little Mill Creek in Ohio. Otherwise, little information on the subject is available.

As a partial solution to the problem of determining rainfall variability with distance, a study was undertaken, using storm data collected on two concentrated rain-gage networks. Data from 25 gages on the 100-square mile Panther Creek network (Fig. 3) for 1950-54 and from 50 gages on the 100 square mile Goose Creek network (Fig. 4) for 1952-54 were used in the study. These networks provided data for distances up to 11 miles from a total of 186 storms having point rainfall amounts ranging from 0.01 inch to 9.15 inches and areal mean rainfalls varying from a trace to 7.21 inches. Analysis was confined to warm season or shower-type rainfall occurring from spring to fall.

Analysis of Average Differences

The rain gage nearest the center of the area in each network was designated as the comparison gage. For each storm on each network, differences were calculated between the total storm rainfall at the comparison gage and that recorded at each of the other network gages. The data were first grouped according to distance from the comparison gage. At each distance, the differences between the various network gages and the comparison gage were further grouped in class intervals according to point rainfall amounts (storm size) at the comparison gage.

Graphical plots of the grouped data indicated one of the two following general equations would provide the best data fit:

$$\text{Log } E = k + 1 \text{ Log } P + m \text{ Log } D \quad (1)$$

$$\text{Log } E = k + 1 P^n + m \text{ Log } D \quad (2)$$

In Equations (1) and (2), E represents the average difference between the total storm rainfall at the comparison gage and at points located at distance D from the comparison gage, when the point rainfall recorded at the comparison gage is P. The regression constants are represented by k, 1, m and n.

The data from both networks were then combined to obtain the empirical expressions:

$$\text{Log } E = -0.796 + 0.49 \text{ Log } P + 0.32 \text{ Log } D \quad (3)$$

$$\text{Log } E = -1.359 + 0.51 P^{0.5} + 0.31 \text{ Log } D \quad (4)$$

where E and P are in inches and D is in miles.

Confidence Limits

For practical application, an estimate of storm rainfall at some point at a distance D from the comparison gage is more useful if an interval or range about the estimate can be determined with some measure of confidence that the estimate is within this range. The 95 per cent confidence bands are frequently used for this purpose. To establish confidence limits, an estimate of the sampling standard deviation is required. Consequently, expressions for an estimate of the standard deviations of the differences between the comparison gage rainfall and that occurring at various distances from the comparison gage were obtained from the same data used in deriving Equations (3) and (4). The expressions obtained are

$$\text{Log } s = -0.398 + 0.49 \text{ Log } P + 0.32 \text{ Log } D \quad (5)$$

$$\text{Log } s = -0.961 + 0.51 P^{0.5} + 0.31 \text{ Log } D \quad (6)$$

The 95 per cent confidence bands for P were estimated by taking two times the standard deviation and adding and subtracting from the corresponding value of P.

Equation Comparisons

Multiple correlation coefficients of 0.74 and 0.78 were obtained from Equations (3) and (4), respectively. These correlation coefficients indicate there is little difference in the goodness of fit provided by these two equations. Graphical plots of the grouped data indicated that Equation (4) gives a somewhat better fit at high and low values of P, while Equation (3) fits best at the intermediate values of P.

A comparison is given in Table 8 of the E values obtained for various P values at a distance (D) of five miles. Only small differences in E are obtained from the two empirical equations below P values of three inches. Above three inches, Equation (4) produces appreciably higher values of E than Equation (3). However, only a small portion of the point rainfall observations from which the empirical equations were derived exceeded three inches.

TABLE 8

COMPARISONS BETWEEN EQUATIONS (3) AND (4)

P (in.)	E (in.) at 5 Mi.	
	Eq. (3)	Eq. (4)
0.10	0.08	0.10
0.25	0.14	0.13
0.50	0.19	0.17
1.00	0.27	0.23
2.00	0.38	0.38
3.00	0.45	0.55
5.00	0.59	1.00

From the hydrologic standpoint, at least, the variation of rainfall with distance in heavy storms is usually of greater interest than rainfall variations in light storms. Since Equations (3) and (4) predict significantly different values of E above P values of three inches, an effort was made to de-

termine which equation appears most applicable at high values of P. Although the data used in the study indicated Equation (4) provided a better fit at the high P values, it was desired to further test the relation with independent data.

For this purpose, data were used from two unusually heavy Illinois storms: the July 9, 1951 storm in North Central Illinois,⁽¹²⁾ and the July 18-19, 1952 storm in Rockford and vicinity.⁽¹³⁾ The Water Survey conducted extensive field surveys following these storms which provided adequate rainfall data for constructing detailed isohyetal maps. A rectangular grid overlay was used with the isohyetal maps from these two storms to obtain data on rainfall variations with distance. Each 3-mile interval on the grid overlay was considered an observation point and rainfall differences were obtained from the underlying isohyetal map at distances of three, six, and nine miles from each observation point in each of four directions - north, east, south and west. This method produced a total of 760 observations in the two storms. Point rainfall values at the observation points ranged from 2.0 to 10.6 inches. Equations(3) and (4) were then tested by determining how many of the 760 observations fell within the 95 per cent confidence bands for each equation. It was found that 94 per cent of these observations fell within the 95 per cent confidence bands of Equation (4) compared to 80 per cent for Equation (3). These results indicate that Equation (4) is more reliable for predicting differences in point rainfall with distance in heavy storms, as suggested earlier by graphical plots of the original data upon which the two empirical equations were based.

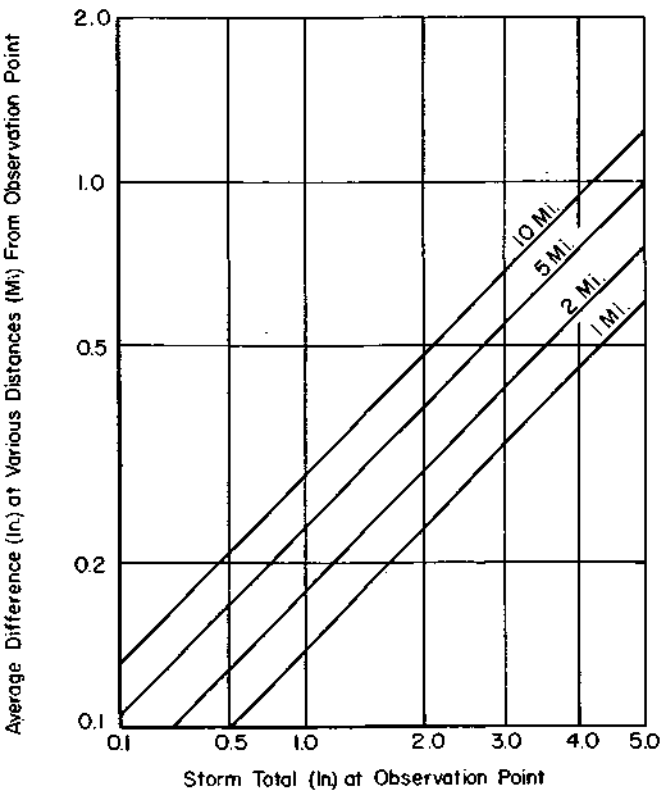


FIGURE 31 VARIATION OF POINT RAINFALL WITH DISTANCE

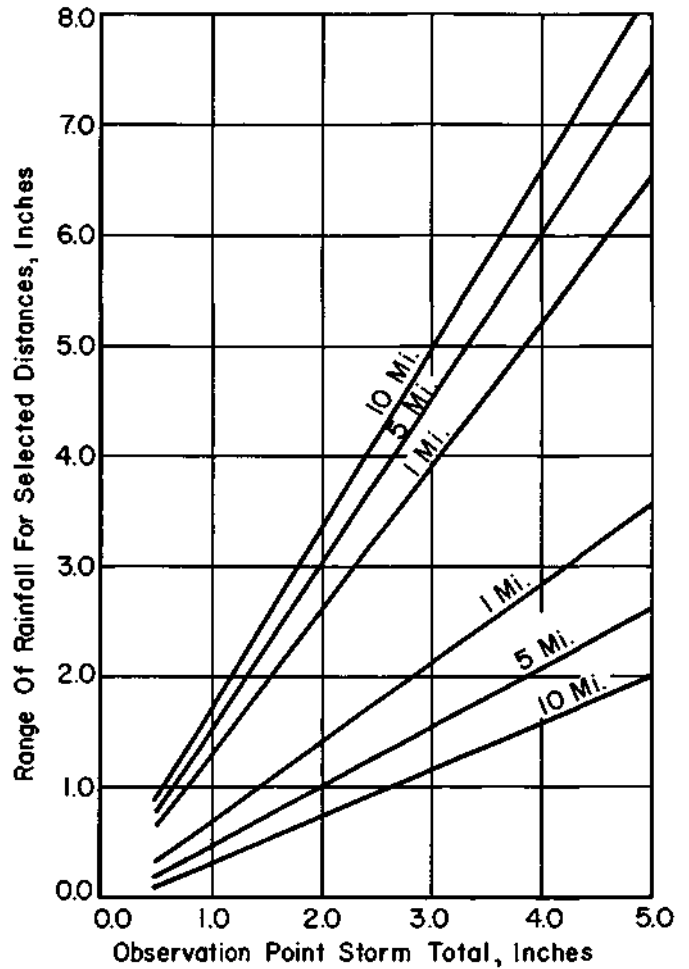


FIGURE 32 95 PER CENT CONFIDENCE RANGE FOR VARIATION OF POINT RAINFALL WITH DISTANCE

A graph derived from Equation (4) for predicting the average difference in storm rainfall between points at various distances is given in Figure 31. The 95 per cent confidence bands, based upon Equation (6), for selected values of D are presented in Figure 32. The great variability in shower-type rainfall is well illustrated in Figure 32. For example, within a distance of one mile from a gage recording a rainfall of one inch, differences up to 0.35 inch or 35 per cent are indicated by the 95 per cent limits; at five miles, differences up to 0.55 inch occur; and at 10 miles, differences reach 0.70 inch.

Consideration of Additional Variables

In an earlier, limited study using data for 33 storms over the Goose Creek network during 1953⁽¹⁴⁾ analysis was performed to determine if a more efficient equation might be obtained by substituting other independent variables into Equation (1) in addition to P and D. The data had not been fitted to Equation (2) at the time of this analysis.

The only practical variables which can be used in an expression such as Equation (1) are those which can be read from the rain-gage chart at the observation gage. It was reasoned that consideration of storm duration (T), mean rate of rainfall (Ra), and maximum rate of rainfall (Rm) might

improve the prediction efficiency of expressions such as (3) and (5) which utilize only P and D. The maximum 5-minute rainfall rate for each storm was used to represent the maximum storm rate.

Multiple correlation coefficients between standard deviation (s) and various combinations of P, D, T, R_a , and R_m were computed to determine whether the correlation would improve from consideration of the three additional variables. The various coefficients are shown in Table 9. The squares of the coefficients, expressed in per cent, are also shown. These values indicate the relative efficiency of the various combinations of independent variables.

The results presented in Table 9 indicate that the three additional variables are about equal in efficiency. Since the product of R_a and T is equivalent to P, their use as variables in an expression already containing P appeared doubtful. However, to more thoroughly explore the problem, tests involving these two variables in conjunction with P were made. Table 9 shows that including R_a and T with P increased the efficiency by only eight per cent (42 to 50). The same efficiency was obtained by using R_a and T without P (last line of Table 9). Using T, R_a and R_m in conjunction with P and D increased the prediction efficiency by only 10 per cent.

Considering the relatively small improvement in efficiency shown by the more complex expressions and the additional work involved in getting data to use with them, Expressions (3) to (6) appear more practical for prediction purposes. Undoubtedly there are other factors which would be useful in increasing the efficiency of Equations (3) to (6). An important factor, for instance, is the storm path with reference to the location of the measurement gage. However, it is impossible to estimate the storm path from a single gage, and only factors which could be obtained from a single recording gage were investigated in this study.

TABLE 9

MULTIPLE CORRELATION COEFFICIENTS

Independent Variables	Multiple Correlation (C)	C ² (%)
PD	0.65	42
PDR _m	0.71	50
PDT	0.70	49
PDR _a	0.70	49
PDR _m T	0.71	50
PDR _m R _a	0.71	50
PDTR _a	0.71	50
PDR _m TR _a	0.72	52
DTR _a	0.71	50

AREAL REPRESENTATIVENESS OF POINT RAINFALL

Introduction

The accuracy with which a point rainfall measurement represents the mean rainfall for areas of varying sizes in the vicinity of the point observation is pertinent to the design of rain-gage networks for various purposes and in the interpretation of data from existing networks. Information regarding the relation between point rainfall and areal mean storm rainfall is especially applicable to hydrologic problems.

The lack of concentrated rain-gage networks over areas of various size, which are necessary for deriving point-areal mean relations, has in the past limited development of empirical relations. Some limited data for areas of 375, 1500 and 8000 square miles have been provided by the U.S. Weather Bureau.⁽⁸⁾

As a partial solution to the above problem, rainfall data collected on several concentrated networks in central Illinois have been utilized to derive empirical relations between point and areal mean rainfall for areas ranging from 0.03 to 400 square miles. Point rainfall was measured at the center of each area and empirical equations developed for storm, weekly, and monthly periods. In addition, storm data for areas of 10 to 100 square miles were used to obtain an empirical relation between point and areal mean rainfall for conditions when the point rainfall is measured at a gage displaced from the areal center by various distances.

Available Data

Data used in this study were collected on the networks illustrated in Figures 2-8, comprising areas ranging from 0.03 to 400 square miles. In addition, the Goose Creek and Panther Creek

networks were subdivided to provide data for areas of 10, 25, and 50 square miles. The various networks provided data for nine areal sizes from which a total of 1900 storm observations were available for derivation of empirical relations. The sampling scheme is illustrated in Figure 33, using the 1954 Goose Creek network.

All data used in the study were collected during spring, summer, and early fall; consequently, the developed relations are most applicable to shower-type rainfall. While the results are based on Illinois data, they should be approximately representative for the Midwest, in general, and for other areas having similar climate and topography.

Accuracy of Areal Rainfall Estimates From a Centered Gage

Average Error. Various graphical plots were made of data for each areal size, relating point rainfall at the center of each area to the difference between the point observation and the areal mean rainfall as measured by all gages within that particular area. Inspection of these graphical plots indicated that one of the following general equations would fit the data best:

$$\text{Log } E = k + 1 \text{ Log } P \quad (1)$$

$$\text{Log } E = k + 1 P^m \quad (2)$$

In these expressions, P is the point rainfall for either the storm, weekly, or monthly observation at the center of a given area; E represents the difference between point and areal mean rainfall in the given area; and k, 1 and m are regression constants. Values for k and 1 for storm, weekly, and monthly rainfall are shown in Table 10 for each network based on Equation (1).

TABLE 10

REGRESSION CONSTANTS FOR STORM, WEEKLY AND
MONTHLY EQUATIONS ON VARIOUS AREAS

Area (sq. mi.)	Storm		Weekly		Monthly	
	k	1	k	J	k	1
0.03	-2.155	0.46	-2.097	0.61	-2.301	0.72
0.60	-1.538	0.46	-1.469	0.61	-1.347	0.38
4	-1.377	0.47	-1.260	0.73	-1.252	0.86
10	-1.377	0.36	-1.229	0.62	-1.268	0.84
25	-1.222	0.52	-1.051	0.68	-1.252	0.78
50	-1.167	0.51	-1.060	0.78	-1.174	0.80
100	-1.131	0.50	-1.065	0.66	-1.131	0.74
280	-0.914	0.45	-0.783	0.69	---	---
400	-0.932	0.53	---	---	---	---

The values of 1 vary at random, whereas the k values show an increasing trend with area. Consequently, it was felt that the data from all networks could be combined into a single expression of the form:

$$\text{Log } E = k_1 + 1_1 \text{ Log } P + n \text{ Log } A \quad (3)$$

relating the measurement error of areal mean rainfall to the point rainfall (P) recorded at the

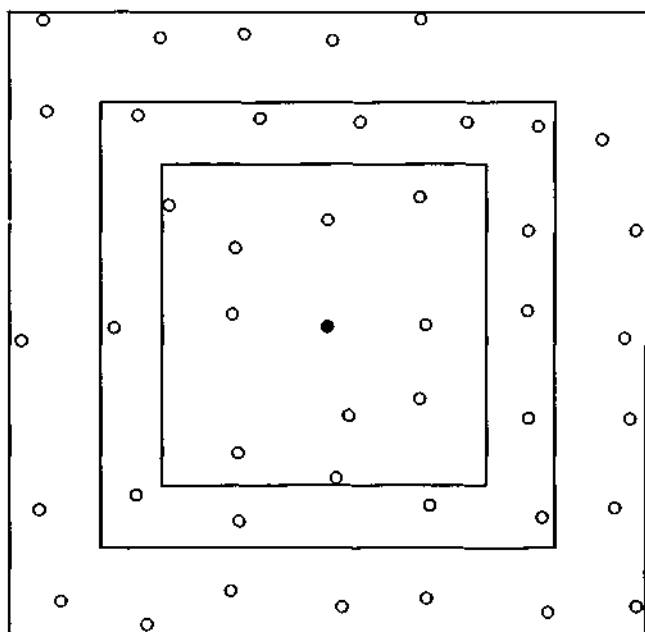


FIGURE 33 25, 50 AND 100 SQUARE MILE AREAS, GOOSE CREEK 1954

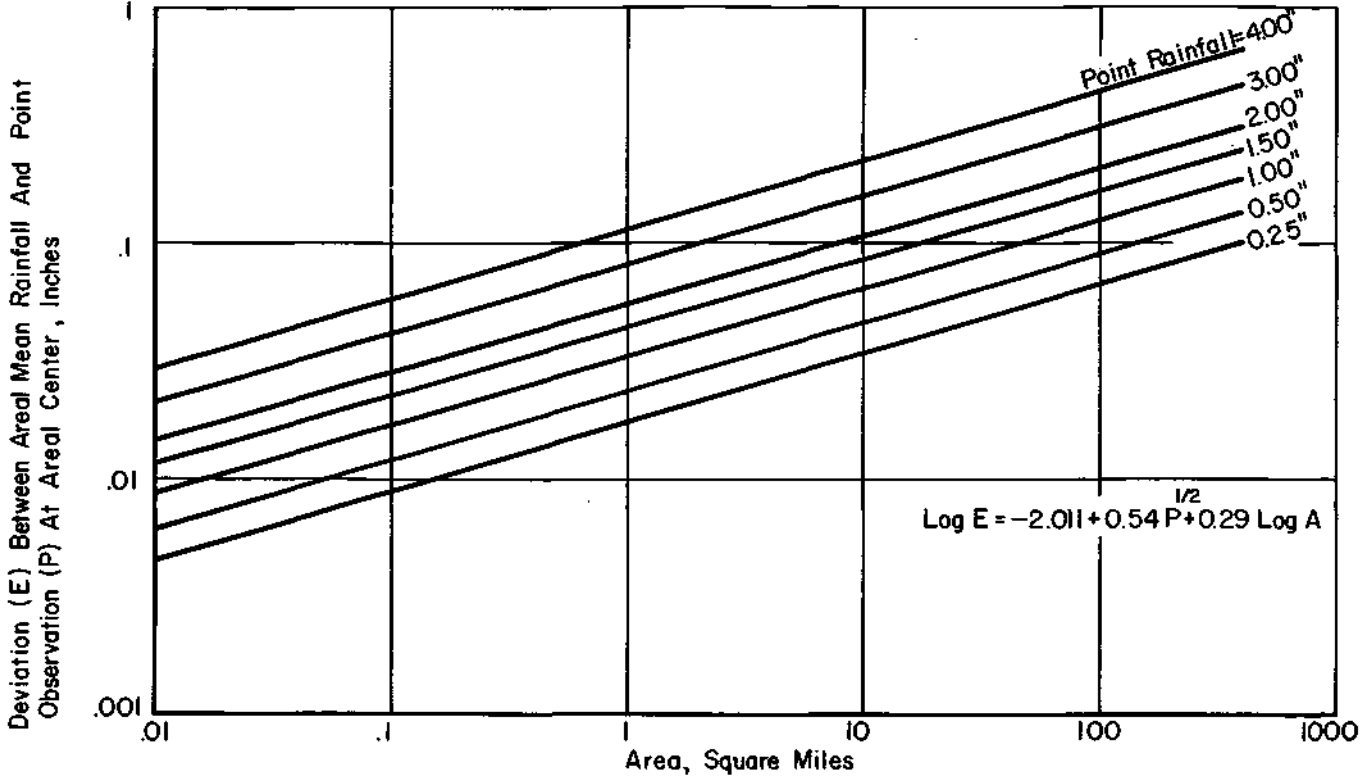


FIGURE 34 STORM RELATION BETWEEN POINT AND AREAL MEAN RAINFALL BASED ON AVERAGE DEVIATIONS

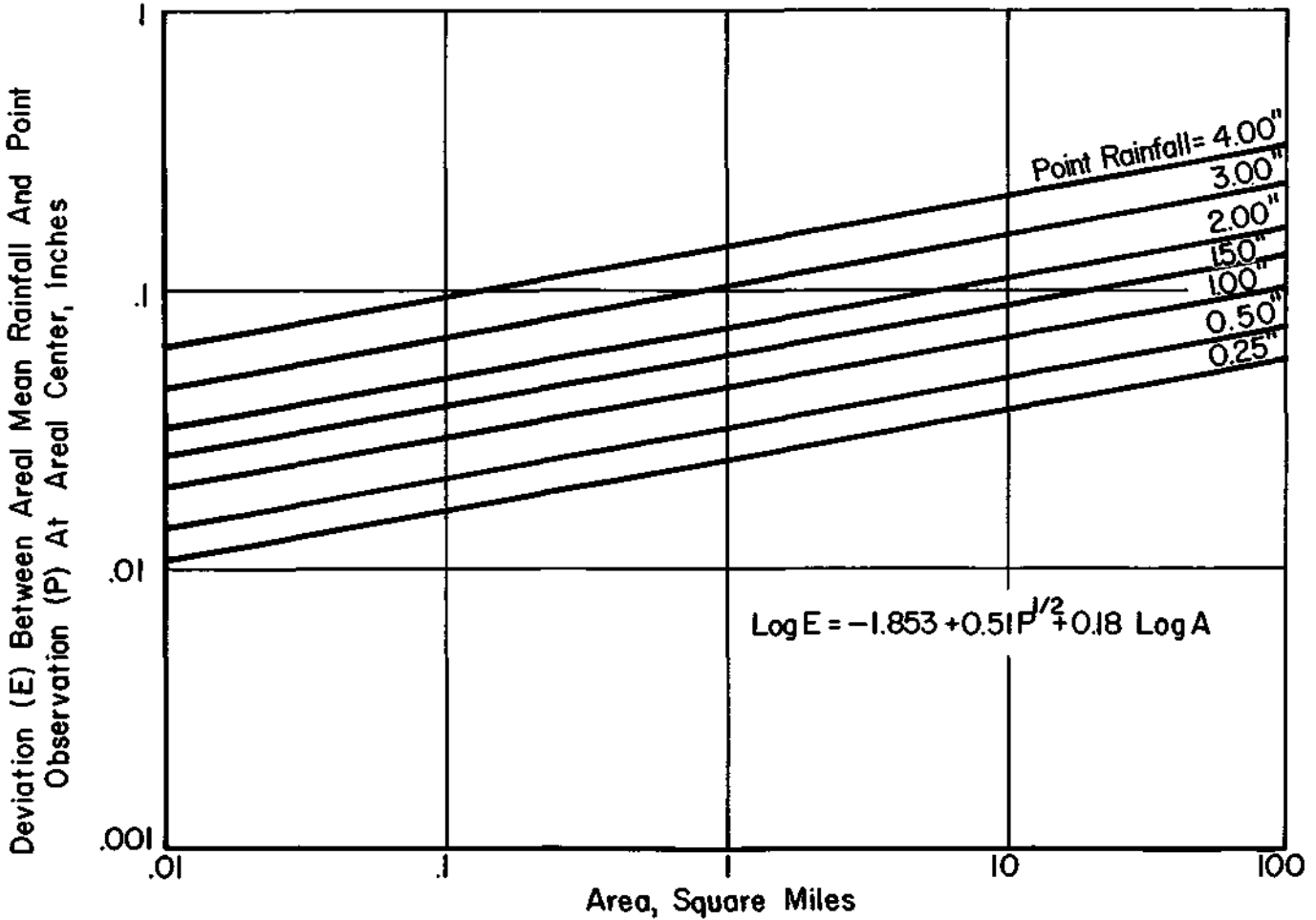


FIGURE 35 WEEKLY RELATION BETWEEN POINT AND AREAL MEAN RAINFALL BASED ON AVERAGE DEVIATIONS

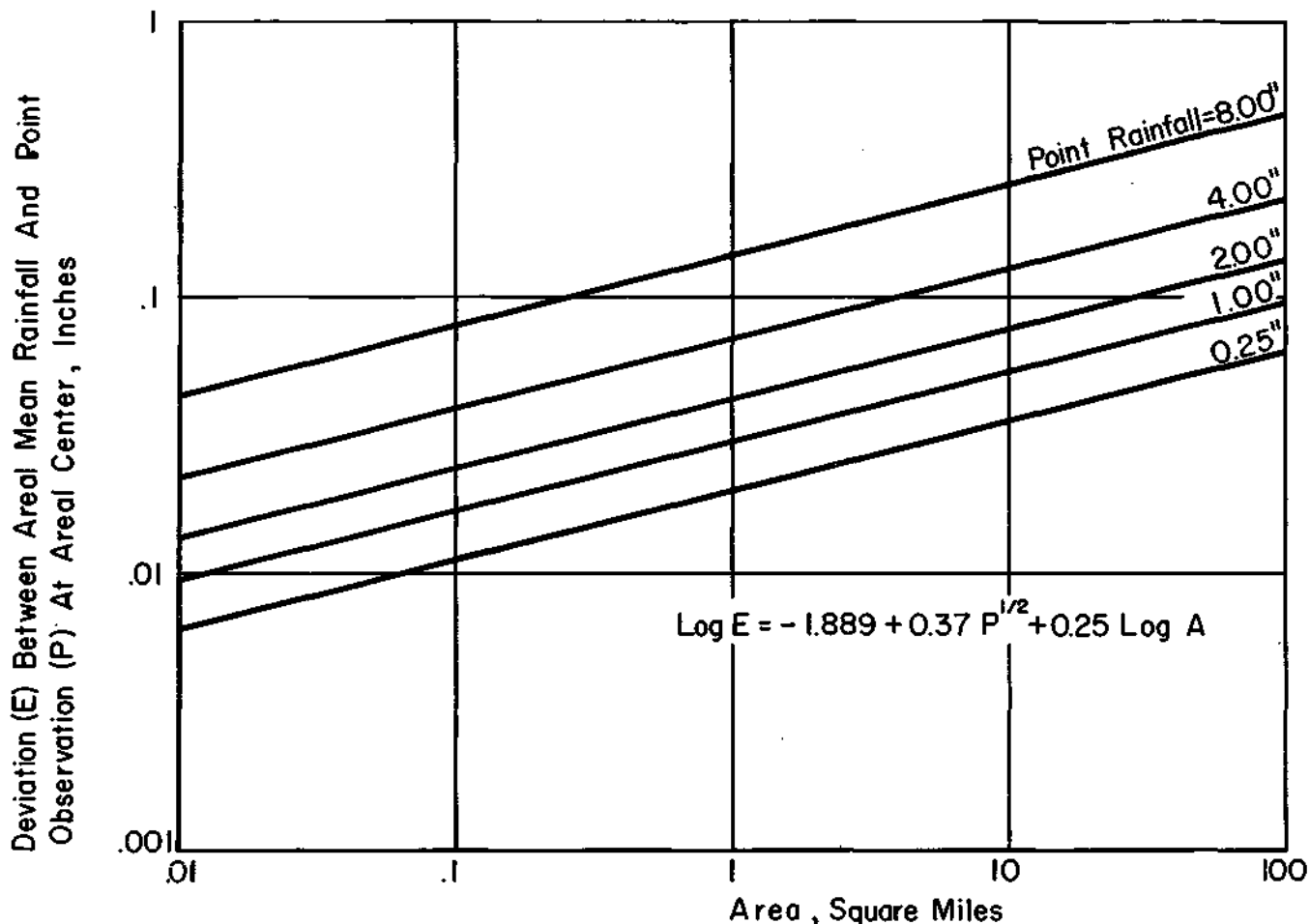


FIGURE 36 MONTHLY RELATION BETWEEN POINT AND AREAL MEAN RAINFALL BASED ON INDIVIDUAL DEVIATIONS

center of the area and to the size of the area (A). The constants k_1 , l_1 , and n were determined by the method of least squares, and the following empirical equations for storm, weekly, and monthly rainfall were obtained.

$$\text{Log } E = -1.341 + 0.50 \text{ Log } P + 0.29 \text{ Log } A \quad \text{(Storm)} \quad (4)$$

$$\text{Log } E = -1.285 + 0.58 \text{ Log } P + 0.20 \text{ Log } A \quad \text{(Weekly)} \quad (5)$$

$$\text{Log } E = -1.559 + 0.71 \text{ Log } P + 0.26 \text{ Log } A \quad \text{(Monthly)} \quad (6)$$

For comparison purposes, the data were next fitted to an expression of the form:

$$\text{Log } E = k_2 + l_2 P^m + n_1 \text{ Log } A \quad (7)$$

in which E , P , and A represent the same quantities as in Equation (3), and k_2 , l_2 , m , and n_1 are again regression constants. The resulting empirical equations are:

$$\text{Log } E = -2.011 + 0.54 P^{0.5} + 0.29 \text{ Log } A \quad \text{(Storm)} \quad (8)$$

$$\text{Log } E = -1.853 + 0.51 P^{0.5} + 0.18 \text{ Log } A \quad \text{(Weekly)} \quad (9)$$

$$\text{Log } E = -1.889 + 0.37 P^{0.5} + 0.25 \text{ Log } A \quad \text{(Monthly)} \quad (10)$$

Multiple correlation coefficients were then determined for Equations (4), (5), (6), (8), (9), and

(10) and are presented in Table 11. These correlation coefficients indicate there is no significant difference in the goodness of fit provided by Equations (3) and (7). The smaller correlation coefficient obtained with the monthly data is due primarily to the fact that analysis was performed on ungrouped data, whereas the storm and weekly analyses were performed on grouped data. The number of individual monthly observations did not permit grouping. There were only 255 monthly values compared to 663 weekly totals and 1900 storm observations.

Graphical plots of the grouped data used in Equations (4), (5), (8), and (9) indicated that Equations (8) and (9) provide a somewhat better fit at high and low values of P . A similar occurrence was noted between these two general types of equations in the study of the variation of point rainfall with distance discussed in the previous section of this bulletin.

TABLE 11

MULTIPLE CORRELATION COEFFICIENTS

Equation Number	Correlation Coefficient	Rainfall Type
(4)	0.89	Storm
(8)	0.90	Storm
(5)	0.85	Weekly
(9)	0.85	Weekly
(6)	0.62	Monthly
(10)	0.60	Monthly

A comparison of the E values obtained for various P values from Equations (4) and (8) for storm rainfall on an area of 100 square miles is presented in Table 12. Only small differences in E are obtained from the two empirical equations below P values of three inches. Above three inches, Equation (8) produces appreciably higher values of E than Equation (4). As mentioned previously, indications are that empirical equations derived from Expression (7) fit heavy rainfall data better. Since heavy rainfall is of prime interest to the hydrologist, further analytical efforts have been concentrated on this form of equation. Equations (8), (9) and (10) are represented graphically in Figures 34, 35, and 36.

TABLE 12
COMPARISONS BETWEEN EQUATIONS (4) AND (8)

P (i")	E (in.) for 100 Square Mile Area	
	Eq. (4)	Eq. (8)
0.10	0.04	0.06
0.25	0.07	0.07
0.50	0.10	0.09
1.00	0.14	0.13
2.00	0.20	0.22
3.00	0.25	0.32
5.00	0.32	0.60

A comparison of E values obtained from the storm, weekly and monthly equations is shown in Table 13. As expected, all three equations show that the average difference between point and areal mean rainfall (E) increases as the storm size, represented by the point measurement at the areal center, increases. For a point rainfall measurement of a given magnitude, a trend exists for E to decrease with increasing sampling time as repre-

sented by storm, weekly and monthly values. This trend becomes more pronounced as the point rainfall at the areal center increases. It would appear, therefore, that a centered gage measures areal mean rainfall with an increasing degree of accuracy as the sampling period increases. Such a trend is to be expected. The weekly rainfall is usually the result of several storms and the monthly total ordinarily contains more storms than the weekly total. In the absence of significant topographic or climatic features, the areal distribution of rainfall will tend to become more uniform as the number of storms increases, because individual storms tend to travel in various paths across a given area.

TABLE 13
COMPARISON BETWEEN STORM, WEEKLY AND MONTHLY RELATIONS

Point Rainfall (in.)	Av. Difference (in.) Between Point and Mean Rainfall for 100-Square Mile Area		
	Storm	Weekly	Monthly
0.25	0.07	0.06	0.06
1.00	0.13	0.10	0.10
2.00	0.22	0.17	0.14
4.00	0.45	0.34	0.22

Confidence Limits. An estimate, P, of the areal mean rainfall becomes more meaningful when some measure is made of the possible error in the estimate. It is desirable to determine an interval about P with some measure of confidence that the areal mean is in that interval. To establish confidence limits, an estimate of the sampling standard error was required. This was made from 14 groups of storms having about the same P values. These classes, expressed in inches, are shown in Table 14. A standard deviation was computed for each of the class intervals in Table 14. The constants k, l, m and n were again deter-

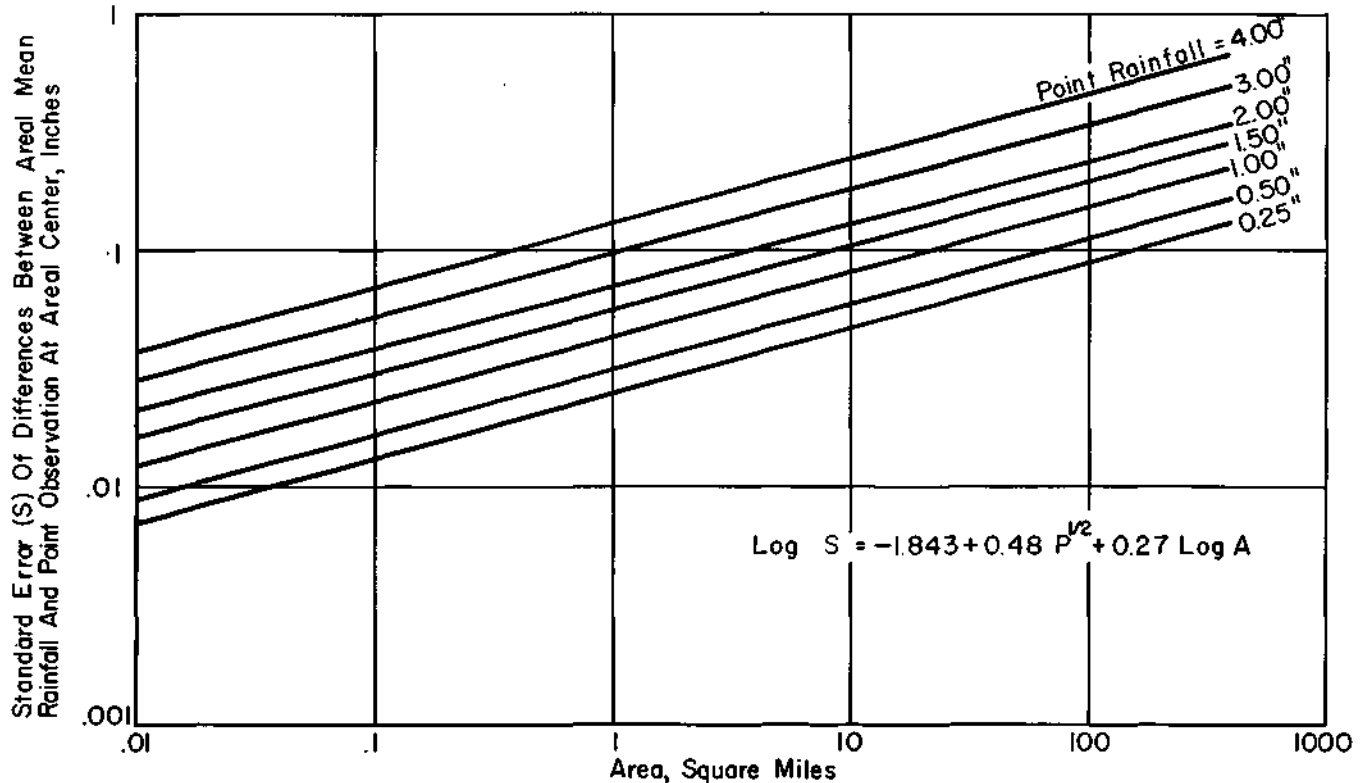


FIGURE 37 STORM RELATION BETWEEN POINT AND AREAL MEAN RAINFALL BASED ON STANDARD ERRORS

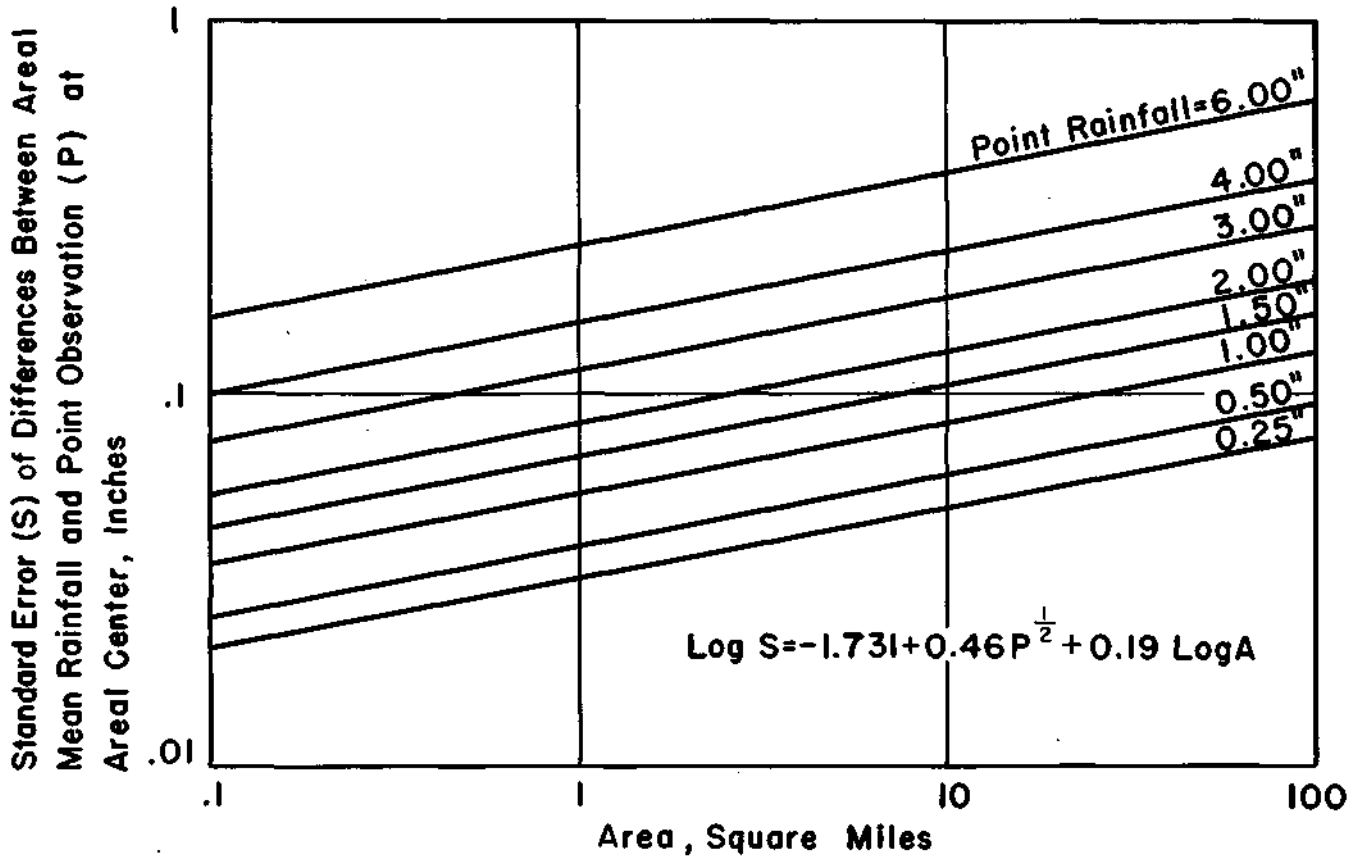


FIGURE 38 WEEKLY RELATION BETWEEN POINT AND AREAL MEAN RAINFALL BASED ON STANDARD ERRORS

mined for equations of the form represented by Expression (7). The resulting equations for storm and weekly rainfall are:

$$\text{Log } s = -1.843 + 0.48 P^{0.5} + 0.27 \text{ Log } A \quad (11)$$

(Storm)

$$\text{Log } s = -1.731 + 0.46 P^{0.5} + 0.19 \text{ Log } A \quad (12)$$

(Weekly)

In these equations, *s* (inches) represents the best estimate of the standard error, *P* (inches) represents the mid-point of the class intervals, and *A* represents the area in square miles. Multiple correlation coefficients for Equations (11) and (12) were 0.85 and 0.82, respectively. Figures 37 and 38 show a graphical relation between *A* and *s* for several *P* values for storm and weekly rainfall. An insufficient number of monthly totals prevented the determination of a monthly relationship.

The 95 per cent confidence limits for storm and weekly areal mean rainfall were estimated by computing $p \pm 2 s$ from Equations (11) and (12). The resulting limits are presented for several values of *A* in Figures 39 and 40. Other confidence limits may be determined if desired. For example 70, 80, 90 and 99 per cent confidence limits for storm

and weekly areal mean rainfall may be estimated by multiplying *s* from Equations (11) and (12) by 1.05, 1.30, 1.67 and 2.66, respectively, and adding and subtracting from *P*.

Areal Rainfall Estimates from an Off-Center Gage

Frequently, rain gages are not located at or near the center of the area of interest. The nearest gage may even be outside the boundary of the area. It is logical to expect that a rain gage which is located at a distance from the areal center will on the average give a less accurate estimate of the areal mean than a gage located at the center. The following paragraphs summarize an analysis to determine the accuracy of storm areal mean rainfall estimates from gages located at various distances from the center of several areas of different sizes.

Data from areas of 10, 25, 50, and 100 square miles were analyzed. Analysis techniques were similar to those used in comparing areal mean rainfall with the rainfall amount obtained from a centrally-located gage. An examination of graphical plots of the data indicated that an expression of the form

$$\text{Log } E = a + b P^c + d \text{ Log } A + e \text{ Log } D \quad (13)$$

followed the trend of the data satisfactorily. In this expression, *E* represents the average of the differences, *A* is the network area, *D* is distance from the areal center, *P* represents rainfall amounts at

TABLE 14

STORM GROUPS (IN.) USED IN STANDARD ERROR COMPUTATIONS			
0.01-0.10	0.41-0.50	0.81-0.90	2.01-3.00
0.11-0.20	0.51-0.60	0.91-1.00	3.01-4.00
0.21-0.30	0.61-0.70	1.01-1.50	
0.31-0.40	0.71-0.80	1.51-2.00	

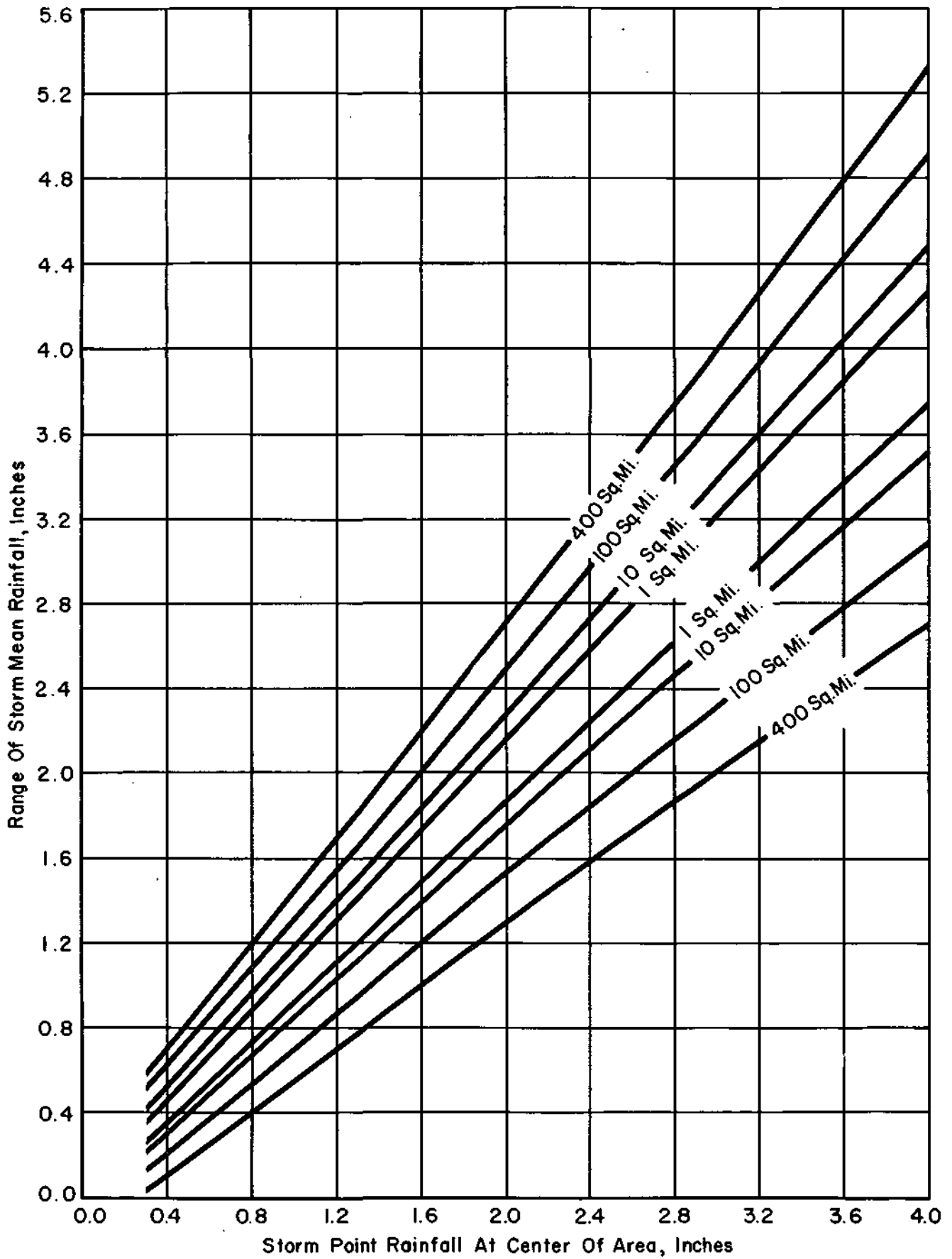


FIGURE 39 95 PER CENT CONFIDENCE RANGE FOR STORM RAINFALL

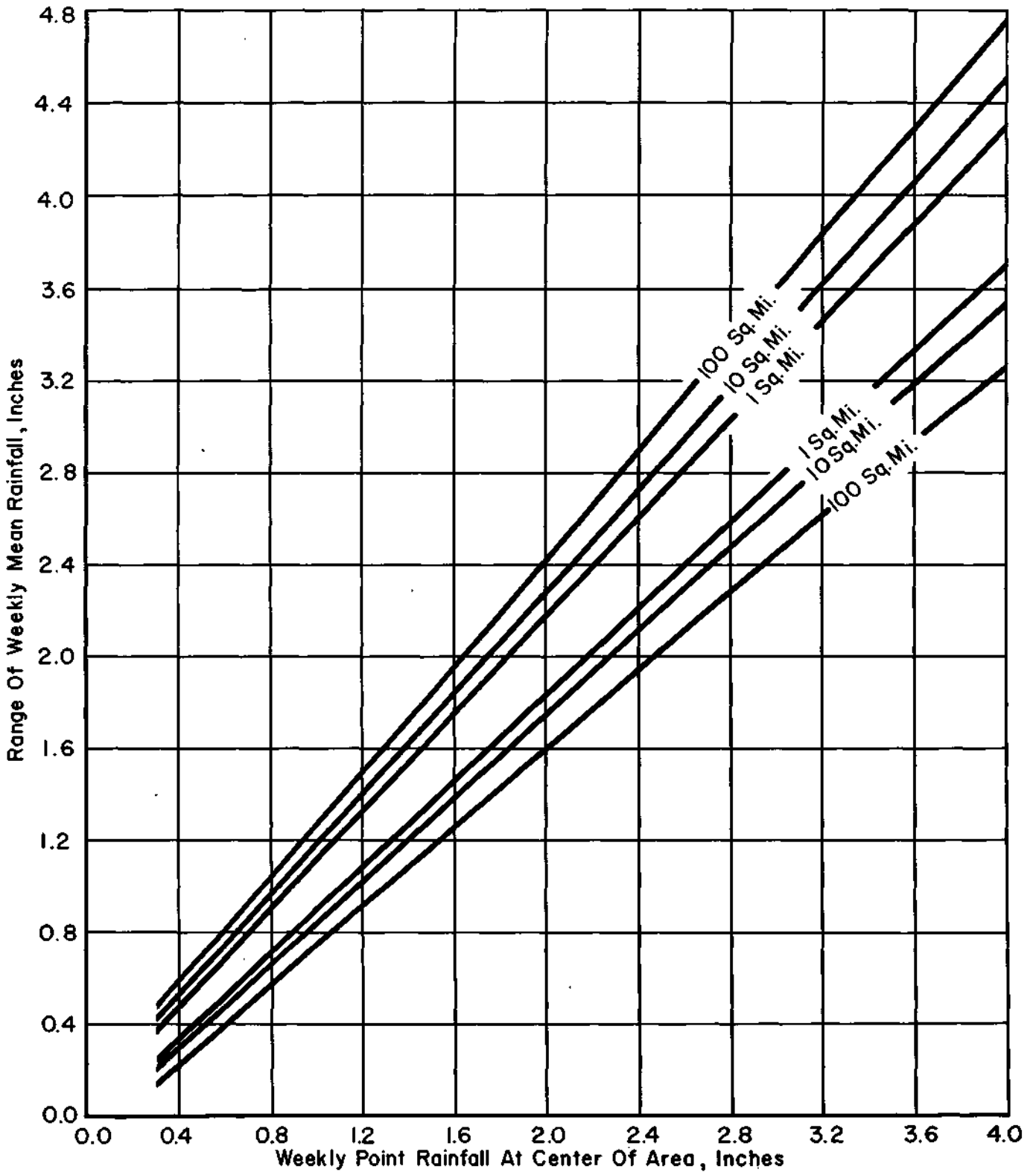


FIGURE 40 95 PER CENT CONFIDENCE RANGE FOR WEEKLY RAINFALL

the observation gage; a, b, c, d, and e are regression constants.

The equation obtained by fitting Expression (13) to the data is:

$$\begin{aligned} \log E = & -1.411 + 0.51 P^{0.5} \\ & -0.01 \log A + 0.37 \log D \end{aligned} \quad (14)$$

In this equation E and P are in inches, A is in square miles and D is in miles. The relation is illustrated for an area of 100 square miles in Figure 41.

Within the limits of the data used, the magnitude of the coefficient of Log A suggests that area was not an important variable in the analysis. This

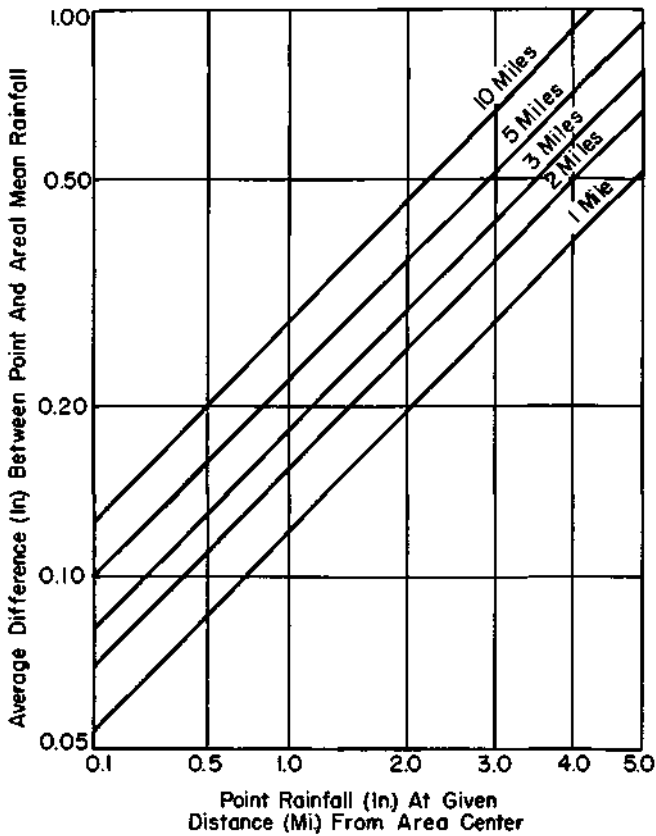


FIGURE 41 EFFECT OF GAGE LOCATION ON SINGLE GAGE ESTIMATES OF MEAN RAINFALL ON 100 SQUARE MILE AREA

result is rather difficult to rationalize. However, it may be due to the fact that a gage located at any given distance from the center of two areas of different size is relatively closer to the center of the larger area. Consequently, the gage may be in an equally good position for sampling the mean rainfall in both areas.

An empirical equation for the standard deviation was determined for use in estimating confidence limits. This equation is:

$$\begin{aligned} \log s = & -1.179 + 0.41 P^{0.5} \\ & - 0.01 \log A + 0.30 \log D \end{aligned} \quad (15)$$

where s is in inches and P , A , and D have the same definition and units of measurement as they had in Equation (14). The 95 per cent confidence limits for various values of P , A , and D may be computed from $P \pm Z s$.

Since A contributes very little to the value of E and s in Equations (14) and (15), the area variable could be omitted without significant error within the limits of area tested in this study. These equations would then be of the same form as Equations (4) and (6) in the variation of rainfall with distance study discussed in the previous section of this bulletin. The coefficient of $P^{0.5}$ is the same and the coefficient of $\log D$ nearly equal in both studies. These results suggest that the estimators P and D give practically the same measurement error in both analyses.

RELIABILITY OF STORM MEAN RAINFALL ESTIMATES

Introduction

In the previous section, the accuracy of areal rainfall estimates obtained from a single gage at or near the center of an area was investigated. However, an estimate of average rainfall may be required for an area on which more than one gage occurs. Consequently, an analysis was made to determine an estimate of both the average error and the standard error involved in measuring areal mean rainfall by means of various gage densities within several areas of different size.

Data Used

Data from the Panther Creek, Goose Creek, El Paso and east central Illinois networks were included in the analysis. Only shower and thunderstorm rainfall were considered. The 100-square mile Goose Creek network was subdivided into networks comprising 25 and 50 square miles for the 1952, 1953, and 1954 seasons. Two 200-square mile networks were chosen; one from the 280-square mile El Paso network (Fig. 2) operated in 1948 and 1949, and the other from the 400-square mile east central Illinois network (Fig. 5) operated in 1955 and 1956. These data permitted an analysis for areas of 25, 50, 100, 200, and 400 square miles.

Sampling Procedures

More than one sampling plan was considered to ascertain the most applicable plan for sampling areal mean rainfall. Three sampling plans were tried on a 100-square mile network. These included the random start, a plan which combined centrally located samples with random start samples, and a single best-centered sampling plan.

A random sampling procedure (not used in this study) allows the selection of gages in each sample to be determined entirely by chance. A stratified random sampling plan provides a more consistently uniform distribution of gages in each sample than that obtained by a purely random plan, but allows the selection of gages to be determined more by chance than does a random start sampling plan, for example. Sampling plans which involve the selection of centrally located gages in contiguous areas require the omission of a considerable number of observations from the analysis. A random start systematic sampling procedure provides a plan for spreading the sample observations over the network, and at the same time, permits the use of data from all gages.

Random Start. The sampling procedure for the random start systematic sampling plan can be illustrated by reference to Figure 42. When the total number of gages in a network is 48 and it is desired to take samples of 3 gages, the 48 gages are divided into 16 contiguous groups of 3 gages each. According to the random start plan, a starting position is selected in one group of gages. One gage in approximately the same location is automatically designated in each of the other groups to complete the observations in each sample. In a

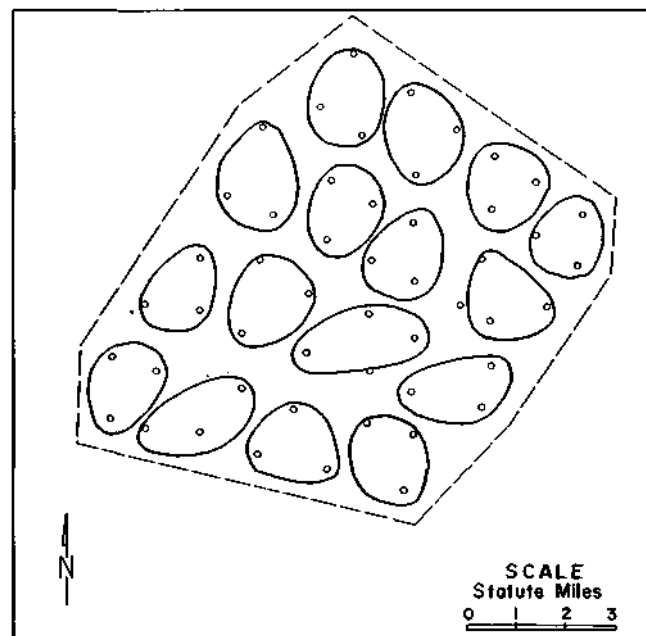


FIGURE 42 GROUPS OF GAGES FROM WHICH 3 RANDOM START SYSTEMATIC SAMPLES OF SIZE 16 WERE SELECTED

network of 48 gages, there are three possible samples of 16 which are treated as having equal probability of being an actual sample of 16 gages. Other sample sizes may be designated in a similar manner.

Combined Sampling Plan. The random start sampling plan does not provide for a single gage sample. When the sample size is decreased to one gage, the random start plan of dividing the network into groups of contiguous gages becomes the same as selecting one observation at random. The variance of these estimates would be equivalent to the purely random sampling variance for single gage samples. There is also a tendency for the random start systematic sampling plan to approach random sampling for other small samples, because the spread of observations in each sample becomes less uniform over the areas as the sample size decreases. This feature of the random start plan allows sampling errors for the small sample sizes which are somewhat larger than would be observed normally in actual practice, for the reason that gages in an operating network usually approach a uniform distribution.

When one is designing a network, each rain gage would logically be placed relatively close to the center of the area to be gaged. A centrally-located gaging plan should permit sampling errors of a magnitude less than a plan in which gage locations were left partially or wholly to chance. This argument may be advanced for random start systematic sample sizes of 2, 3, 4, and possibly 6 and 8 gages in 100 square miles. Consequently, a sampling plan was tried which involved sample sizes of 1, 2, 3, 4, 6, and 8 which were obtained from a centrally located plan as illustrated in Figures 43-A through 43-F.

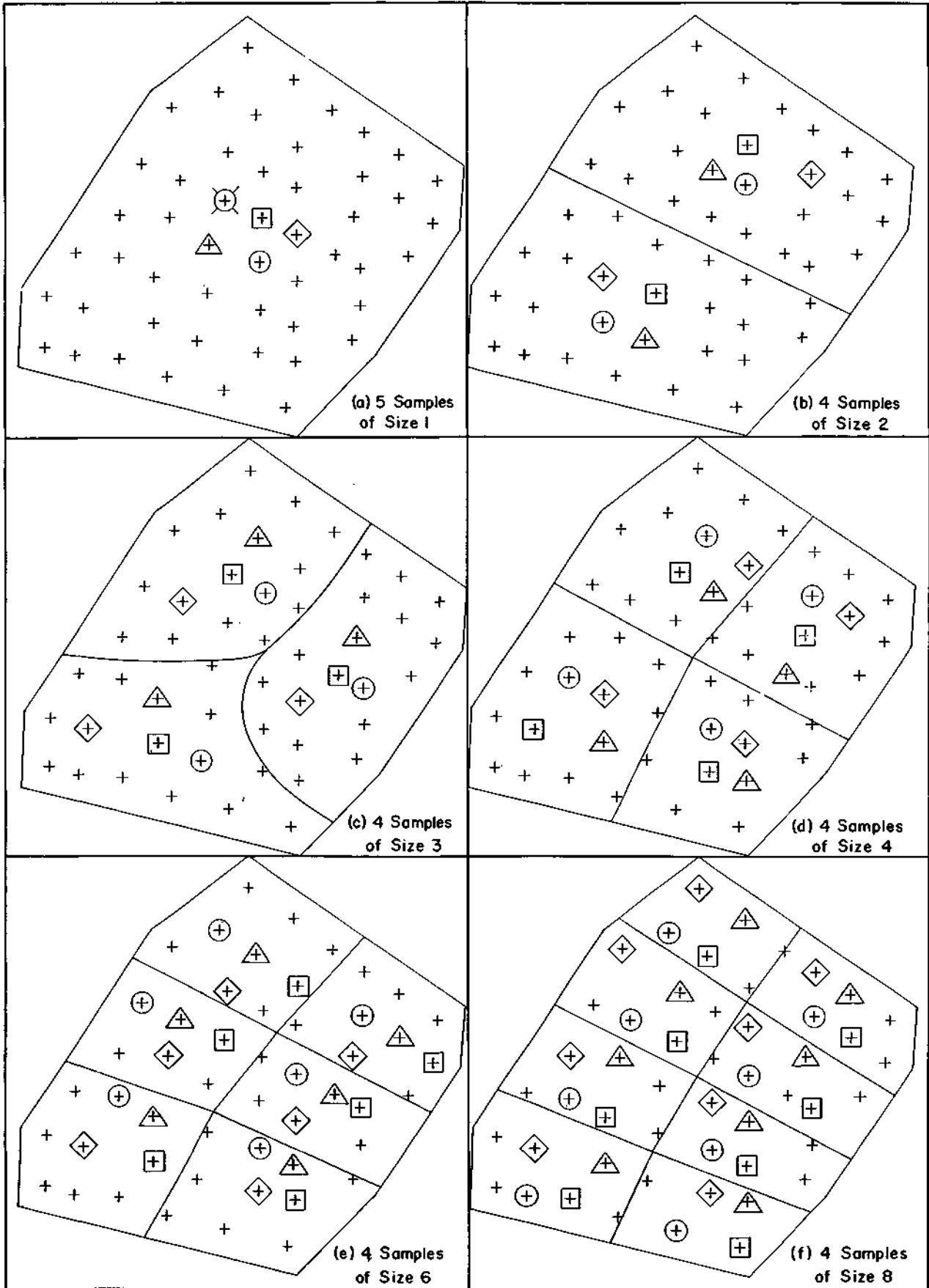


FIGURE 43 COMBINED SAMPLING PLAN FOR SAMPLES OF SIZE 1, 2, 3, 4, 6 AND 8

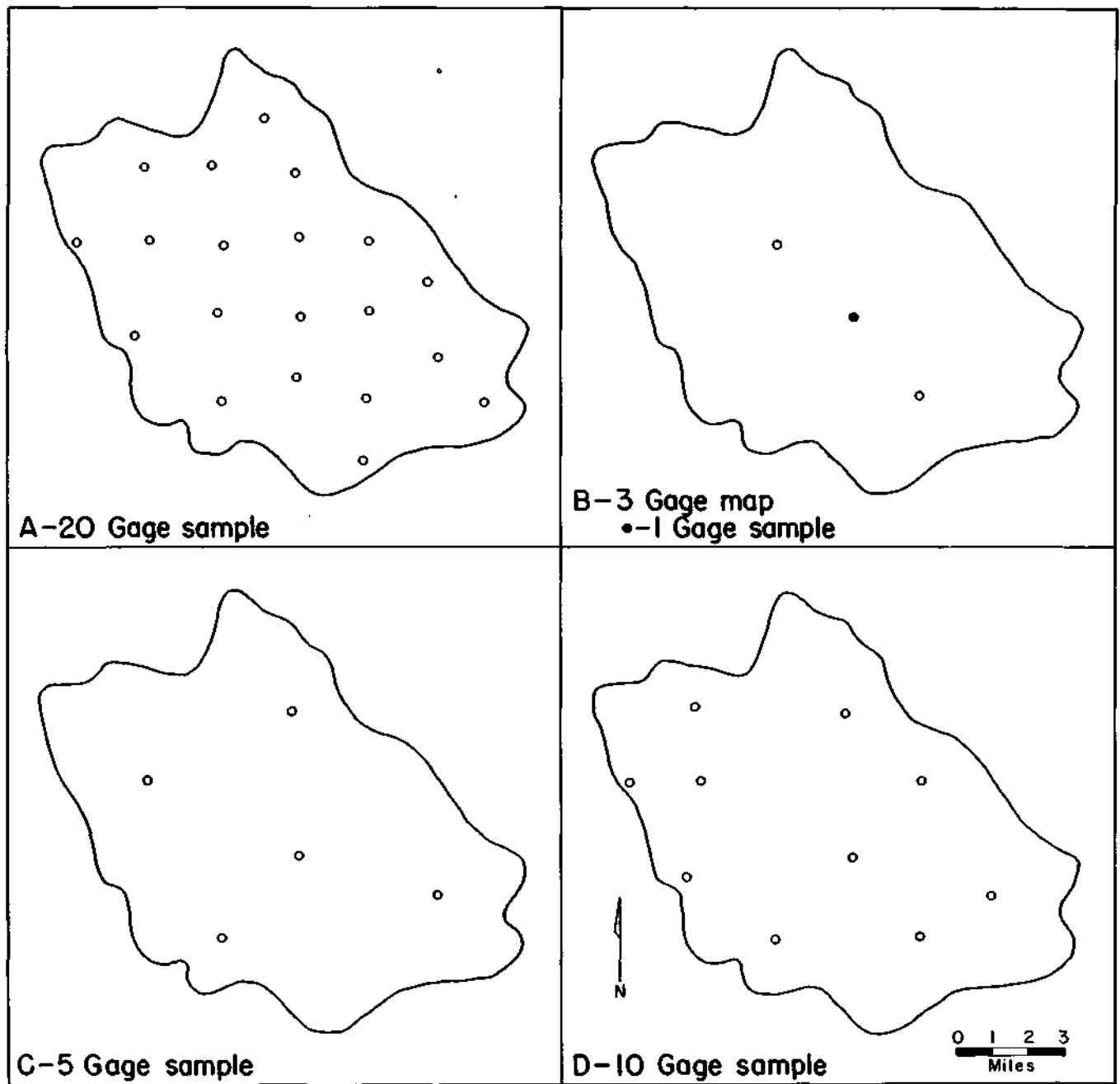


FIGURE 44 BEST-CENTERED SAMPLING PLAN FOR PANTHER CREEK NETWORK

For samples of size 1, five gages were selected within 1-1/4 miles of the geographic center of the network to represent the possible samples for this size. For samples of size 2, 3, 4, 6, and 8 the network was divided into 2, 3, 4, 6, and 8 sections, respectively. Gages located near the centers of these sections were designated as observation stations. As the sample size increased beyond eight, it became impossible to select samples which would be more centrally located than the random start samples. Consequently, the random start systematic plan was used for designating samples having more than eight gages.

Best-Centered. The third sampling plan which was selected was that defined as the one best sub-

sample for each gage density, that is, approximately a uniform grid or centered systematic sample. This sampling plan has one advantage over either of the other two described, because it more closely approaches the practical network design. The best-centered plan has the advantage of providing data that allow for easy calculation of either the average or the standard error of mean rainfall. However it has the disadvantage of being dependent on a single subjective selection of a best sample. This plan does not utilize information that was gathered at all the other gages of the network except in the estimation of the network average. Gage locations used for this sampling plan are shown in Figures 44A through 44D.

Analytical Procedure

The main problem in the analysis was the estimation of the true variance of the estimated average precipitation, P , about the true average precipitation for the network area under consideration. An estimate of this variance leads to an expected measure of the error involved in sampling with each different gage density. The computation consisted mainly of two steps. The first step was the determination of the deviations from the network mean by the following formula

$$d = (P - \bar{P}) \quad (1)$$

where d represents the absolute value of the difference between P , the sample mean rainfall from a sample of N gages, and \bar{P} , the areal mean rainfall based on the total number of gages in the network.

The second step in determining an estimate of the error involved the fitting of a regression system to the deviations. The regression lines provide values which are designated as the estimate of the error of P about \bar{P} . A discussion of the regression system follows.

From graphical plots of the data it was observed, in general, that the deviation of the sample estimate from \bar{P} increased as P increased, although there was considerable fluctuation in this upward trend. Also, the deviations generally increased as the number of observations (rain gages) in the sample decreased. Undoubtedly, there are many other factors which contribute to the variability of these deviations from storm to storm, such as the (1) meteorological factors causing the storm, (2) location of the storm core with respect to the center of the network, (3) duration of the storm, and (4) rate of rainfall. However, it is difficult to express (1) and (2) quantitatively and P is a function of (3) and (4).

Graphical plots indicated that the average magnitude of the deviations was also a function of N . Mathematical expressions of the form

$$\text{Log } s = a + b \text{ Log } P + c \text{ Log } N \quad (2)$$

and

$$\text{Log } s = a + b P^m + c \text{ Log } N \quad (3)$$

appeared to provide the best fit to the data. In these expressions, s represents the standard deviation of the absolute values of d from Expression (1). The goodness of fit of Expression (2) was determined in preliminary analyses.

Results of Analysis on 100-Square Mile Network

Random Start. When Expression (2) was fitted to the deviations obtained by the random start systematic sampling plan, the multiple correlation coefficient was 0.52. Although this correlation is significant, a correlation of greater degree is desirable for predicting the expected deviation between the sample and the areal mean rainfall.

It was felt that a part of the variation not accounted for by the regression system was due to

variation in the distribution of rainfall over the network among storms of similar mean rainfall. A practical quantitative measure of areal rainfall distribution which can be included in Expression (2) is difficult to obtain. It was thought that the duration of rainfall might partially reflect the areal distribution, since the distribution of point rainfall amounts may depend upon the storm duration factor. Consequently, the duration factor, T , was added to Expression (2) and the goodness of fit of an expression of the form

$$\text{Log } s = a_1 + b_1 \text{ Log } P + c_1 \text{ Log } N + e_1 \text{ Log } T \quad (4)$$

was determined. Fitting Expression (4) to the data resulted in a multiple correlation of 0.53. It is evident that the duration variable did not significantly increase the efficiency in predicting the expected deviation. Consequently, it was felt that adding the duration factor to the regression system did not warrant the extra work involved.

Combined Sampling Plan. When Expression (2) was fitted to the data for the deviations obtained from the combined sampling plan, the resulting multiple correlation coefficient was 0.70. This increase in the correlation coefficient from 0.52 for the random start plan apparently reflects a general increase in stability of the sample estimates from the more uniform distribution of gages for the small sample sizes.

Another independent variable was then introduced into the previous regression system in order to examine more thoroughly the estimate of the sampling variation. An expression of the following form

$$\text{Log } s = a_2 + b_2 \text{ Log } P + c_2 \text{ Log } N + e_2 \text{ Log } s_{\bar{P}} \quad (5)$$

was fitted to the data, where $s_{\bar{P}}$ is the standard deviation of the entire network of gage readings, e is a constant, and the other symbols represent the same quantities as they did in previous discussions. The $s_{\bar{P}}$ variable represents the best available estimate of variation in the areal precipitation pattern. The sampling error for various sample sizes should depend considerably upon the variability of the precipitation pattern. When Expression (5) was fitted to the data the multiple correlation was increased from 0.70 to 0.84. The simple correlation coefficients between $\text{log } s$ and $\text{log } P$, $\text{log } N$, and $\text{log } s_{\bar{P}}$ were 0.40, 0.58 and 0.65, respectively.

From the preceding correlation coefficients it is evident that the expected sampling error is highly dependent upon the variation in rainfall, as measured by the standard deviation of a relatively dense network of rain gages. It is also evident, as would be expected, that the sampling error has a higher degree of correlation with variation of rainfall than with either mean rainfall or gage density.

It should be noted that the insertion of the standard deviation of point rainfall totals from all gages into the equation produces an estimate that is not practical from the hydrologic standpoint. Dense networks of rain gages are seldom used except in research. The hydrologist frequently needs a means of estimating the sampling error for mean rainfall

amounts which have been obtained from a sparse network of gages. Consequently, the standard deviation, s_p of point rainfall amounts included in each sample was inserted into Expression (5) in place of $s_{\bar{P}}$. For example, if five gages were included in a sample, s_p would be the standard deviation of the five point rainfall amounts. The magnitude of s_p is a measure of the precision of a sample mean rainfall value. This variable should have an influence upon estimates of the sampling error for areal mean rainfall values. Inserting this variable into the expression resulted in a multiple correlation of 0.71. This is a very small increase over the 0.70 coefficient which was obtained from Expression (5). Consequently, it must be concluded that the s_p variable is not useful as a third independent variable. The inefficacy of s_p probably reflects the fact that the variation of sample standard deviations within storms approximated the variation in the standard deviations of a particular set of gage readings from storm to storm. Effectiveness of the sample standard deviation variable increased as sample size increased. However, the larger variation associated with small sample sizes offset most of the effect of the standard deviations for larger sample sizes. The efficiency of standard deviation as a third independent variable reached a maximum when all gages were included, as was the case when the $s_{\bar{P}}$ variable was used.

Best-Centered. A standard deviation of d values from Expression (1) was obtained by an adjustment similar to that used by Linsley and Kohler in their analysis of data from a concentrated network near Wilmington, Ohio.⁽¹⁵⁾ Storm data were grouped into classes on the basis of sample mean rainfall as measured by a sample of N gages. A standard deviation was computed for each class. Expression (2) was then fitted to the data, using the standard deviation for each class as the dependent variable. The sample size and the mid-point of the rainfall for each class were the independent variables. A multiple correlation coefficient of 0.86 was obtained with this regression system.

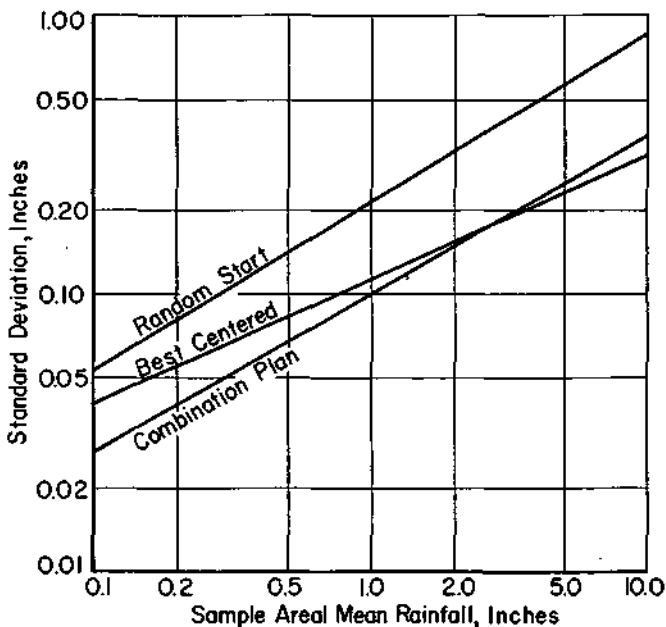


FIGURE 45 COMPARISON OF STORM SAMPLING PLANS ON A 100 SQUARE MILE AREA

Comparison of Results from Three Sampling Plans

A comparison of sampling error equations for the three sampling plans can be made by reference to Figure 45. It is evident that the random start plan will predict considerably higher errors than either of the other plans. The other two sampling plans resulted in errors which are very similar in magnitude within the range of data used. The a and c values for the best-centered and the combination plan are almost identical. The differences between the b values could be attributed to sampling variation.

Results of Analysis for Areas of Different Size

Average Error. The best-centered sampling plan approaches the practical situation which hydrologists must contend with in using the results of sampling error analyses. In addition, this plan ranked well in the comparison with other sampling plans which were considered. Consequently, the best-centered sampling plan was chosen for a more complete analysis of data involving areas of 25, 50, 100, 200, and 400 square miles.

As noted previously in the sections on variation of point rainfall with distance and areal representativeness of point rainfall, graphical plots of the data indicated that an equation for average error, E , of the form

$$\text{Log } E = a_3 + b_3 P^{0.5} + c_3 \text{Log } N \quad (6)$$

would provide a better fit to the data at high and low values of P than an expression of the form given in (2). Consequently, an expression of the form shown in (6) was applied to data for all five areas. The values of a_3 , b_3 , and c_3 are tabulated in Table 15.

TABLE 15
REGRESSION CONSTANTS

Area (Sq. Mi.)	Log E			Log S		
	a_3	b_3	c_3	a_4	b_4	c_4
25	-1.720	0.65	-0.73	-1.556	0.60	-0.63
50	-1.597	0.56	-0.55	-1.421	0.53	-0.60
100	-1.439	0.59	-0.65	-1.275	0.49	-0.63
200	-1.305	0.49	-0.56	-1.220	0.50	-0.58
400	-1.356	0.54	-0.48	-1.198	0.50	-0.54

More data should be added to the analysis to substantiate the trends in b_3 and c_3 . The Water Survey has rain-gage networks in operation which will furnish these data.

Since gage density is a more commonly used variable than the sample size variable, the constants a_3 and c_3 presented in Table 15 were adjusted to express the sample size factor in terms of gage density by the substitution

$$\text{Log } N = \text{Log } A - \text{Log } G \quad (7)$$

where G is in square miles per gage. Equations for $\text{Log } E$ with the adjusted constants are shown in Table 16.

Although the computed E tends generally to increase with area, the individual equations permit

TABLE 16
EQUATIONS FOR AVERAGE AND STANDARD DEVIATIONS

Area (Sq. Mi.)	Log E =	a ₅	+	b ₄	p ^{0.5}	+	c ₅	Log G
25	=	-2.740		0.65			0.73	
50	=	-2.531		0.56			0.55	
100	=	-2.739		0.59			0.65	
200	=	-2.594		0.49			0.56	
400	=	-2.605		0.54			0.48	
Combined	=	-2.642	+	0.794	A ^{-0.7} P ^{0.5}	+	0.966	A ^{-1.2} Log G
	Log s =	a ₆		b ₅	P ^{0.5}		c ₆	Log G
25	=	-2.395		0.60			0.63	
50	=	-2.440		0.53			0.60	
100	=	-2.535		0.49			0.63	
200	=	-2.555		0.50			0.58	
400	=	-2.603		0.50			0.54	
Combined	=	-2.506	+	0.692	A ^{-0.6} P ^{0.5}	+	0.746	A ^{-0.5} Log G

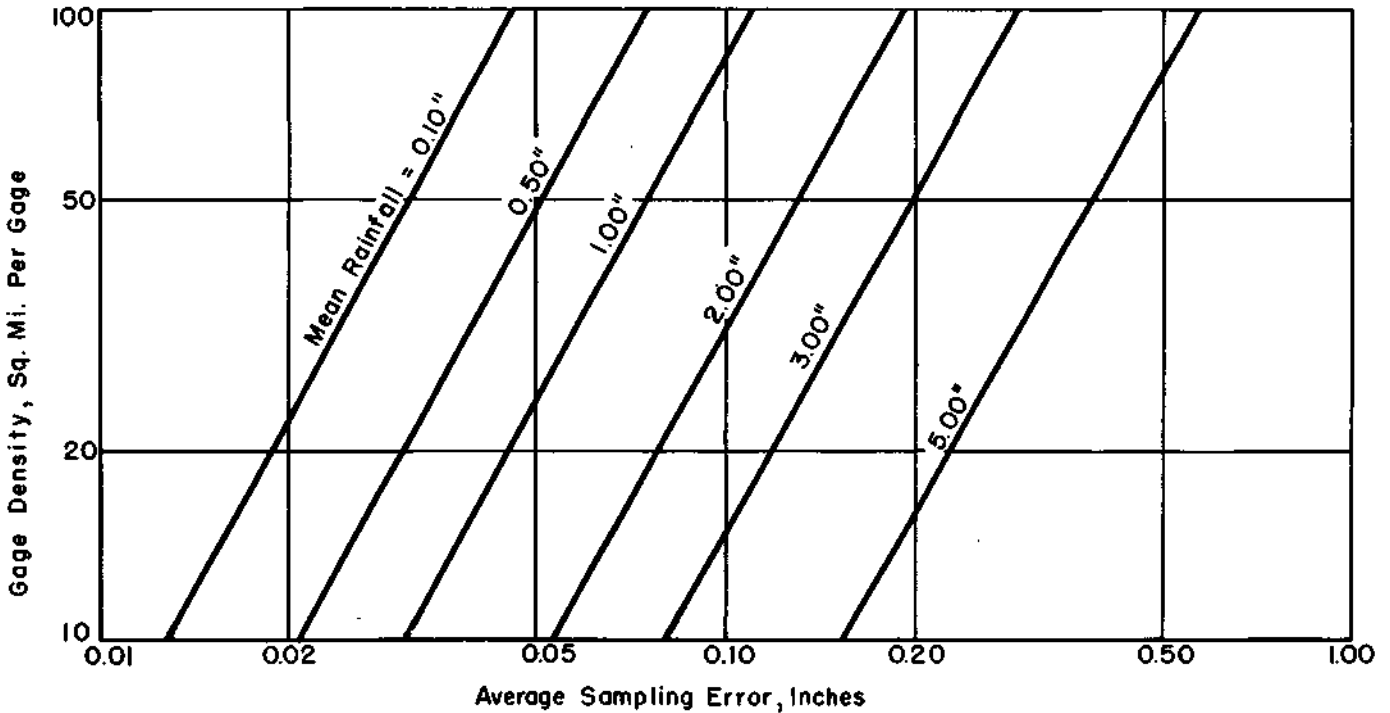


FIGURE 46 RELATION BETWEEN SAMPLING ERROR, STORM SIZE, AND GAGE DENSITY ON 100 SQUARE MILE AREA

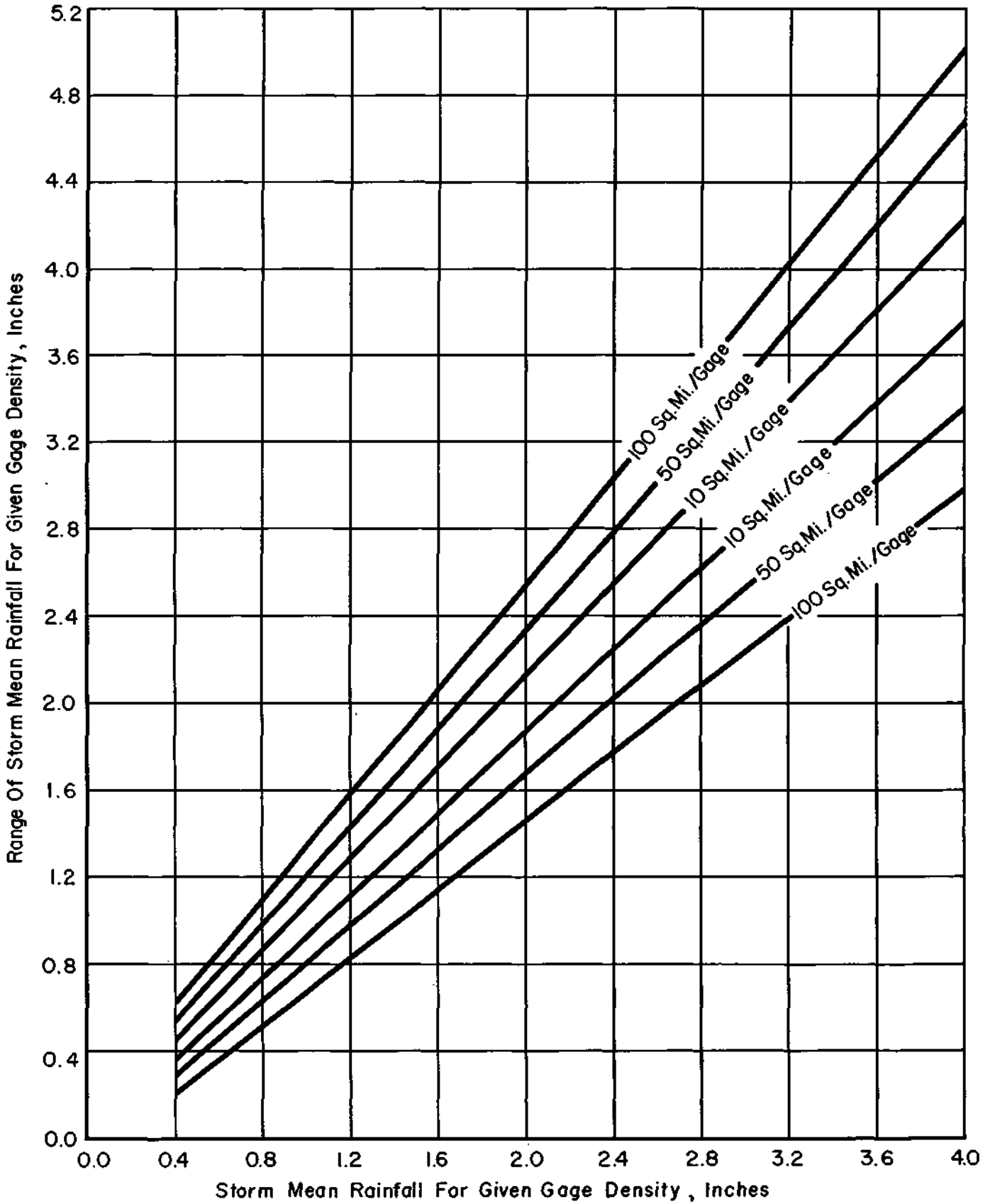


FIGURE 47 95 PER CENT CONFIDENCE RANGE OF STORM MEAN RAINFALL FOR VARIOUS GAGE DENSITIES

random fluctuations in this trend. A combined equation which would represent all five areas was desired for the purpose of smoothing and for interpolating between areas. Since the constants represented by a_5 vary at random, an average of these values may be used in a combined equation. As previously noted, there is a tendency for the values of b_4 and C_5 to decrease in magnitude as the area increases. Consequently, the values of the b_4 and c_5 were expressed as a function of area by expression of the following form:

$$b_4 = k A^1 \quad (8)$$

and

$$c_5 = k_1 A^1 \quad (9)$$

The combined equation for Log E which represents all five areas in the analysis is shown in Table 16. Relations for a 100-square mile area obtained from the combined equation are presented in Figure 46.

Confidence Limits. To establish confidence limits, an estimate of the sampling standard deviation was required. This estimate was obtained by replacing Log E in Expression (6) of Log s and fitting the resulting expression to the data, as was done for Log E.

Standard deviations were computed for the same class intervals used in determining Log E. The constant values are shown in Table 15. The values of a_4 and c_4 were adjusted for the gage density factor and the resulting equations for individual areas and for all areas combined are shown in Table 16.

The combined areal equation for Log s can be used to establish confidence limits for areal mean rainfall. The 95 per cent confidence limits for P were estimated simply by taking $2s$ and adding and subtracting from the corresponding value of P. The resulting bands are represented for selected values of G for the 100-square mile area in Figure 47.

EXCESSIVE RAINFALL RELATIONS ON
100-SQUARE MILE AREA

Data collected from 20 recording rain gages during 1950-53 on the 100-square mile Panther Creek watershed (Fig. 3) were used in a limited analysis of excessive rainfall relations. The following excessive rainfall definition of the U.S. Weather Bureau was used in the study

$$R = T + 20 \quad (1)$$

where R is the rainfall depth in inches and T is the period of observation in minutes. Excessive rates for periods of 30, 60, and 120 minutes were investigated. The above definition gives lower limits of 0.50, 0.80, and 1.40 inches for the 30-, 60-, and 120-minute periods, respectively. In addition to the Panther Creek data, data from 48 gages on the 100-square mile Goose Creek network (Fig. 4) were available for 1953-54, and these have been utilized to a limited extent in the analysis.

Gage Density to Observational Frequency Relations

The effect of gage density upon the frequency of observation of excessive rainfall values in a 100-square mile area was examined first. For this purpose, the Panther Creek network was subdivided into networks of 10, 5, 2, and 1 gages, keeping the distribution in each set as uniform as possible. Similarly, on the Goose Creek area, networks of 24, 12, 6, 3, and 1 gages were selected. The number of excessive amounts recorded by one or more gages for each of the various networks within both areas was then tabulated. Use of special recording rain gages having 12.6-inch diameter orifices and 6-hour charts enabled recording of 15-minute excessive amounts on the Goose Creek area, in addition to those for the 30-, 60-, and 120-minute periods.

Results of this first phase of the study are shown in Table 17. The expected trend for the observational frequency of excessive amounts to increase with increasing gage density is apparent. Of particular interest are the data for 24 and 48 gages in the Goose Creek network. The very slight increase in frequency in going from 24 to 48 gages

TABLE 17

RELATION BETWEEN EXCESSIVE RAINFALL FREQUENCY AND GAGE DENSITY

Number of Gages	Number of Cases for Given Time Period (Min.)				Total
	15	30	60	120	
<u>Goose Creek Network. 100 Sq. Mi.. 1953-54</u>					
1	14	14	5	2	35
3	22	19	14	3	58
6	24	22	14	3	63
12	28	25	18	5	76
24	33	28	21	6	88
48	34	28	22	7	91
<u>Panther Creek. 100 Sq. Mi.. 1950-53</u>					
1	--	21	14	5	40
2	--	34	17	10	61
5	--	41	25	14	80
10	--	49	31	15	95
20	--	52	33	18	103

indicates that the optimum gage density for a 100-square mile area, considering all factors, is probably between 20 and 30 gages. It appears that storms of adequate intensity to provide excessive values for the time periods investigated are of sufficient areal extent and of sufficient duration to be almost always observed by a network of 20 to 30 gages.

Effect of Gage Density on Observed Maximum

The effect of gage density on the maximum observed excessive amounts within a 100-square mile area was investigated next, using the 1950-53 data for Panther Creek. For this purpose, networks of 20, 10, 5, and 2 gages within the 100 square miles were used. For each storm, a ratio of the maximum amount observed on the network to the amount observed at the central gage in the network was computed. This was done for each network and for 30-, 60-, and 120-minute periods whenever excessive values were recorded by one or more of the 20 gages making up the network of maximum density. Average ratios were then calculated for each of the several networks within the 100-square mile area. The results of this study are summarized in Table 18 where the average ratios for each network within the 100-square mile area are presented for 30-, 60-, and 120-minute periods. The relation is further illustrated in Figure 48.

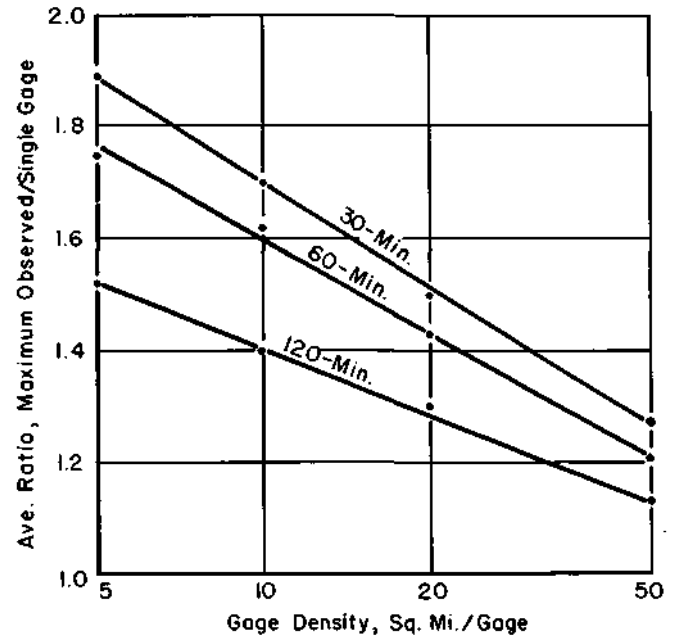


FIGURE 48 EFFECT OF GAGE DENSITY ON MAXIMUM OBSERVED EXCESSIVE RATES

TABLE 18

EFFECT OF GAGE DENSITY ON OBSERVED MAXIMUM AMOUNTS

Number of Gages	Av. Ratio, Maximum Observed/Central Gage Amount for Given Time Periods (Min.)		
	30	60	120
20	1.89	1.75	1.52
10	1.70	1.62	1.40
5	1.50	1.43	1.30
2	1.27	1.21	1.13

As expected the ratio tends to increase with increasing gage density. The ratio appears to be still increasing at an appreciable rate when the maximum network of 20 gages is reached.

Point-Areal Mean Relations

Next, the relation between point excessive and areal mean excessive amounts was investigated. The areal mean was obtained in each storm by averaging the heaviest amount observed at each of the 20 rain-gage stations for the periods of 30, 60, and 120 minutes. That is, the individual amounts making up the mean may have occurred at different times at the various network stations although all occurred in the same storm period. This definition of the mean was considered more desirable than that obtained by calculating means at a given time during the storm for all gages. The core of heavy rainfall, especially in thunderstorms, frequently covers a relatively small area; consequently, the heaviest storm rates occur at different times in moving across an area of 100 square miles. Since such factors as soil erosion and sedimentation appear to be closely related to the short-period, heavy rainfall rates experienced in storms, the method used for calculating the means was considered to have the most practical application.

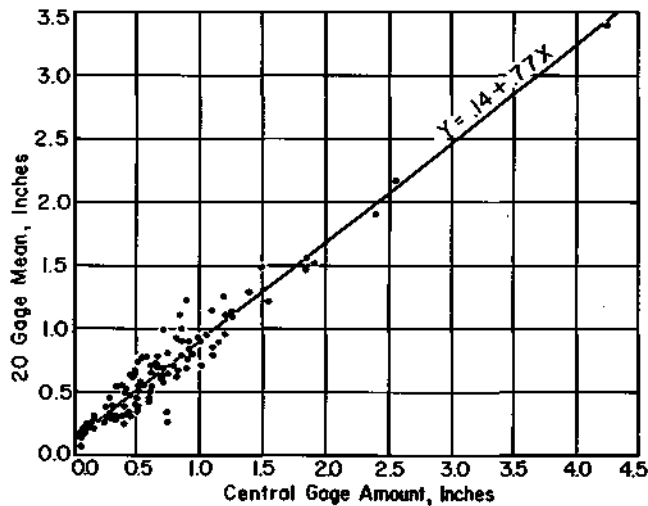


FIGURE 49 RELATION BETWEEN POINT AND AREAL MEAN RATES UNDER EXCESSIVE RATE CONDITIONS

Figure 49 illustrates the relations between the point rainfall observed at the central gage and areal mean rainfall for 30-, 60-, and 120-minute periods. The three periods were combined into one relation after separate graphical plots indicated insignificant differences among the relations for individual periods. Points in Figure 49 include all cases in which an excessive amount was recorded by one or more gages in the 20-gage network. The regression equation indicates that the point rainfall observed at the center of a 100-square mile area is slightly above the areal mean rainfall when excessive amounts are experienced (above 0.50 inch). This trend is to be expected when storm movement

is considered. For example, assume two thunderstorms of the same size and same intensity, one passing over the network with its core passing through the center of the network, while the core of the other storm passes along or near the border of the network. Obviously, the heaviest rates will be observed at the central gage when a given storm passes through or near the center of the network and these storms will also provide the most frequent areal mean excessive rates. A correlation coefficient of 0.96 was obtained between the 20-gage mean and the central-gage point rainfall.

Observations used in the preceding analysis of point-areal mean relations included a considerable number in which neither the central-gage amount nor the areal mean rainfall represented an excessive amount, since only one excessive value among the 20 gages was required for inclusion in the analysis. To determine whether the inclusion of values below the excessive level materially affected the point-areal relation, another analysis was made in which only those cases with an excessive amount at the central gage were included. This analysis resulted in development of a regression equation given by

$$Y = 0.11 + 0.78 X \quad (2)$$

where Y is the areal mean rainfall in inches and X is the central gage amount in inches. This equation is insignificantly different from the one illustrated in Figure 49. A correlation coefficient of 0.97 was obtained compared to 0.96 for the curve in Figure 49. Results indicate that Figure 49 can be used for estimating the areal mean maximum or areal mean excessive rainfall on a 100-square mile basin for short periods within storms, when a point rainfall observation is available at or near the center of the area.

A study of the data indicated the central gage gives a very good measure of the frequency of excessive areal mean rainfall. For example, on Panther Creek during 1950-53 the number of areal mean excessive values was practically the same as the number observed at the central gage. For a 30-minute period, 21 excessive amounts were observed on both a point and areal basis. For a 60-minute period there were 14 point excessive amounts and 13 areal excessive amounts, while for a 120-minute period there were 5 excessive values for both cases. Combining all three periods, there were 40 excessive amounts observed at the central gage compared to 39 cases of excessive areal mean rainfall. However, this does not mean that the point and areal mean rates all occurred in the same storms. By comparison, it was found that excessive areal means occurred 17 out of the 21 times that excessive amounts were observed at the central gage. Similarly, 11 out of 14 point excessive amounts occurred in conjunction with excessive areal mean values for the 60-minute period, while all five of the point and areal excessive amounts coincided for the 120-minute period.

Figure 50 is an illustration of the occurrence of excessive rainfall amounts over the network during an exceptionally heavy storm during the evening of June 8, 1951. Heavy excessive amounts were observed at all stations within the network

during the storm period. An areal average of 7.21 inches fell during the entire storm which lasted about four hours. Figure 51 illustrates the distribution of excessive rainfall in the area by means of area-depth curves. It is interesting to note that the square-root relation for total storm rainfall discussed in the section on area-depth relations provides a good fit in these cases of unusually heavy short-period amounts within a storm.

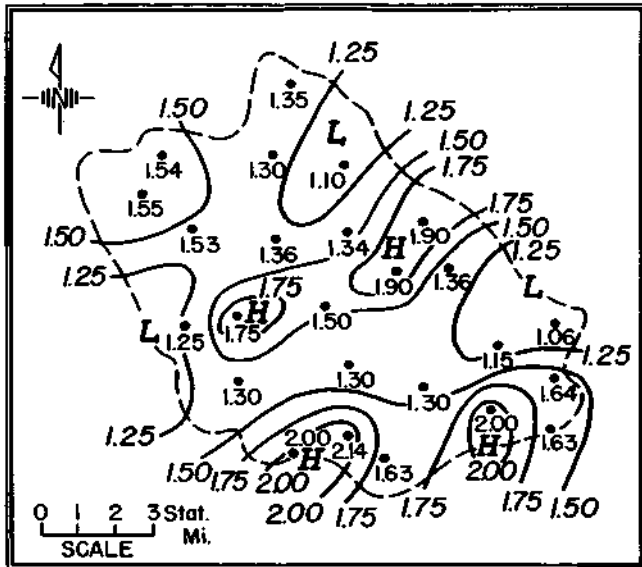


FIGURE 50 30-MINUTE EXCESSIVE RATES, JULY 8, 1951

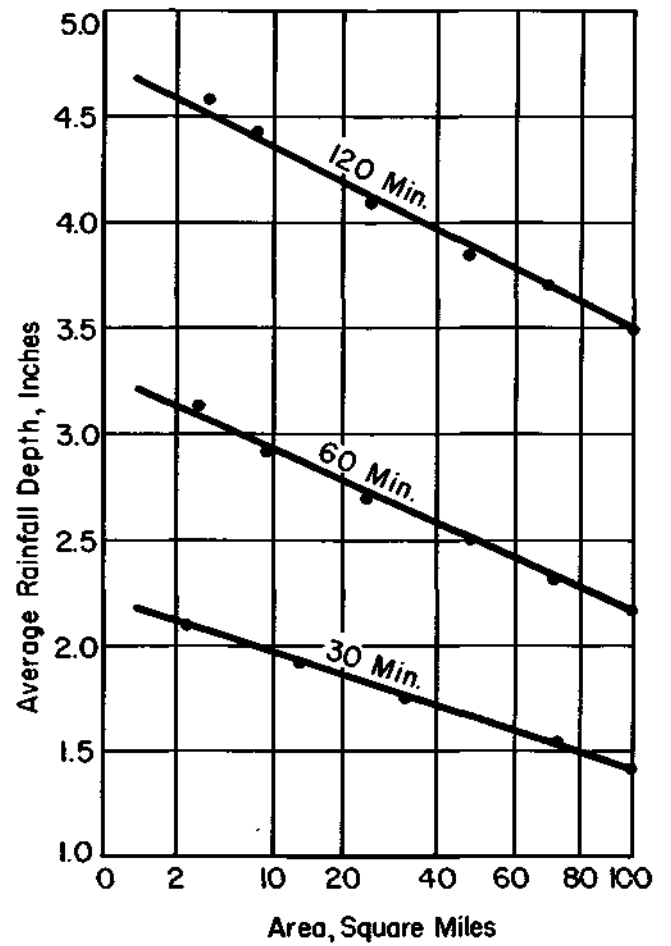


FIGURE 51 EXCESSIVE RATE AREA-DEPTH RELATIONS, JULY 8, 1951

RELATION BETWEEN POINT AND AREAL
RAINFALL FREQUENCIES

Although much information has been published on point rainfall frequencies, little data are presently available in the literature on areal rainfall frequencies. The following presents limited information on the subject, obtained from a 20-gage network on the 100-square mile Panther Creek watershed during the period 1948-53.

Using data from this network, comparisons have been made between point and areal mean rainfall frequencies for the above 6-year period for areas

of 25 and 50 square miles within the 100-square mile network. Because of minor changes in some of the gage locations from year to year, it was not possible to obtain a 6-year comparison for the 100-square mile area. However, data were available for a 3-year comparison and these results are also given.

Within each area, the point rainfall frequencies were obtained from the rain gage in the center of the area. Areal mean rainfall was calculated from

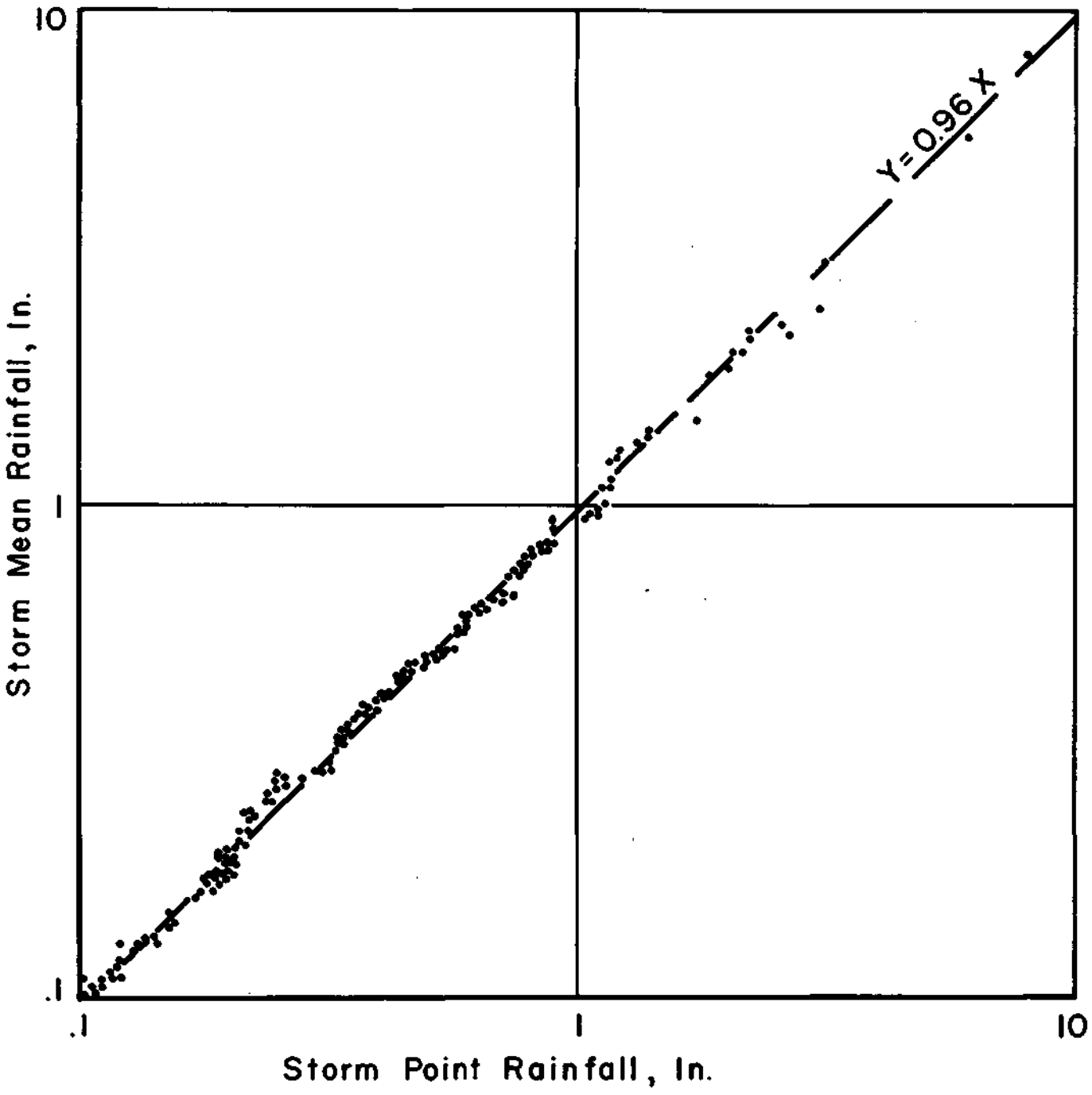


FIGURE 52 COMPARISON BETWEEN POINT AND AREAL MEAN RAINFALL AT EQUAL FREQUENCIES ON 25 SQUARE MILE AREA

the arithmetical average of all gage observations. Within the 25- and 50-square mile areas studied, there were 6 and 12 gages, respectively. To obtain comparisons between point and areal frequencies, all storms for each area were ranked by mean rainfall. Similarly, storm point rainfall totals at the center of each area were ranked. The rankings then provided a frequency distribution of point and areal mean rainfall within a 6-year period for the 25- and 50-square mile areas and within a 3-year period for the 100-square mile area. Regression equations and correlation coefficients were obtained between point and areal mean rainfall frequencies for each area, treating equal positions of rank as pairs of observations. To illustrate the pairing procedure, the highest point rainfall observed at the center of the 25-square mile area, 8.22 inches, was paired with the highest mean rainfall for this area during the 6-year comparison period, which was 8.16 inches. Obviously, the paired observations in many cases occurred in different storms, since the data were paired on a frequency distribution basis.

Relations were developed for storm rainfall, in which a single storm was defined as all rainfall unseparated by a break in precipitation of six hours or more. Consequently, several showers were frequently included in a storm as defined in this study. The results are perhaps also indicative of daily rainfall. The study was confined to shower-type rainfall, the type of storm from which flash floods on small areas occur. The results are con-

sidered indicative and not definitive of point-areal frequency relations.

The regression equations obtained for the 25- and 50-square mile areas were $Y = 0.96X$ and $Y = 0.94X$, respectively. The 6-year point-areal comparison for the 25-square mile area is illustrated in Figure 52.

Results of the study indicate that an excellent relationship exists between point and areal rainfall frequencies. A correlation coefficient of 0.99 was obtained between point and areal rainfall for both the 25- and 50-square mile areas. For the 100-square mile area, a correlation coefficient of 0.99 was obtained and the regression equation was $Y = 0.97X$, very close to the equations obtained for the 25- and 50-square mile areas. Indications are that areal mean rainfall frequencies are close to, but slightly less than, equivalent point rainfall frequencies for small areas.

A 3-year comparison for another set of 25- and 50-square mile areas within the 100-square mile watershed produced regressions of $Y = 0.97X$ for both areas, agreeing closely with the 6-year comparisons. A 3-year frequency comparison was also made using data only for excessive rainfall rates, based on the definition of excessive rainfall given in the previous section of this bulletin. Combining data for excessive 30- and 60-minute amounts, a regression equation, $Y = 0.92X$, was obtained.

A MICROMETEOROLOGICAL STUDY OF
RAINFALL VARIABILITY

Introduction

Analyses of rainfall data from several concentrated rain-gage networks in central Illinois during recent years have revealed the frequent presence of rainfall gradients exceeding 0.25 inch per mile in shower-type rainfall. The relation between rainfall variability and either distance or area is pertinent in the determination of gage density requirements for specific purposes, such as: the collection of small scale climatological data, hydrologic projects involving runoff and sedimentation investigations, agricultural research, and studies concerned with establishing the utility of radar for quantitative precipitation measurements. Also, the magnitude of rainfall variability with distance should be considered in determining the sensitivity and calibration accuracy required for recording rain gages, especially those employed in routine observational programs where concentrated networks are not feasible.

As part of a program to investigate the quantitative relations existing between rainfall variability and distance, a micro-network of rain gages was established in 1953. Since the greatest variation in rainfall with distance normally occurs with shower-type rainfall, data were collected during the spring, summer and fall seasons of 1953-54. Similar observations on a mesometeorological scale were available for comparison purposes from other networks described in the section on rain-gaging facilities.

Description of Network

A micro-network of 18 gages was established on level meadow land at the University of Illinois Airport. Its design was based upon available infor-

mation concerning rainfall gradients obtained from rainfall studies on several concentrated watershed networks during 1948-52. The network consisted of pairs of 8-inch non-recording gages spaced six feet apart at each of nine stations which were located at intervals of 300 feet to form a square grid pattern (Fig. 8). Information on storm duration and rainfall intensity was obtained from a recording rain gage installed adjacent to the micro-network. Wind data were obtained from an Aerovane system located about 0.5 mile from the network.

The calibration of each gage was checked before installation. The level of each gage was checked periodically and the gages kept as free of dirt, insects and other foreign material as possible. Measurements of rainfall were made for each occurrence of precipitation. These measurements were made as soon as possible after the end of each storm to minimize evaporation effects. Careful attention was given to gage exposures, maintenance, and observational techniques. To minimize the reading error, experienced observers read the rain-gage amounts to the nearest .001 inch.

Analysis of Data

Data were collected from 93 storms from March to November, during 1953 and 1954. For each storm, average precipitation differences were calculated for the various sets of gages located 6, 300, and 600 feet apart on the grid pattern. Results of this analysis, classed by storm size, are shown in Table 19. The mean maximum differences shown in Table 19 are the averages for the highest difference observed in each storm. The absolute maximum is the highest reading obtained during the 1953-54 test period for each class of storm size, as measured by the network mean rainfall.

TABLE 19
DIFFERENCES BETWEEN GAGE PAIRS

	Differences (in.) for Given Storm Sizes (in.)			
	0.01-0.19	0.20-0.49	0.50-0.99	1.00-1.99
<u>6-Foot Pairs</u>				
Average	0.003	0.005	0.009	0.020
Mean Maximum	0.009	0.013	0.022	0.047
Absolute Maximum	0.015	0.046	0.041	0.110
Number of Storms	46	19	15	13
<u>300-Foot Pairs</u>				
Average	0.005	0.009	0.013	0.027
Mean Maximum	0.013	0.025	0.034	0.079
Absolute Maximum	0.026	0.049	0.048	0.165
Number of Storms	46	19	15	13
<u>600-Foot Pairs</u>				
Average	0.006	0.012	0.016	0.038
Mean Maximum	0.015	0.027	0.034	0.087
Absolute Maximum	0.034	0.047	0.070	0.231
Number of Storms	46	19	15	13

Reference to Table 19 shows that average 6-foot differences for storms having mean rainfall up to 0.50 inch are rather insignificant. However, appreciable differences were usually observed with the heavier storms and occasionally with light storms. Since the differences have a definite tendency to increase with storm size, they cannot be attributed solely to reading error. Another factor which may have contributed to the differences observed between the 6-foot pairs is the turbulence created in the wind flow about the gages. There was no way in which to separate the effects of reading and turbulence errors from the real differences occurring in the surface rainfall pattern. Considering the careful attention which was given to gage exposures, gage maintenance, and observational techniques, it is believed that the differences which were obtained between the 6-foot pairs represent the minimum to be expected in shower-type rainfall. For the 6-foot pairs a correlation coefficient of 0.79 was obtained between average storm differences and storm size.

The trend for the average difference to increase with increasing storm size and with distance is further illustrated by the summarized data for the 300-foot and 600-foot pairs in Table 19. A correlation coefficient of 0.80 was obtained between average difference and mean rainfall for the 300-foot pairs. Similarly, a correlation coefficient of 0.72 was obtained with the 600-foot pairs.

The data were further examined for differences between 6-foot gage pairs arising from meteorological factors other than mean rainfall. These factors include storm duration, mean rainfall rate, and wind. Results of this phase of the study are presented in Table 20, where the relative variability of the average differences has been related to each meteorological factor. The variability factor was obtained for each storm by dividing the average difference for pairs at a given distance by the areal mean rainfall and multiplying by 100 to convert the factor to per cent.

TABLE 20

RELATIVE VARIABILITY TRENDS FOR
6-FOOT GAGE PAIRS

Av. Variability (%) for Given Size of Event				
Mean Rainfall, in.				
0.01-0.09	0.10-0.19	0.20-0.49	0.50-0.99	1.00-1.99
6.1	2.5	1.9	1.4	1.3
Storm Durations, hrs.				
0.1-2.0	2.1-4.0	4.1-6.0	6.1-12.0	12.1-24.0
5.8	1.9	2.1	1.9	2.0
Mean Rainfall Rate, in/hr				
0.01-0.05	0.06-0.10	0.11-0.20	0.21-0.30	Over 0.30
5.8	2.7	2.3	2.2	1.8
Wind Speed, mph				
0-5	6-10	11-15	16-20	21-30
3.6	3.7	2.8	2.8	2.4

Examination of Table 20 shows that the relative variability tends to decrease with increasing mean rainfall, this trend being more pronounced for the light storms. A similar trend was observed for storm duration up to four hours, after which, there appeared to be no significant change in the average relative variability with increasing storm duration. Mean rainfall rate produced its greatest effect upon the relative variability at low values. A slight trend was observed for the relative variability to decrease with increasing magnitude of wind speed, the average relative variability tending to level off with high values of wind speed.

Because of the magnitude of the computations involved, no attempt was made to combine all the possible variables into a multiple regression equation, especially since a relatively high correlation was obtained between the various differences and storm size of mean rainfall. Scatter diagrams relating the 6-foot relative variability to mean rainfall, wind speed, storm duration, and mean rainfall rate are illustrated in Figure 53.

For comparison with the small scale differences in Table 19, some results from the study discussed in the section on the variation of point rainfall with distance are summarized in Table 21. The relations shown in this table were obtained from observations in shower-type rainfall collected on the Panther Creek and Goose Creek networks shown in Figures 3 and 4.

The magnitude of the variability between 6-foot 300-foot and 600-foot pairs on a monthly and seasonal basis is illustrated in Table 22. A trend for average differences between gage pairs to increase with distance and with areal mean rainfall was found for both monthly and seasonal precipitation. This trend was less pronounced than that found between average differences and storm mean rainfall. Correlation coefficients of 0.60, 0.58, and 0.48 were obtained between monthly rainfall and average differences of 6-foot, 300-foot and 600-foot pairs, respectively. Although a maximum monthly difference of 0.27 inch was observed between 600-foot pairs on one occasion, average monthly differences were generally less than 0.05 inch.

Computations were made of the accuracy with which the central gage within the grid pattern measured the storm mean rainfall for the entire area. Results are summarized in Table 23 where the average, standard and maximum errors have been related to storm size. Mean rainfall was obtained from the arithmetical average of all gages. The errors were found to increase with increasing storm size, although remaining relatively small.

TABLE 21

VARIATION OF POINT RAINFALL WITH DISTANCE

Storm Size (in.)	Av. Difference (in.) at Given Distance		
At Given Point	1 Mile	3 Miles	
0.10	0.06	0.09	
0.25	0.08	0.11	
0.50	0.10	0.14	
1.00	0.14	0.20	
1.50	0.18	0.26	
2.00	0.23	0.33	

TABLE 22
MONTHLY AND SEASONAL DIFFERENCES BETWEEN GAGE PAIRS

	Mean Rainfall, in.	Difference (in.) for Given Distance					
		6-Ft		300-Ft		600-Ft	
		Av.	Max.	Av.	Max.	Av.	Max.
<u>1953</u>							
April	1.30	0.022	0.067	0.023	0.054	0.032	0.094
May	1.53	0.022	0.047	0.028	0.078	0.028	0.059
June	3.39	0.016	0.034	0.032	0.100	0.039	0.079
July	3.15	0.036	0.057	0.032	0.080	0.036	0.066
Aug.	0.59	0.012	0.032	0.016	0.036	0.021	0.040
Sept.	0.41	0.006	0.016	0.008	0.031	0.014	0.039
Oct.	1.74	0.028	0.061	0.039	0.120	0.055	0.123
<u>1954</u>							
March	1.18	0.013	0.034	0.023	0.060	0.023	0.044
April	4.61	0.043	0.083	0.083	0.234	0.145	0.270
May	4.34	0.026	0.053	0.025	0.081	0.029	0.074
June	2.59	0.050	0.112	0.044	0.122	0.055	0.102
July	2.79	0.020	0.036	0.037	0.090	0.054	0.125
Aug.	4.51	0.028	0.055	0.027	0.088	0.025	0.083
Sept.	0.30	0.007	0.014	0.013	0.032	0.025	0.036
Oct.	4.51	0.032	0.057	0.028	0.076	0.044	0.110
<u>1953</u>							
Apr.-Oct.	12.11	0.053	0.092	0.102	0.234	0.167	0.327
<u>1954</u>							
Mar.-Oct.	24.83	0.113	0.219	0.175	0.429	0.200	0.482

TABLE 23
RELATION BETWEEN AREAL MEAN RAINFALL AND
CENTRAL GAGE POINT RAINFALL

	Storm Mean Rainfall, in.				
	<u>0.01-0.09</u>	<u>0.10-0.19</u>	<u>0.20-0.49</u>	<u>0.50-0.99</u>	<u>1.00-1.99</u>
Average Error	0.003	0.003	0.005	0.007	0.013
Standard Error	0.004	0.004	0.007	0.009	0.017
Maximum Error	0.013	0.011	0.017	0.025	0.044
Number of Storms	28	18	19	15	13

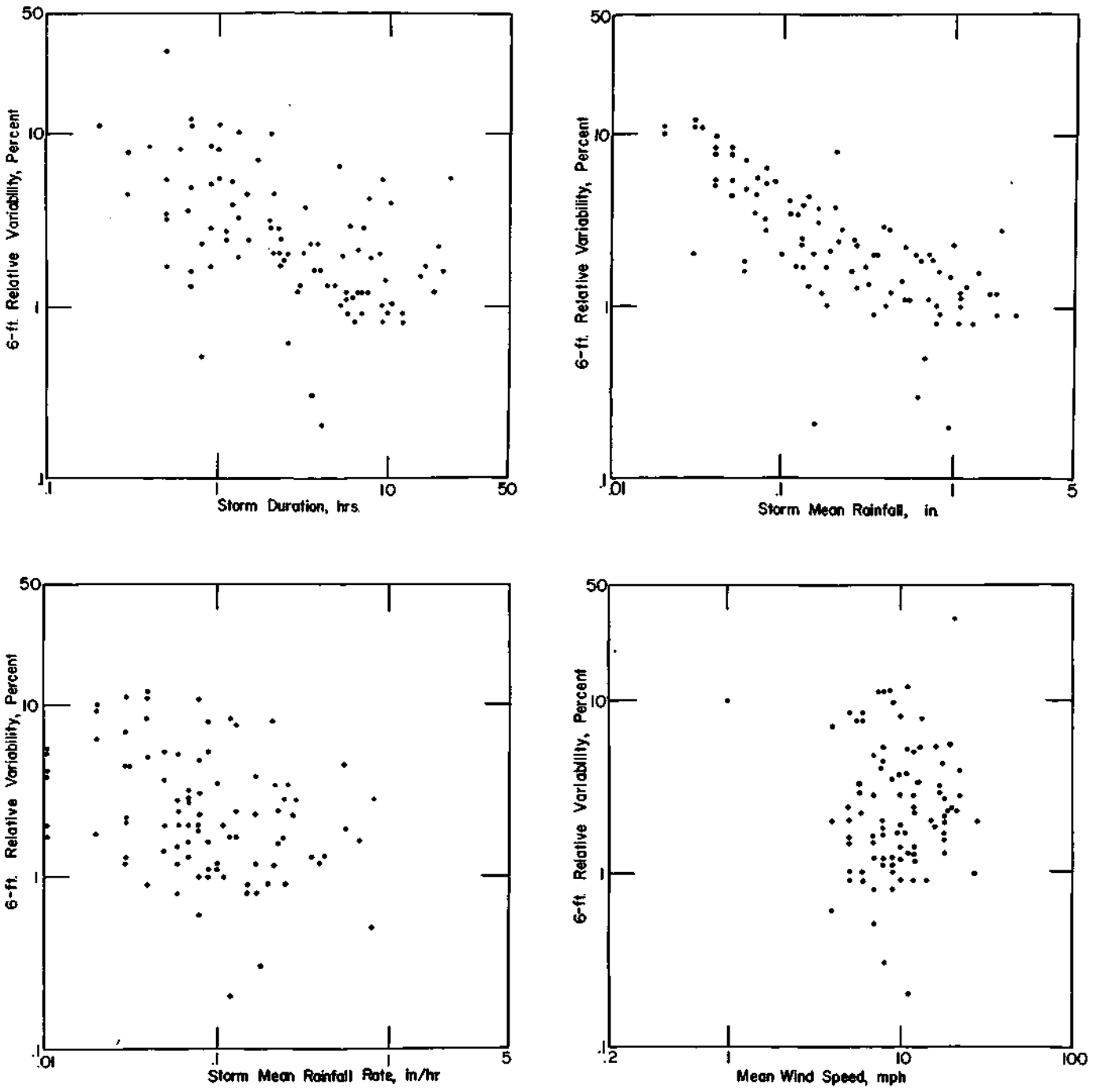


FIGURE 53 EFFECT OF SEVERAL METEOROLOGICAL FACTORS ON RELATIVE VARIABILITY OF STORM RAINFALL

REFERENCES

1. The Thunderstorm, Report of the Thunderstorm Project (Joint Project of Air Force, Navy, NACA, Weather Bureau), U. S. Dept. of Commerce, Weather Bureau, Washington, D. C, June 1949.
2. Neill, J. C, Analysis of 1952 Radar and Rain Gage Data, Report of Investigation No. 21, State Water Survey Division, Urbana, Illinois, July 1953.
3. Huff, F. A., Neill, J. C, and Spock, M., Evaluation of Low-Powered 3-cm Radar for Quantitative Rainfall Measurements. Research Report No. 4 under U. S. Army Signal Corps Contract DA-36-039 SC-64723 (State Water Survey Division Report of Investigation No. 29), Urbana, Illinois, 1956.
4. Yarnell, D. L., Rainfall Intensity-Frequency Data, U. S. Dept of Agriculture, Misc. Pub. No. 204, Washington, D. C, August 1935.
5. Rainfall Intensity-Duration-Frequency Curves, Tech. Paper No. 25, U. S. Dept. of Commerce, Weather Bureau, Washington, D. C, December 1955.
6. Storm Rainfall of Eastern United States, Miami Conservancy District, Dayton, Ohio, 1936.
7. Storm Rainfall in the United States, Depth-Area-Duration Data, U. S. Corps of Engineers, Office of Chief of Engineers, Washington, D. C, 1945.
8. Thunderstorm Rainfall, Hydromet. Report No. 5, U. S. Dept. of Commerce, Weather Bureau, Washington, D. C, 1947.
9. Huff, F. A., and Stout, G. E., "Area-Depth Studies for Thunderstorm Rainfall in Illinois," Trans. AGU, 33, 4, (State Water Survey Division Circular No. 39) August 1952.
10. Chow, V. T., Discussion of "Area-Depth Studies for Thunderstorm Rainfall in Illinois," Trans. AGU, 34, 4, August 1953.
11. Hudson, H. E. Jr., Stout, G. E., and Huff, F. A., "Rainfall Studies Using Rain Gage Networks and Radar," Proc. ASCE, Sep. 178, March 1953.
12. The Storm of July 8, 1951 in North Central Illinois. Report of Investigation No. 14, State Water Survey Division, Urbana, Illinois, 1952.
13. Larson, B. O., Hiser, H. W., and Daniels, W. S., The Storm of July 18-19, 1952 in Rockford, Illinois and Vicinity, Report of Investigation No. 24, State Water Survey Division, Urbana, Illinois, 1955.
14. Huff, F. A., and Neill, J. C, "Variation of Point Rainfall With Distance", Proc. ASCE, 82, SA1, Feb. 1956.
15. Linsley, R. K. and Kohler, M. A., "Variations in Storm Rainfall Over Small Areas," Trans. AGU, 32, 2, April 1951.